



MASTERARBEIT / MASTER'S THESIS

Titel der Masterarbeit / Title of the Master's Thesis

„On the synthesis of potentially bioactive, chiral
aminophosphonic acids“

verfasst von / submitted by

Tamara Dinhof, BSc

angestrebter akademischer Grad / in partial fulfilment of the requirements for the degree of

Master of Science (MSc)

Wien, 2021

Studienkennzahl lt. Studienblatt /
degree programme code as it appears on
the student record sheet:

UA 066 862

Studienrichtung lt. Studienblatt /
degree programme as it appears on
the student record sheet:

Masterstudium Chemie

Betreut von / Supervisor:

Dr. Katharina Pallitsch, Bakk. MSc

Acknowledgements

Ich möchte mich an dieser Stelle bei allen bedanken, die mich während der Anfertigung dieser Masterarbeit unterstützt haben.

Zuerst möchte ich mich herzlich bei Kathi bedanken, für die Möglichkeit in ihrer großartigen Gruppe meine Masterarbeit machen zu dürfen und für die stets herausragende Betreuung ihrerseits. Neben hilfreichen Anregungen und konstruktiver Kritik war bei ihr auch vor allem die Freude an der Arbeit immer spürbar, was mich noch mehr motivierte.

Ein besonderer Dank geht an Toda und Lukas, die mir zu jeder Zeit bei Fragen hilfreich zur Seite gestanden sind und durch ihre herzliche Art meine Arbeit im Labor noch schöner gemacht haben.

Ich möchte auch Ertan danken, der mir im Labor eine große Hilfe war.

Außerdem bedanke ich mich herzlich beim Team des NMR Zentrums, der Massenspektrometrie, dem Mikroanalytischen Laboratorium sowie dem Zentrum für Kristallstrukturanalyse.

Ebenso möchte ich mich bei allen Kolleginnen und Kollegen des Instituts für organische Chemie bedanken, die eine angenehme Atmosphäre geschaffen haben.

Ein großer Danke geht an meinen Freund, meine Eltern und meine ganze Familie, die mir immer zur Seite standen und mich während des gesamten Studiums unterstützt haben. Vor allem meiner Mama möchte ich an dieser Stelle noch einmal danken.

Abschließend möchte ich mich noch bei allen bedanken, die zu meiner Masterarbeit beigetragen haben, die ich hier nicht namentlich aufgezählt habe.

Content

1. Introduction.....	1
1.1 Phosphorus.....	1
1.2 Organophosphorus compounds.....	1
1.2.1 Overview	1
1.2.2 Phosphonates in nature	2
1.3 Industrial importance of synthetic phosphonates.....	4
1.3.1 Phosphonates as enzyme inhibitors.....	4
1.3.2 Phosphonates as herbicides.....	6
1.3.3 Bisphosphonates in medicine	7
1.3.4 Antiviral phosphonates	8
1.3.5 α -Aminophosphonic acids.....	10
1.4 Environmental impact.....	12
1.5 Overview of phosphonate biosynthetic pathways	13
1.6 Biodegradation pathways of phosphonates	16
1.6.1 Phosphonate metabolism	16
1.6.2 The <i>pho</i> -regulon	17
1.6.3 Radical (C-P-lyase) mechanism.....	19
1.6.4 Hydrolytic (β -electron-sink) mechanism.....	24
1.6.5 Oxidative P-C bond cleavage.....	27
2. Aims of the thesis.....	33
3. Results and discussion.....	35
3.1 Synthesis of chiral α -aminophosphonic acids.....	35
3.1.1 Overview of the new method	35
3.1.2 Synthesis of ketophosphonates	36
3.1.3 Synthesis of enantiopure α -hydroxyphosphonates.....	39

3.1.4 Synthesis of α -azido-phosphonates by Mitsunobu reaction (with HN_3)	44
3.1.5 Phosphaarginine, additional steps: synthesis of (<i>R</i>)-diisopropyl [1-azido-4-bis(<i>tert</i> -butoxycarbonyl)guanidino]butylphosphonate [(<i>R</i>)- 88]	48
3.1.6 Reduction of azides, synthesis of α -aminophosphonates	50
3.1.7 Synthesis of α -aminophosphonic acids	52
3.1.8 Synthesis of α -hydroxyphosphonic acids	53
3.2 Synthesis of (<i>R</i>)-[1-hydroxy-2-(trimethylammonio)ethyl]phosphonate (<i>R</i>)- 58 and its isotopically labeled analogs (<i>R</i>)-1-[^2H]- 58 and (<i>R</i>)-1-[^{13}C]-1-[^2H]- 58	54
4. Experimental part.....	63
4.1 General experimental part	63
4.2 General procedures.....	65
4.3 Synthesis of (<i>R</i>)-phosphaalanine [(<i>R</i>)- 20].....	68
4.4 Synthesis of (1 <i>R</i> ,2 <i>S</i>)-phosphaisoleucine [(1 <i>R</i> ,2 <i>S</i>)- 59]	73
4.5 Synthesis of (<i>S</i>)-phosphaisocysteine [(<i>S</i>)- 62]	77
4.6 Synthesis of (<i>S</i>)-phosphamethionine[(<i>S</i>)- 60]	79
4.7 Synthesis of (<i>R</i>)-phosphaarginine [(<i>R</i>)- 61]	84
4.8 Synthesis of (<i>R</i>)-[1-hydroxy-2-(trimethylammonio)ethyl]phosphonate (<i>R</i>)- 58 and its isotopically labeled analogs (<i>R</i>)-1-[^2H]- 58 and (<i>R</i>)-1-[^{13}C]-1-[^2H]- 58	89
5. Abstract	98
5.1 English abstract	98
5.2 Deutsche Zusammenfassung.....	99
6. References.....	101
7. Appendix.....	108

1. Introduction

1.1 Phosphorus

Phosphorus was first isolated and thus discovered around 1669 by Hennig Brandt, a German alchemist. It is the 11th most abundant element in the earth's crust. Through the ages it was found that phosphorus is an essential nutrient for all living organisms. It is released from rocks into soil and is then taken up by plants. Like this, phosphorus enters the food chain. In most cases it is present as inorganic phosphate ion P_i (PO_4^{3-}). The mass of phosphorus in our biosphere is quite low, however, phosphorus is quite abundant in vertebrates: hydroxyapatite, $Ca_{10}(PO_4)_6(OH)_2$ makes up 70% of the mass of teeth and 60% of the mass of bone. This structural role in bone and teeth accounts for about 85% of the whole body phosphorus content. Apart from this, the remaining 15% have also significant functions. The backbone of deoxyribonucleic acid and ribonucleic acid (DNA/ RNA) chains, which are responsible for replication and storage of all genetic information, are formed by phosphate-bridges. Furthermore, phosphate residues are crucial for many cellular signaling cascades, cellular energy supply as component of adenosine triphosphate (ATP), and they are essential for lipoprotein, phospholipid and cellular membrane formation.¹⁻³

The involvement of these highly oxidized P-containing species in such very important biochemical processes in animals and plants led to intensive studies on their metabolic fate. Hence, the metabolism of phosphates and phosphate esters in nature is very well understood nowadays. However, these highly oxidized compounds, where P is in the oxidation state +V are not the only known phosphorus-containing species. The possible oxidation states of phosphorus range from +V to -III. Among all existing lower oxidized P-containing species, organophosphorus compounds play an outstanding role.⁴

1.2 Organophosphorus compounds

1.2.1 Overview

Phosphonates (+III) and phosphinates (+I) belong to the group of organophosphonates (P-C compounds), containing either one or two direct, covalent phosphorus carbon bonds (figure 1). In the early 1940s, the first organophosphonate, aminomethylphosphonic acid, was synthesized and patented by Pikl *et al.*⁵ After the production of several amino-substituted

phosphonic acids it was concluded that they are very stable and can maybe also found in nature.

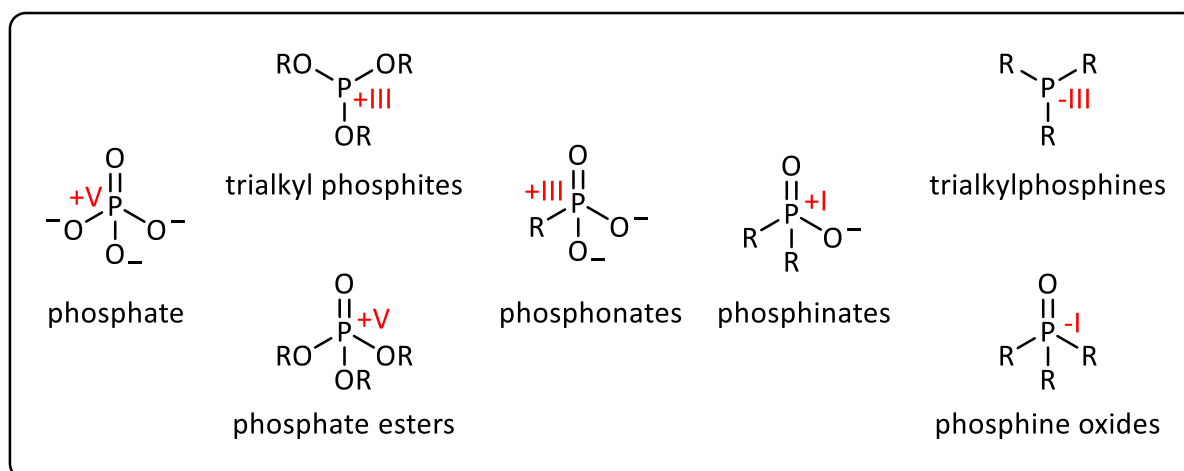


Figure 1: A structural comparison of known oxyphosphorus and carbophosphorus compounds with the oxidation state of phosphorus denoted in red.

Phosphonates and phosphinates are nearly isosteric to phosphate esters but are more stable under harsh thermolytic or hydrolytic conditions and are even stable against the enzymatic activity of phosphatases. Due to these (bio-)chemical and structural properties, the behavior of those compounds inside living systems is of high interest.^{4,6,7} It is believed that phosphonates have been the predominant phosphorus species in the oxygen poor atmosphere on the primitive Earth and hence in early life forms due to the higher energy of the phosphorus-carbon than phosphorus-oxygen bond.⁸

1.2.2 Phosphonates in nature

For a long time, phosphonates were still only known as purely synthetic compounds. It took fifteen more years until 2-aminoethylphosphonic acid (2-AEP, **1**, figure 2) was isolated from sheep rumen protozoa in 1959 and thus became the first known biogenic phosphonate. It is also the most frequently found phosphonate in nature and an integral component of cell membrane phosphonoglycolipids in several eukaryotes.^{4,9} From that discovery onwards, the number of known natural phosphonic acids slowly, but steadily increased and so did the knowledge about their possible applications.

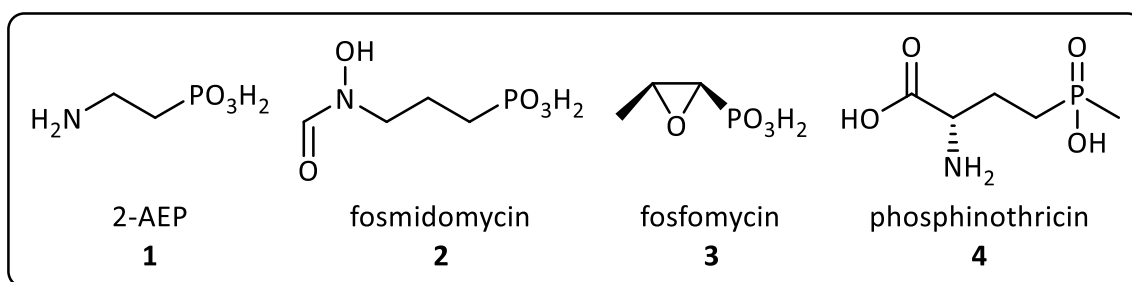
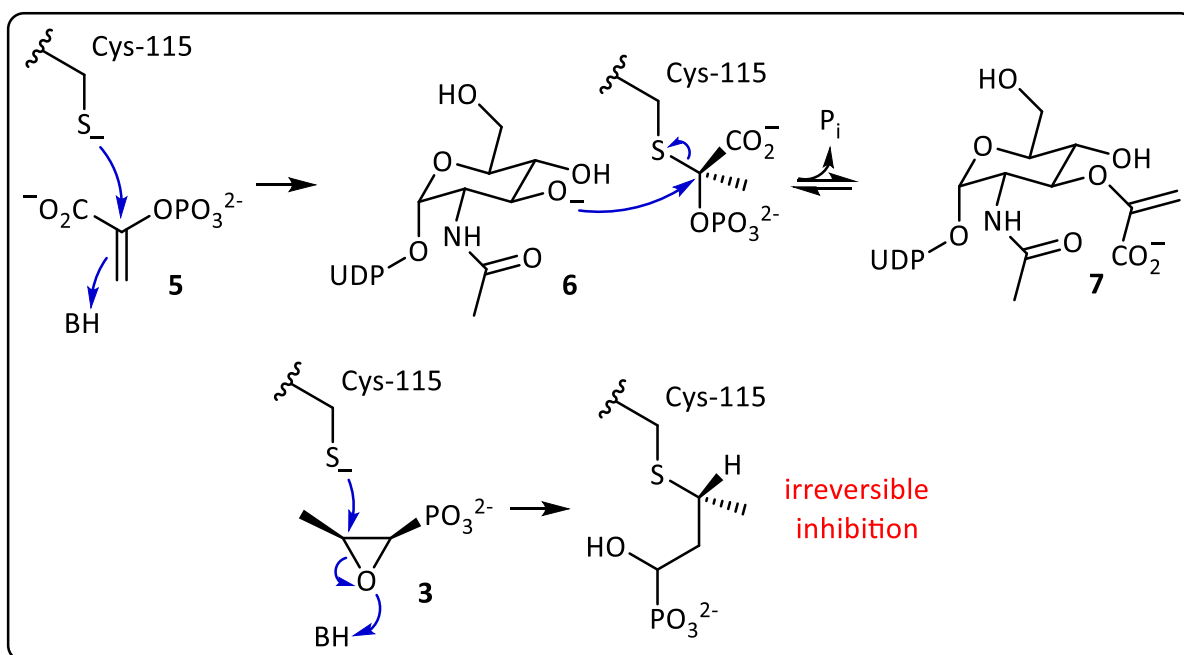


Figure 2: Some important biogenic phosphonates and phosphinates.

Amongst the most important biogenic phosphonates, we find compounds such as fosmidomycin (**2**), which is produced by *Streptomyces*. It blocks a key enzyme of the nonmevalonate isoprenoid biosynthesis pathway of *Plasmodium falciparum*, the pathogen causing Malaria. It was found that in combination with clindamycin its anti-malarial activity is even increased. At the moment, prodrug derivatives of fosmidomycin (**2**) are developed and tested for the treatment of tuberculosis.¹⁰⁻¹²

Another example, fosfomicin (**3**), was first isolated from *Streptomyces* spp. in 1969 and is one of the most used biogenic phosphonates nowadays due to its high antimicrobial activity. Its unique structure, combining an epoxide ring and a phosphonic acid, prevents cross-resistances with other classes of antimicrobial agents. It is active against many gram-positive and gram-negative bacteria, including some multidrug-resistant microorganism, by blocking the first step of bacterial cell wall peptidoglycan biosynthesis performed by the essential enzyme UDP-*N*-acetylglucosamine enolpyruvyl transferase (MurA). Normally, this enzyme couples phosphoenolpyruvate (PEP, **5**) to the 3'-hydroxyl group of UDP-*N*-acetylglucosamine (UNAG, **6**, scheme 1). However, in the presence of **3**, the latter binds irreversibly to the Cys-115, in the active site of MurA. Unfortunately, there are also some bacterial strains with known resistances to **3** like diverse *Chlamydia* species or *Mycobacterium tuberculosis*.¹³⁻¹⁶



Scheme 1: In the first row the natural action of MurA is shown; in the second row, inhibition of MurA by fosfomycin (3) is illustrated.

Phosphinothricin (4) was discovered in 1972 and is now used in agriculture. It is the active component of many commercially available herbicides. This phosphinic acid is produced by different *Streptomyces* strains and acts as irreversible inhibitor for glutamine synthetase, which is an essential enzyme for nitrogen assimilation in all plants. Two of the main advantages of this compound over other herbicides are the good ecological compatibility and low mammalian toxicity.^{17,18}

1.3 Industrial importance of synthetic phosphonates

1.3.1 Phosphonates as enzyme inhibitors

As already discussed, biogenic phosphonic acids have a wide area of application, reaching from herbicidal to anti-malaria and antibacterial activities. The commercialization rate of natural phosphonates is about 15%, which is many times higher than the average of 0.1% for natural products in general.^{19,20} This led to the development of a variety of synthetic phosphonate-based drug that were structurally similar to these natural compounds. Among the already used synthetic phosphonates we find antiviral compounds such as adefovir (9, figure 3), herbicides, as glyphosate (7) or anti-osteoporosis drugs such as the bisphosphonate zoledronate (8). They all act as very selective, mechanism-based enzyme inhibitors.²¹

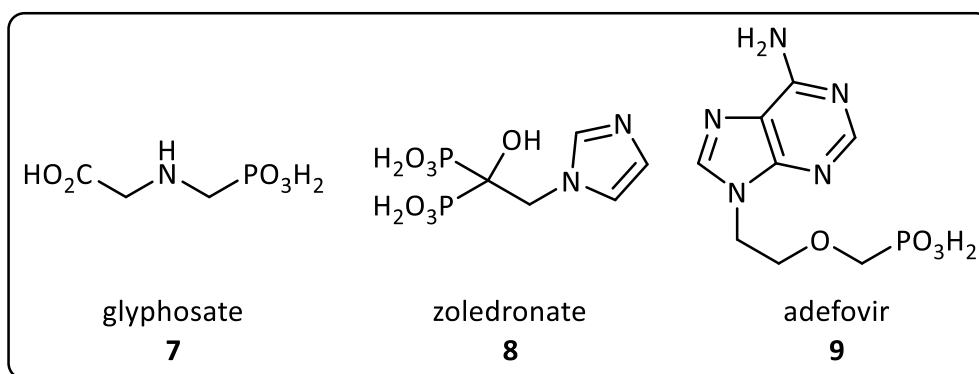


Figure 3: Some important synthetic phosphonates.

Overall, enzyme inhibitors can be divided into reversible and irreversible inhibitors. The latter are of higher interest for medicinal applications. Furthermore, this second group can be subdivided into first- and second-generation inhibitors. The former are structural analogues to the natural enzyme substrates, bearing a reactive group, and thus having a high binding specificity. These substances trigger covalent modifications of the enzyme to be blocked through reactions with nearby amino acid residues. Inhibitors of the second generation bear a latent reactive group. The enzyme mistakes these compounds for its natural substrate or, in some cases the transition state of the enzyme. This leads to an irreversible inhibition of the enzyme or the release of a toxic product. A binding equilibrium on the side of the substrate-enzyme complex is favorable for a good mechanism based enzyme inhibitor, as is a transformation process with first order kinetics.²²

Phosphonates are almost isosteric to phosphate esters and carboxylates, as already mentioned, which makes them good antimetabolites for these compound classes. However, even more intriguingly, phosphonates almost perfectly mimic the tetrahedral transition state of ester/amide hydrolysis and formation reactions (figure 4). Since the transition state is unique for an enzyme and always much more tightly bound than its substrates, molecules that mimic transition states are particularly good, tightly bound inhibitors.^{23,24}

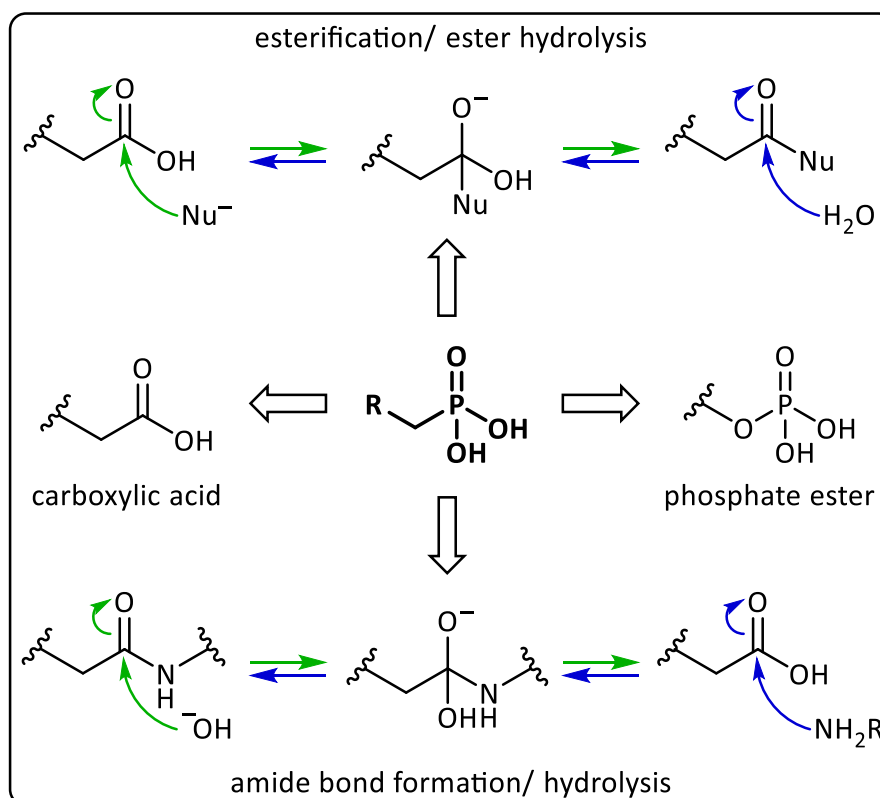
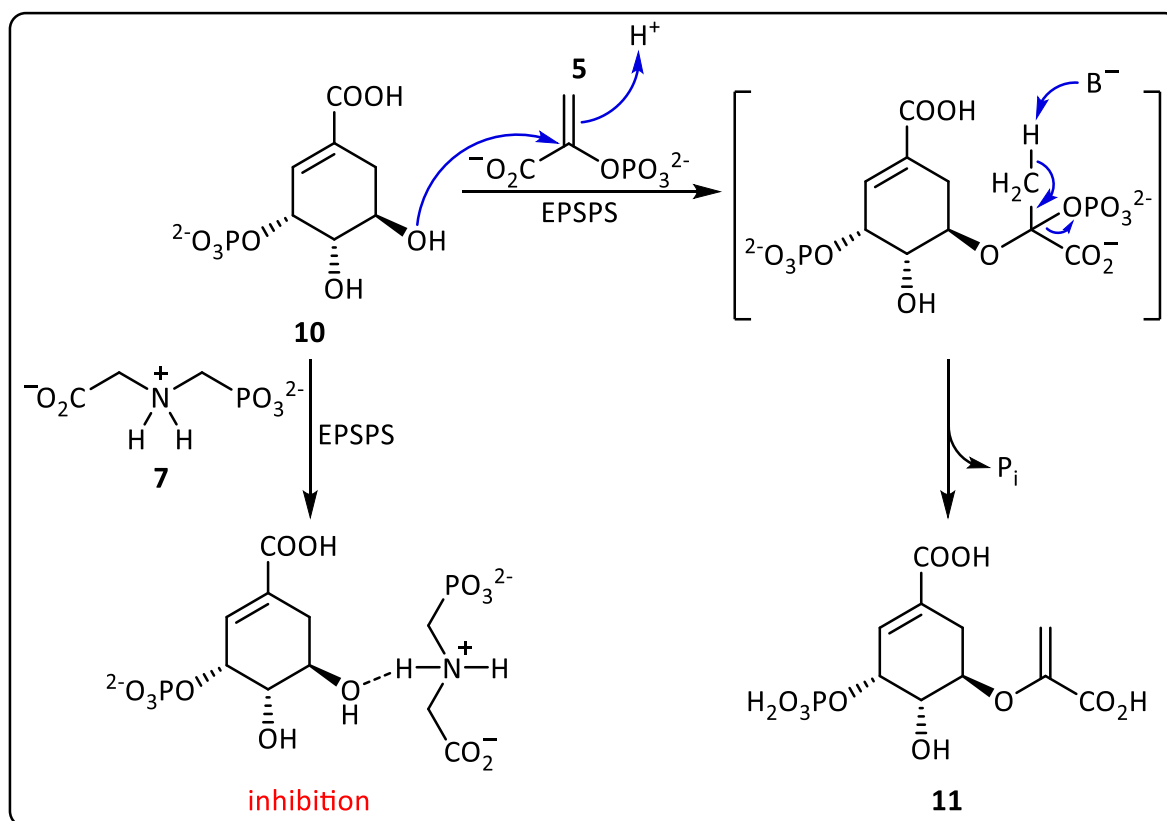


Figure 4: The structural similarities of phosphonates and common enzymatic transition states qualifying them as good enzyme inhibitors.

1.3.2 Phosphonates as herbicides

One of the most widely used and probably most critically discussed phosphonic acid that is acting as a mechanism-based enzyme inhibitor is glyphosate (**7**). It was already developed in 1950, but only 20 years later it was commercialized by Monsanto under the trademark name Roundup®. Glyphosate is acting as a mechanism-based enzyme inhibitor. It effectively blocks the enzyme 5-enolpyruvylshikimate-3-phosphate synthase (EPSPS) in plants, bacteria and fungi. This enzyme performs the enolpyruvyl transfer from phosphoenolpyruvate (PEP, **5**, scheme 2) to shikimate-3-phosphate (S3P, **10**) to produce 5-enolpyruvyl shikimate-3-phosphate (EPSP, **11**), which is a key step in the synthesis of aromatic amino acids in plants.^{25,26} For inhibition of the enzyme the normal binary EPSPS-S3P complex is formed first followed by attack of glyphosate to give a ternary complex of EPSPS-S3P-Glyphosate, thus **7** competes with **5**.²⁷



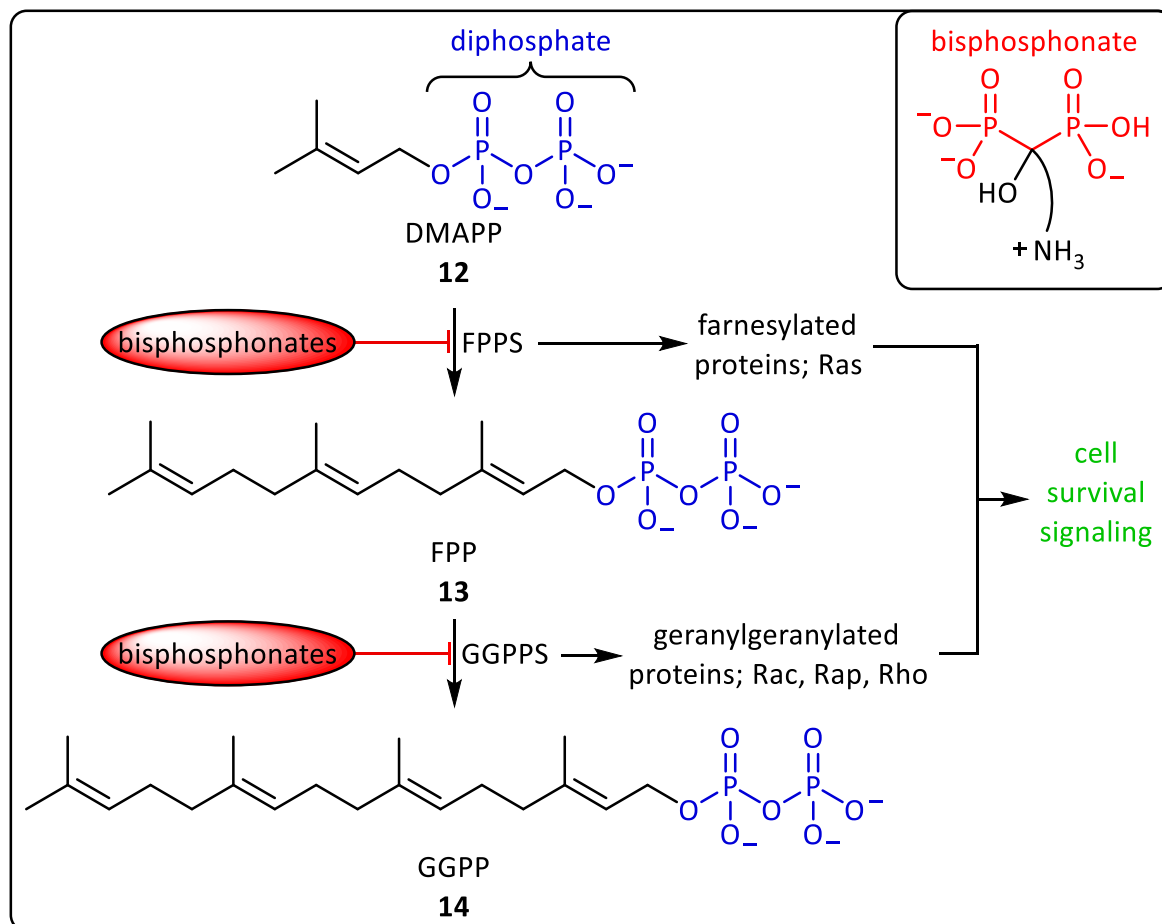
Scheme 2: Comparison of enolpyruvate transfer from PEP (5) to S3P (10) by EPSPS and inhibition of EPSPS by glyphosate (7).

1.3.3 Bisphosphonates in medicine

Medicinal applications for phosphonate-based enzyme inhibitors are also known. Geminal bisphosphonates are approved for the treatment of several bone diseases associated with excessive bone resorption, such as osteoporosis or Paget's disease.^{28,29} This class of compounds has two direct P-C bonds to the same carbon. They are analogs of diphosphate (scheme 3), hence most of these compounds block the formation and aggregation of calcium phosphate crystals, and thus slow down bone matter dissolution. They either bind in a bi- or tri-dental fashion through the two phosphonates and, if present, a hydroxyl group to bone mineral surfaces. Nowadays, tridental bisphosphonates are mainly used due to their higher affinity. The most used bisphosphonates have an additional, protonated, very basic amino group on the carbon side-chain, which is important for some targets.^{30,31}

Those adsorbed bisphosphonates act by inhibiting farnesyl diphosphate synthase (FPPS) and geranylgeranyl diphosphate synthase (GGPPS), which are both key enzymes of the mevalonate pathway (scheme 3) and are essential for lipid biosynthesis. Furthermore, farnesyl diphosphate (FPP, 13) and geranylgeranyl diphosphate (GGPP, 14) are responsible for

posttranslational modifications of small GTPases (e.g. Roh and Rac), which are involved in cell signaling pathways. They block protein prenylation, which leads to osteoclast inactivity and induction of apoptosis.^{25,31}

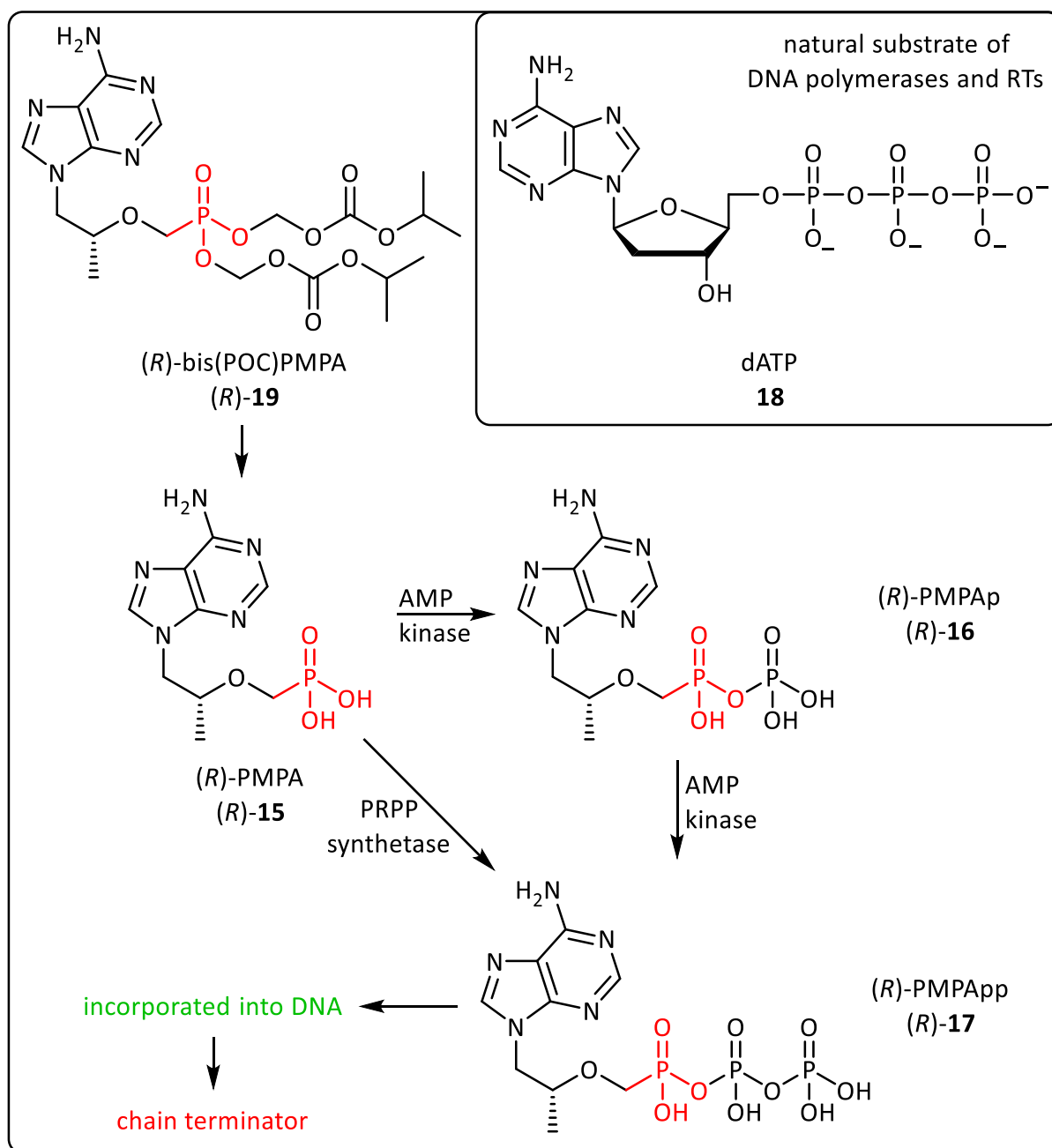


Scheme 3: GGPP biosynthesis pathway and possible target enzymes for inhibition by bisphosphonates.

1.3.4 Antiviral phosphonates

Another group of phosphonates, namely phosphonate-based nucleotide analogues to adenosine, shows great activity against DNA viruses and retroviruses. One famous example is (*R*)-9-(2-Phosphonomethoxypropyl)adenine [(*R*)-PMPA, (*R*)-15] or also called tenofovir, which acts as antiviral and antiretroviral agent by inhibiting viral DNA polymerases and reverse transcriptases (RT). Thus, this compound is active against both the hepatitis B virus and the human immunodeficiency virus (HIV). (*R*)-15 is diphosphorylated either in one step by phosphoribosyl pyrophosphate (PRPP) synthetase or in two consecutive steps by adenosine monophosphate (AMP) kinase to give the active form PMPApp [(*R*)-17] (scheme 4). This

molecule competes with the natural substrate deoxyadenosine triphosphate (dATP, **18**) for DNA incorporation. Once it is incorporated DNA replication is stopped.^{32,33}



Scheme 4: Inhibition mechanism of (R)-15.

In 1997 several analogs of tenofovir were tested, due to its low oral bioavailability and resulting necessary high dosage. One of the tested compounds, tenofovir disoproxil fumarate (TDF), [(R)-bis(POC)PMPA, (R)-19] (scheme 4) showed a comparable selectivity and better bioavailability. Even more intriguingly, it showed a 100-fold higher inhibitory activity compared to the parent compound. However, the cytotoxicity increased proportionally,

indicating a higher intracellular accumulation of PMPApp [(R)-**17**], which is the active as well as the cytotoxic form of this compound.³² In 2001, TDF was approved for the treatment of HIV and in 2008 for the treatment of hepatitis B under the trademark-name Viread®.^{34,35}

1.3.5 α -Aminophosphonic acids

Concerning the high potential of phosphonate-based drugs in the medicinal area, a specific compound class is particularly outstanding and needs further investigation, namely α -aminophosphonic acids. Those are analogs to α -aminocarboxylic acids in which the carboxylate is replaced by a phosphonic acid moiety (figure 5).

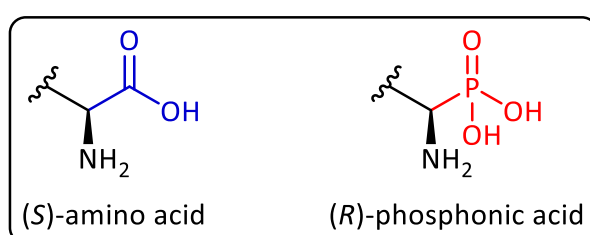
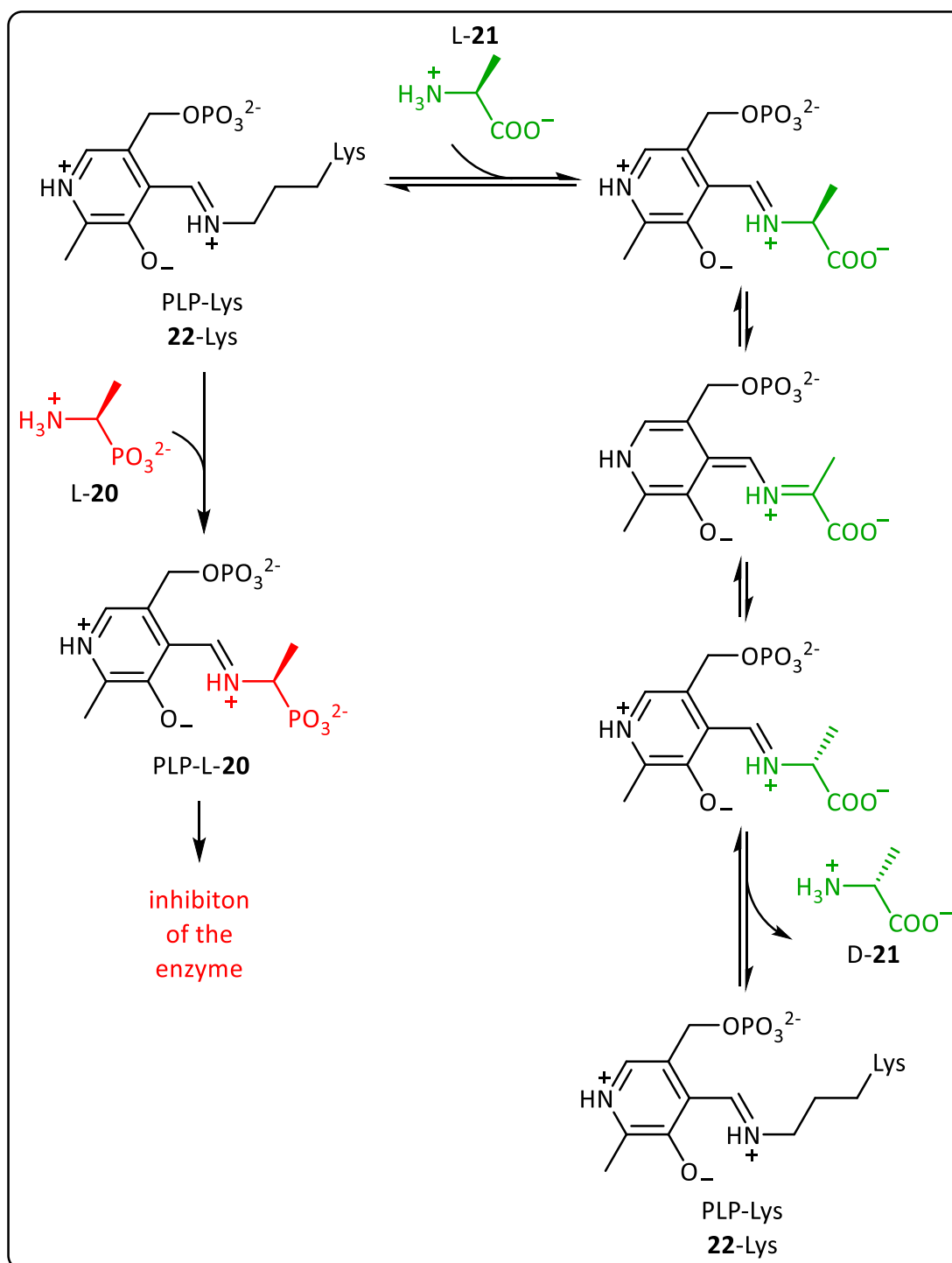


Figure 5: General structure of α -aminocarboxylic acid compared to the general structure of α -aminophosphonic acid.

Although phosphonic acids differ from carboxylic acids in terms of acidity (much more acidic), shape (tetrahedral instead of planar) and steric volume (larger atomic radius of phosphorus compared to carbon), α -aminophosphonic acids are often mistaken as substrates by enzymes or receptors. They effectively mimic the transition state of a large variety of hydrolases following the principle discussed in [chapter 1.3.1](#). Therefore, they can act as highly potent antimetabolites to their respective α -aminocarboxylic acids natural substrates and effectively compete with the corresponding carboxylic acids for binding sites.^{36–38}

One prominent example of an α -aminophosphonic acids which can be used to effectively mimic its carboxylic acid analogues is L-phosphaalanine (L-**20**), which is also known as the antibacterial drug alafosfalin. It inhibits L-alanine racemase, the responsible enzyme for the isomerization from L to D-alanine (L/D-**21**). This pyridoxal 5'-phosphate (PLP, **22**) dependent enzyme (scheme 5) is essential for the production of D-**21**, a component of the peptidoglycan layer of cell walls in gram-negative and gram-positive bacteria. Since L-alanine racemase is unique to bacteria, substances which are able to block this enzyme can be used as antibiotic agents that effectively fight pathogens and have low side effects for the host organism.³⁸



Scheme 5: Comparison of natural mechanism of alanine racemase with alanine (**21**) and the inhibitor phosphoalanine (**20**).

The enzyme is inhibited through binding of the α -aminophosphonic acid to the enzyme on the cofactor and the formation of an external aldimine. Instead of the usually very efficiently hydrolyzed cofactor, PLP-L-**20** binds strongly and tightly to the enzyme active site. Additional interactions of the oxygen atoms of the phosphonate moiety with residues of the active site irreversibly inhibit the enzyme.³⁹

Other example for a clinically used α -aminophosphonates include incadronate, a bisphosphonate, which is used against osteoporosis and the biogenic compound dehydrophos (**28**), an antibacterial substance, which is produced by *Streptomyces luridus* and was discovered in 1984.³⁸

The research in this field is currently still ongoing and compounds belonging to this structural class have a high potential for future applications as effective enzyme inhibitors. For example thizole[5,4-*b*]-pyridine containing α -aminophosphonates are currently tested as antitumor agents⁴⁰, substituted analogues of phosphaphenylglycine should act as inhibitors of phenylalanine ammonia lyase (PAL)⁴¹ and chromone-containing α -aminophosphonates are tested as anti-Alzheimer agents.⁴²

1.4 Environmental impact

Besides the medicinal importance of synthetic and biogenic phosphonates, the metabolic pathways leading to the formation and degradation of phosphonates are also of high environmental importance, although until recently they were thought to be of limited ecological relevance. However, they are especially important in marine ecosystems where phosphorus is the ultimate limiting macronutrient. Compared to other essential nutrients like nitrogen or carbon, inorganic phosphate has a slow cycling and solubility at neutral pH values and ambient temperature and pressure.^{43,44} While dissolved inorganic phosphate (DIP) is still the most readily available form of phosphorus for microbes, the low available amount of DIP in the upper ocean spheres, especially in some regions such as the North Pacific ocean and Subtropical Gyre drastically limits its use. In such regions, dissolved organic phosphorus (DOP) species constitute up to 80 % of the total bioavailable phosphorus, mainly consisting of phosphorus esters and phosphonates in an approximate ratio of 3:1.⁴⁵ Therefore phosphonates, play an important role as phosphorus source. Nowadays we know that about 10% of bacterial genomes encode putative pathways of phosphonate biosynthesis and 40% contain at least one pathway of phosphonate catabolism.⁴⁶ Among marine microorganism, about 10% were found to encode genes for phosphonic acids metabolism.⁴⁷

Thus, both natural and synthetic phosphonates are used as a source of phosphorus by diverse microorganisms, especially in these DIP-poor ecosystems.

Therefore, the degradation and formation of these compounds is of high environmental importance and needs to be studied intensively, especially concerning their huge environmental impact on the global phosphorus and carbon cycles, which only starts to become uncovered.

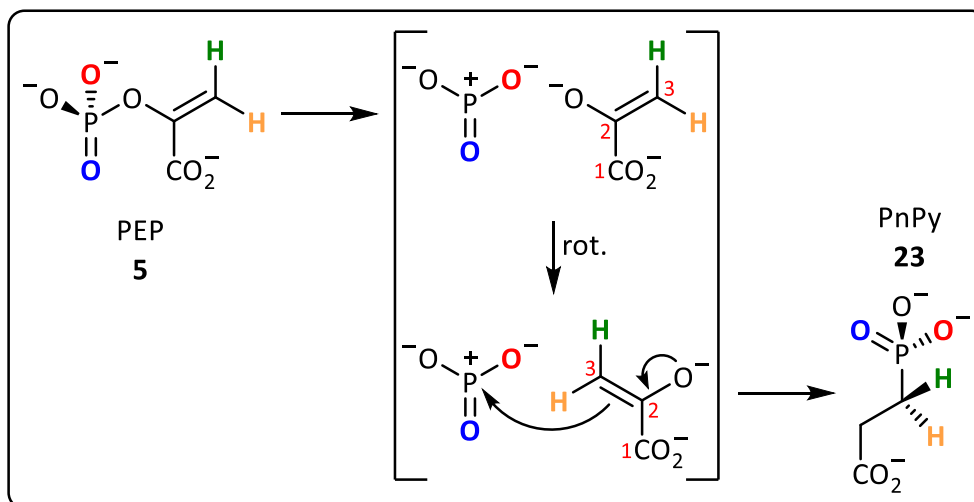
A very prominent example for the ecological impact of phosphonate degradation is its involvement in global warming: For a long time, all known biogenic pathways for the formation of methane were assigned to archaea living under strictly anaerobic conditions. Still researchers observed a CH₄-supersaturation of oxygen rich upper ocean zones. This phenomenon was called methane-paradox. In 2010 this paradox could finally be solved: it was found that the degradation of methylphosphonic acid (MePn, **27**) by the C-P lyase enzyme complex (for mechanism see [chapter 1.6.3](#)) can produce methane and inorganic phosphate in oxygen rich ocean surface waters, which causes a net flow of CH₄ to the atmosphere. However, this was not believed to have a high impact on our climate, even though methane is a potent greenhouse gas, as there was no biogenic source of MePn known that could produce significant amounts of this compound. Some time after, it was found that *Nitrosopumilus maritimus*, belonging to one of the most abundant groups of microorganisms in the oceans is able to synthesize MePn, thus making this degradation a process of high environmental impact.^{48–50}

This phenomenon was recently also observed in freshwater ecosystems, which account for at least 11% of natural global methane emission per year by this mechanism. It is believed that planktonic cyanobacteria e.g. *Synechococcus* are able to produce MePn (**27**) and bacterioplankton in the subsurface water of the lake is able to cleave it to P_i and methane causing the emission. On the contrary, under strictly anaerobic conditions in deep lakes anoxic sediments and lake hypolimnia produce methane. However, due to methane-oxidizing bacteria (MOB), CH₄ is normally oxidized to CO₂ and can thus not reach the surface.⁵¹

1.5 Overview of phosphonate biosynthetic pathways

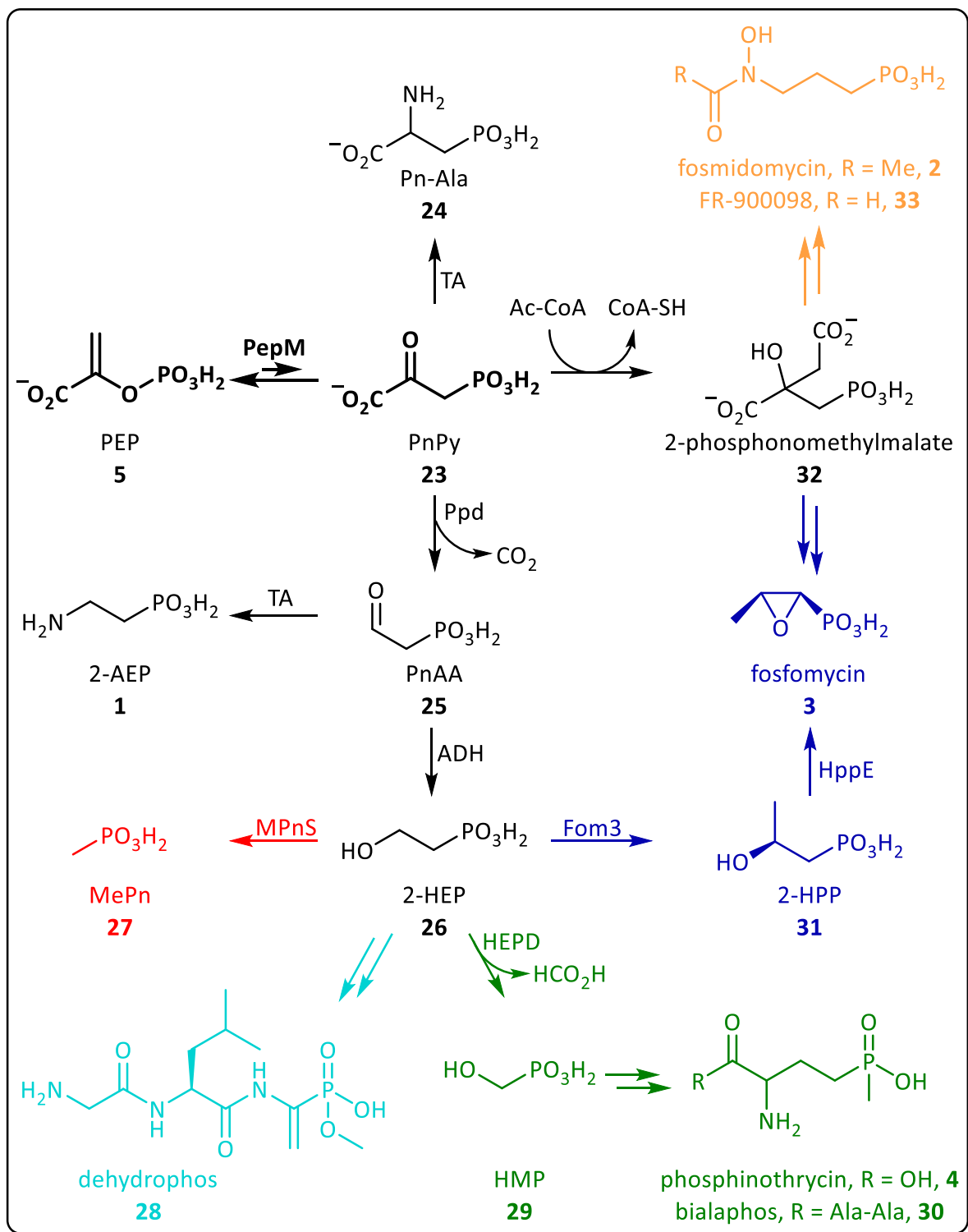
The biosynthesis of almost all phosphonates starts with the transformation of phosphoenolpyruvate (PEP, **5**) to phosphonopyruvic acid (PnPy, **23**) and is catalyzed by the enzyme phosphoenolpyruvate phosphomutase (PepM). Through a retention of stereochemistry at phosphorus, this reaction is believed to go through a dissociative

mechanism with a metaphosphate (mP_i) intermediate (scheme 6). Active side changes would hold the intermediate in position and after rotation of pyruvate, C-3 is able to attack the mP_i .^{4,6,52}



Scheme 6: Proposed dissociative mechanism for PEP mutase with retention of stereochemistry at phosphorus.

Although the equilibrium of this transformation lies 500-fold on the side of PEP, the reaction occurs, because the produced phosphonate is immediately and irreversibly converted. In most cases phosphonoacetaldehyde (PnAA, **25**) is formed by decarboxylation thus shifting the equilibrium of the first reaction (scheme 7).^{4,6,52}



Scheme 7: An overview of phosphonate biosynthetic routes; frequently occurring reactions are shown in black, unique pathways (as to our current knowledge) are highlighted in other colors.

PnAA (**25**), generated by the most common biosynthetic pathway for phosphonate biosynthesis can then be converted to 2-AEP (**1**), by transaminase (TA). Alternatively, it can be

reduced by an alcohol dehydrogenase (ADH) to 2-hydroxyethyl phosphonate (2-HEP, **26**), a very common intermediate in the biosynthesis of a variety of known phosphonates.^{53,54}

Methylphosphonic acid (MePn, **27**) is for example derived from this precursor by action of methylphosphonate synthase and so is dehydrophos (**28**), the only known esterified phosphonate of natural origin, which is used as antibiotic agent.⁵⁵

Hydroxymethylphosphonate (HMP, **29**) is produced from 2-HEP by action of hydroxyethylphosphate dioxygenase (HEPD), a set of very unique reactions can then either lead to the formation of phosphinothrycin (**4**) or the tripeptidic antibiotic bialaphos (**30**).

Alternatively, the enzyme Fom3 catalyzes the formation of 2-hydroxypropylphosphonate (2-HPP, **31**) from 2-HEP which is further converted to fosfomycin (**3**) by 2-hydroxypropylphosphonate epoxidase (HppE).^{6,50}

However, there are also two other options for the necessary irreversible, second reaction after the transformation of PEP to PnPy. One of them is performed by a transaminase (TA), which converts PnPy (**23**) to phosphonoalanine (Pn-Ala, **24**). Another possibility is that an acetate anion from Ac-CoA attacks the carbonyl-C of PnPy (**23**) to give 2-phosphonomethylmalate (**32**), which is the biogenic precursor for fosmidomycin (**2**) and the structurally related compound FR-900098 (**33**).^{6,53}

1.6 Biodegradation pathways of phosphonates

1.6.1 Phosphonate metabolism

The high environmental importance of phosphonates as phosphorus source for microorganisms has not only led to an increased scientific interest in the biochemical processes involved in their formation, but also in their degradation. In the last decades the catabolism of phosphonates of medical and industrial importance have been studied preferentially and are thus best understood today. So far, most studies have focused on the metabolism of the most abundant phosphonates. They are often called the fundamental eight Pn (figure 6).⁴⁶

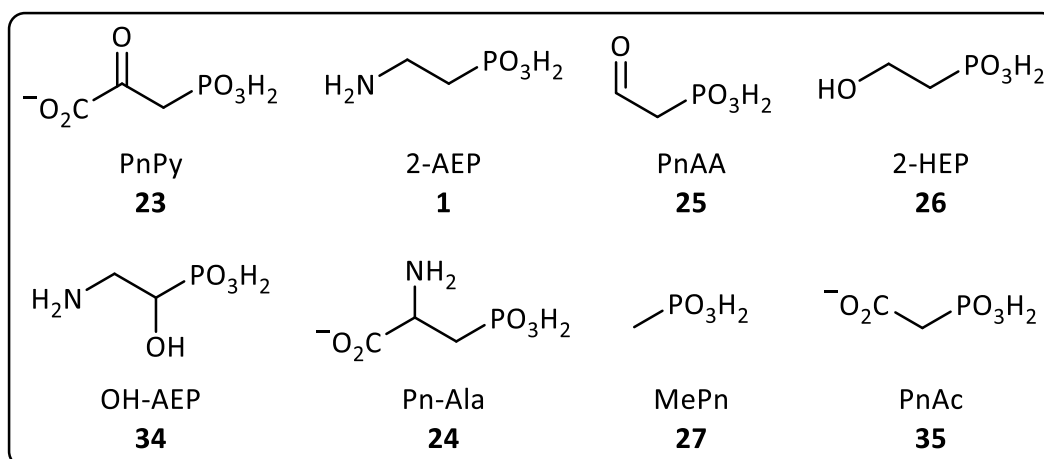


Figure 6: The fundamental eight Pn - common intermediates in Pn biosynthesis and degradation.

A complete understanding of mechanisms leading to phosphonate degradation is also of great interest, due to their favorable drug-like properties. This also fuels the interest in mechanistic details of their degradation with a focus on possible resistance mechanisms. Knowledge in this area will certainly help to develop new synthetic phosphonates in the future and improve the structural features of already known drugs. Although, the knowledge about phosphonates and their mineralization drastically increased within the last few years, there are still many pending questions.⁵²

Microorganisms have developed several different pathways to use phosphonates as alternative phosphorus source. Today, three general degradation pathways are known: the radical (C-P-lyase), the hydrolytic (β -electron-sink) and the oxidative P-C bond cleavage mechanism.²¹ However, there are certainly more pathways to be discovered. In most cases, phosphonate catabolism is dependent on the so-called *pho*-regulon and thus limited to phosphate starvation conditions. Nevertheless, some degradation pathways are independent of the surrounding phosphate concentration.

1.6.2 The *pho*-regulon

Most of the time, the extracellular concentration of phosphate is crucial for the phosphonate degradation rate. It has been best studied in *Escherichia coli* where it consists of more than 30 genes which are divided into eight transcriptional units.⁴ The *pho*-regulon upregulates phosphonate degradation in case of low environmental phosphate levels and downregulates it at high surrounding P_i levels.

An inner membrane histidine kinase and a cytoplasmic transcriptional response regulator are the two-component system, which control the *pho*-regulon, in *E. coli* they are called PhoR and PhoB. The inorganic phosphate specific transporter (Pst) is responsible for the detection of external P_i concentration. It belongs to the family of ATP-binding cassette (ABC) transporters and consist of four subunits: PstS, PstC, PstA and PstB.⁵⁶ The periplasmic phosphate binding protein PstS has high affinity to phosphate and detects the extracellular phosphate concentration (figure 7). The inner membrane channel proteins PstA and PstC let P_i enter, depending on the outside phosphate level. PstB, an ATP-dependent permease component, contributes the energy required for P_i transport.⁵⁷

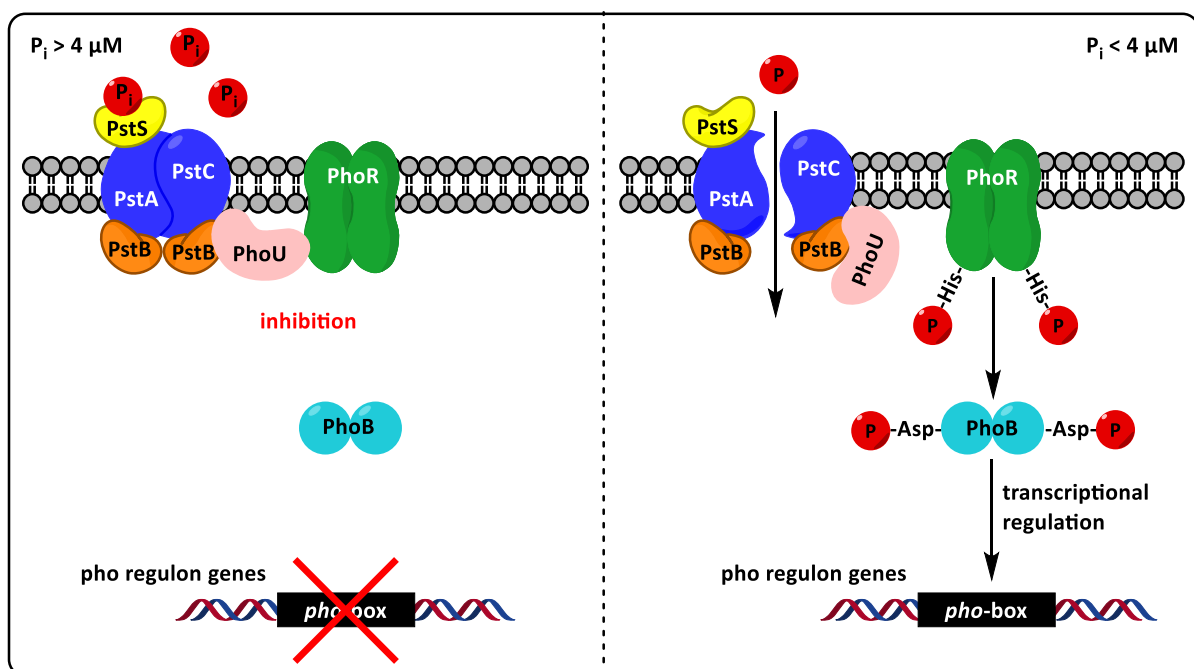


Figure 7: The response of bacteria to high and low surrounding P_i concentrations and the related regulation of phosphorus compound uptake.

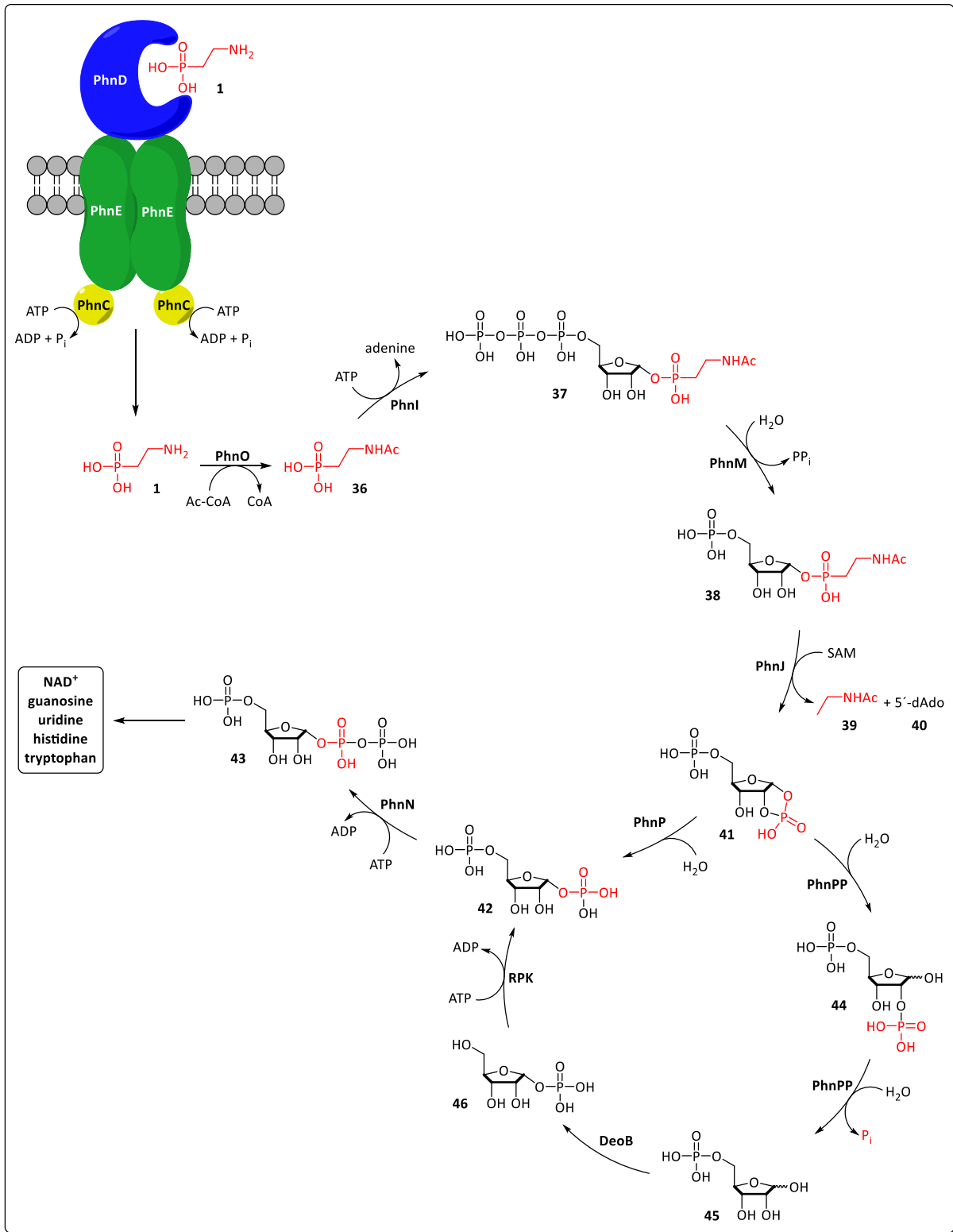
If the extracellular phosphate level drops below $4 \mu M$, PstS decouples from PstA and PstC, and a conformational change occurs, whereby inorganic phosphate and organophosphonates can enter the cell. A histidine group of PhoR autophosphorylates and then PhoR transfers the phosphoryl group to an aspartate group of PhoB. This activates Pho B, a DNA-binding protein, which is now able to bind to the Pho-box and activates the transcription of Pho-regulated genes. If PstS is saturated with P_i , PhoU inhibits PhoR and dephosphorylation of PhoB occur. Thus, the cleavage of phosphonate P-C bonds, which produces P_i automatically inhibits further

phosphonate uptake. P-C bond cleavage strategies that are dependent on the *pho*-regulon are thus limited to phosphate starvation conditions.^{56,58–60}

1.6.3 Radical (C-P-lyase) mechanism

One of the three known phosphonate degradation pathways is catalyzed by the so-called C-P-lyase complex, which was discovered in 1963. However, the very complex mechanism is still not fully elucidated.^{21,61–63}

The C-P-lyase pathway is encoded by a 14 gene cistron, namely *phnCDEFGHIJKLMN*OP. In *E. coli* the phosphonate transport system is encoded by *phnCDE*, *phnF* is a regulatory protein, the C-P-lyase activity itself is attributed to *phnGHIJKLM* and *phnNOP* are accessory catabolic enzymes. C-P-lyase is found in many types of bacteria in which all the genes *phnGHIJKLM* are found, but they may differ in their arrangement (scheme 8).^{64,65}



Scheme 8: An overview of the CP-Lyase pathway

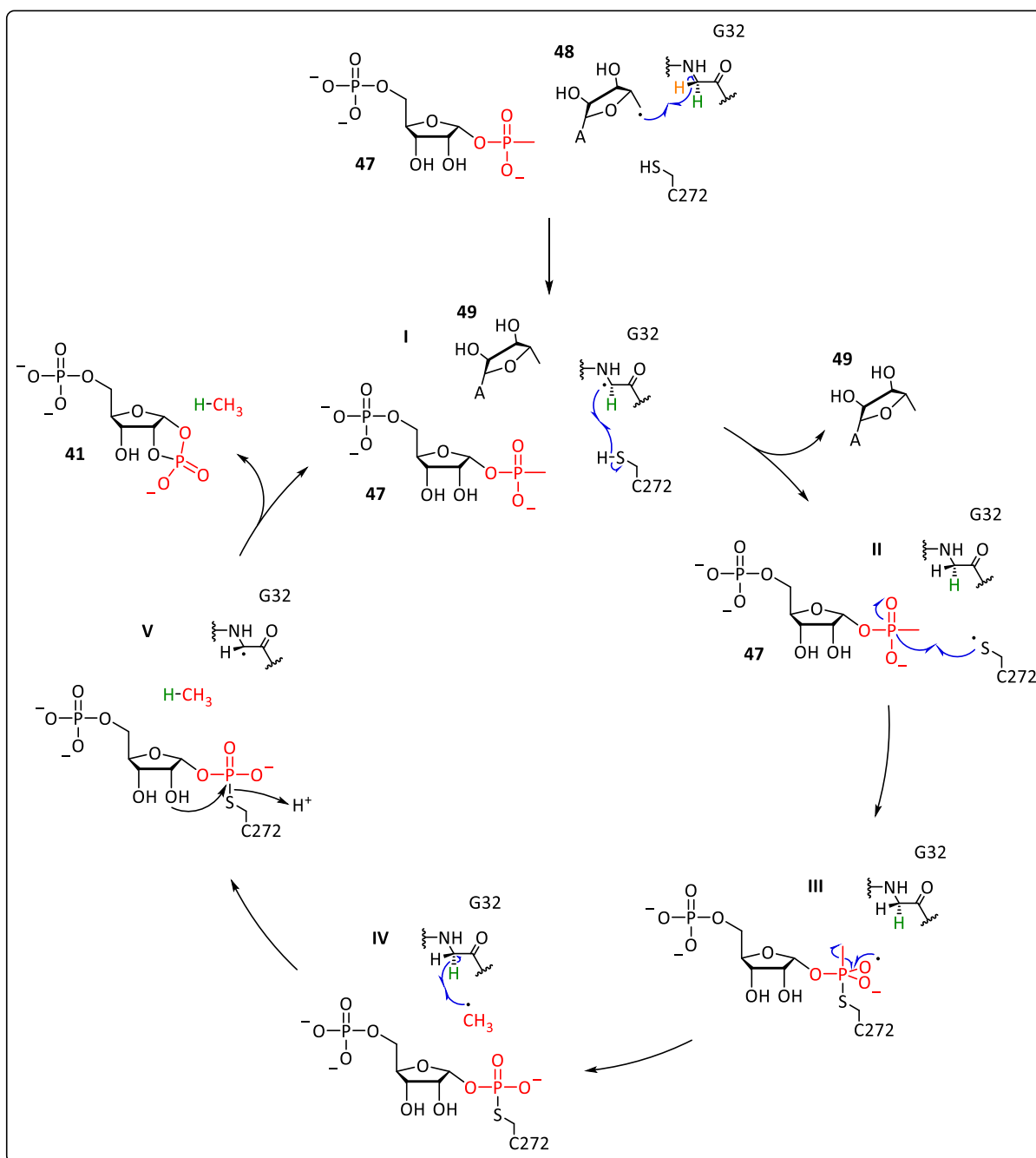
Phn D is a periplasmic binding protein to which the dianionic phosphonate binds very tightly at the end of the binding pocket. After cellular uptake by PhnCDE, an ABC-type phosphonate

transporter, phnO catalyzes a transfer of an acetyl group from Ac-CoA to the nitrogen of aminoalkylphosphonic acid, in case the substrate bears an NH₂-group.^{66,67}

A following ATP- and GTP-dependent hydrolyzation and ribosylation of intermediate **36** is catalyzed by PhnI to obtain 5-triphosphate- α -D-ribosyl phosphonate (**37**) and adenine. Raushel *et al.* could show, that the multi-protein complex PhnG₂H₂I₂KL₂ is necessary to catalyze a subsequent nucleophilic attack on the anomeric carbon of Mg-ATP by methylphosphonic acid (**27**) to get D-ribose-5-triphosphate and adenine, with PhnK being not essential for this process.⁶⁸ Its exact role has still not been elucidated.^{67,69}

The hydrolyzation of the α - β phosphoryl bond is performed by PhnM, a member of the amidohydrolase superfamily. The obtained α -phosphate is hydrolyzed to give 5-phospho- α -D-ribosyl alkylphosphonate **38**.

The actual C-P bond cleavage step is catalyzed by PhnJ to convert D-ribosyl alkylphosphonate **38** to α -D-ribosyl 1,2-cyclic phosphate **41**. Mechanistic studies using MePn (**27**) as substrate showed that all four cysteine residues of PhnJ are necessary for catalytic activity (scheme 9).^{66,70}



Scheme 9: C-P-lyase – a detailed look on the C-P bond cleavage step catalyzed by PhnI.

During this key step an 5'-deoxyadenosyl radical (**48**) is formed by electron donation from an [4Fe-4S]⁺ cluster to SAM. The pro-R hydrogen (yellow) of G32 is abstracted and the formation of 5'-deoxyadenosine (**49**) and an active site glycy radical can be observed (**I**). Afterwards this radical attacks the hydrogen of Cys-272 and a thiyl radical is formed (**II**) which then produces the phosphothioester intermediate (**IV**) by releasing a methyl radical (**II-IV**). Subsequently, the pro-S hydrogen (green) of Gly-32 reacts with this radical to form methane (**V**).^{66,70,71}

The next step is the PhnP-catalyzed regiospecific hydrolysis of **41** to give α -D-ribose-1,5-diphosphate (**42**).^{66,72,73}

The last step catalyzed by the C-P lyase complex is a regiospecific phosphorylation performed by PhnN. The phosphorus group of the former phosphonate is transferred to a diphosphate.^{67,74,75}

This pathway has a broad substrate specificity, accepting branched and substituted alkylphosphonic acids as well as aromatic compounds (figure 8). The products of the C-P lyase reaction are always inorganic phosphate and a hydrocarbon.

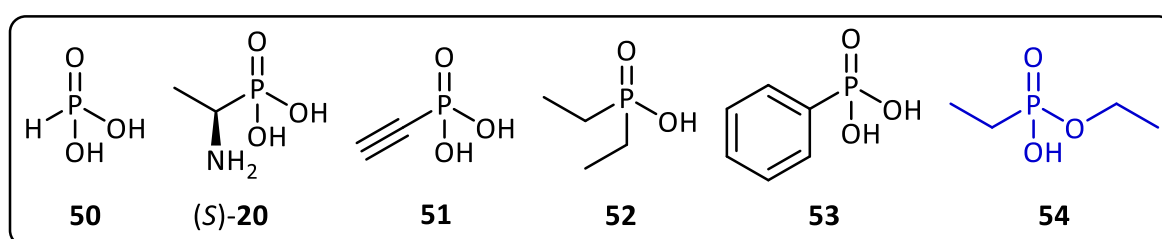
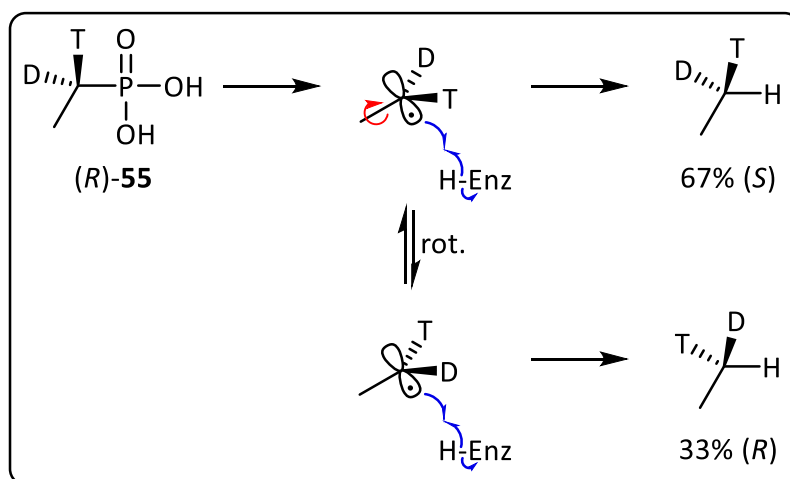


Figure 8: Substrates that can be processed (black) or cannot be processed (blue) by the C-P lyase complex.

As shown, C-P bonds can be cleaved independently from the hybridization state of the involved carbon atom. Phosphinates are equally processed by this enzyme complex. In some cases, the cleavage activity is depending on the stereochemistry of the substrate: while (S)-**20** is a phosphorus source for *E. coli*, its (R) enantiomer is not. Varying Pn-transport systems and specificities of C-P-lyase from different bacterial strains create a diverse, organism related substrate scope for this degradation pathway.⁶⁶

While many different alkylphosphonic acids are processed via this pathway, alkylphosphonate esters like **54** cannot be metabolized in any specie.^{66,76}

In experimental studies with isotopically labeled ethylphosphonic acid {1-[²H₁]-1-[³H]-(*R*)-**55**} 67% retention and 33% inversion of configuration at C-1 were observed (scheme 10). The mechanism thus probably involves a neutral ethyl radical at C1 that can be attacked from either side by an active-site hydrogen radical.⁶⁶

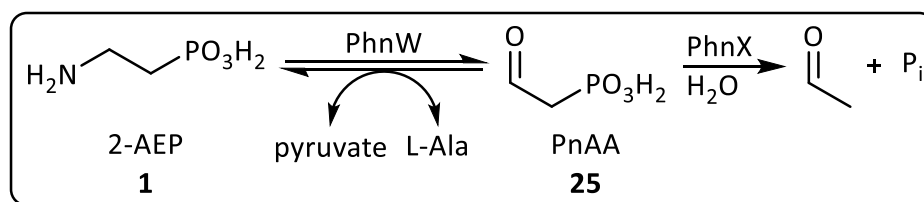


Scheme 10: Experimental proof of the stereochemical of the C-P lyase reaction.

1.6.4 Hydrolytic (β -electron-sink) mechanism

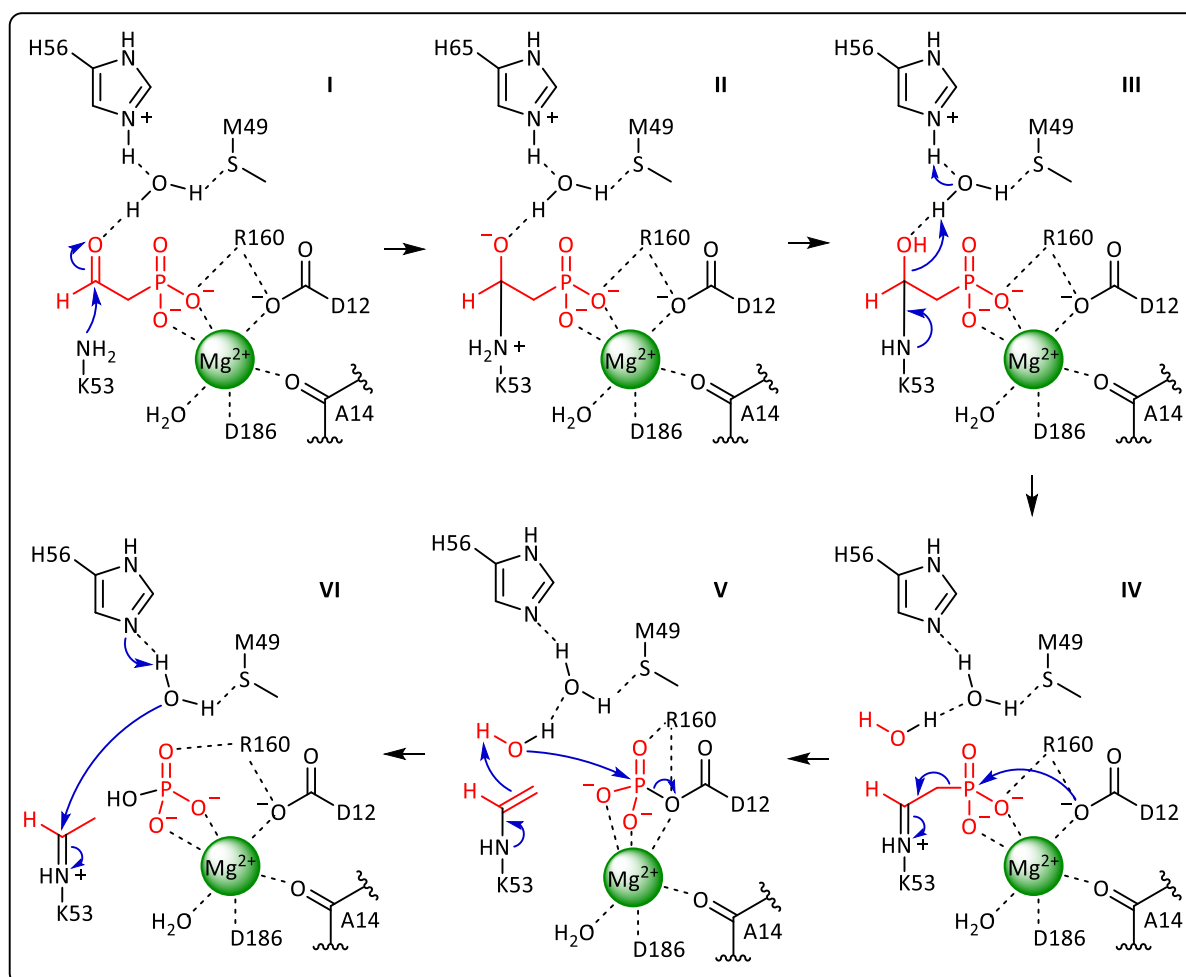
Another possibility for P-C bond cleavage is the co-called β -electron-sink pathway. In this case an electron withdrawing group in β -position to the phosphorus is necessary as the name already indicates. During attack of an active site nucleophile such as water at the phosphorus atom, a carbanionic species is formed, which is stabilized by delocalization either due to an adjacent carboxyl- or a carbonyl group. Currently three concrete enzymes which use this electron sink mechanism are known. They are called phosphonoacetaldehyde hydrolase (Phn X), phosphonopyruvate hydrolase (PPH) and phosphonoacetate hydrolase (Phn A).^{66,77}

Phosphonoacetaldehyde hydrolase, was first isolated from *Bacillus cereus* and described by La Nauze in 1970. He also found that the enzyme is dependent on Mg^{2+} . Furthermore, he investigated the inhibitory effect of ions such as SO_3^{2-} on this enzyme.⁷⁸ *Bacillus cereus* is able to use the natural phosphonate 2-AEP (**1**) as sole phosphorus source. Hence, the phosphonate degradation pathway is not under the control of the *pho*-regulon. In addition, synthetic PnAA (**25**) was also found to be converted, therefore, it was concluded to be an intermediate of this degradation mechanism. Later, Wanner discovered that the degradation of 2-AEP by this hydrolytic pathway is actually a two-step process catalyzed by PhnW and PhnX (scheme 11).^{66,79,80}



Scheme 11: Hydrolytic degradation pathway of 2-AEP (1) via PnAA.

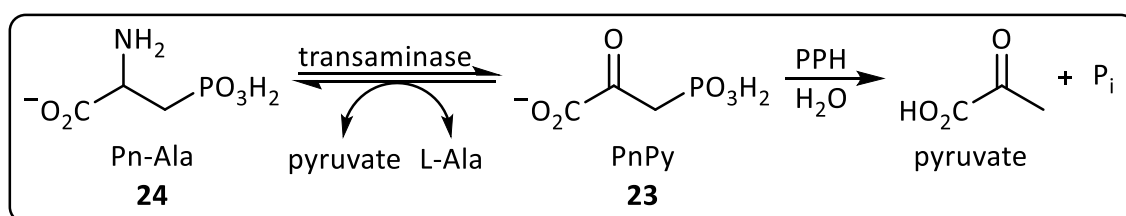
The former encodes a transaminase that converts **1** to **25** using pyruvate as amino group acceptor and forming alanine as side product. PhnX is the enzyme which performs the actual P-C bond cleavage step and belongs to the haloacid dehalogenase (HAD) superfamily of hydrolases.^{66,81} La Nauze found that PhnX forms a Schiff base-type intermediate (scheme 12) with a lysine side chain (**IV**). This positively charged Schiff base intermediate acts as the required electron sink for stabilization of the carbanion leaving group.



Scheme 12: Proposed mechanism of the reaction of PhnX with PnAA (25) as substrate.

The next step is a phosphoryl-transfer to D-12, a second active site nucleophile in PhnX, whereupon an enamine is formed (**V**). The cleavage of the intermediates from the enzyme is still not fully elucidated but the K53-enamine-intermediate presumably acts as a base. Subsequent deprotonation by H56 and hydrolyzation of K53-iminium-intermediate (**VI**) finally produces acetaldehyde.^{67,82,83}

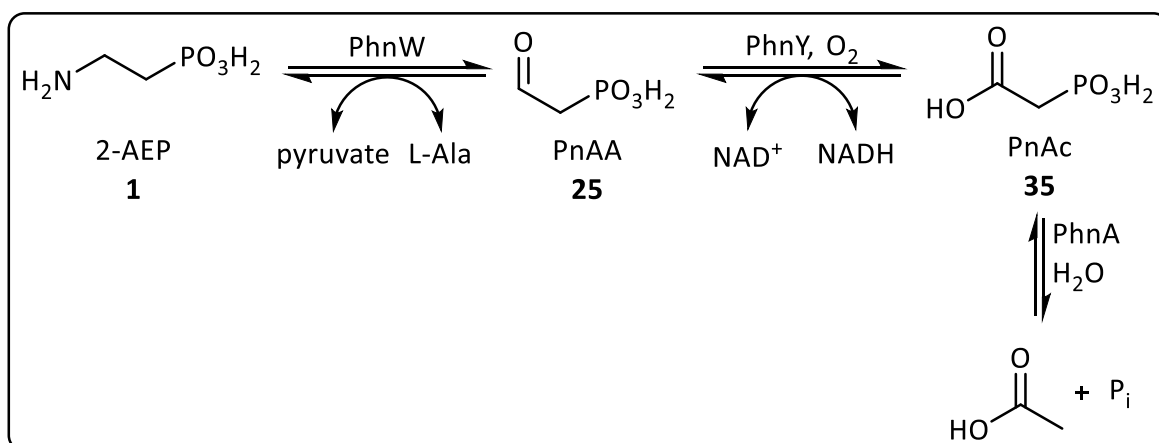
Phosphonopyruvate hydrolase (PPH), the second known enzyme responsible for hydrolytic P-C bond cleavage, was discovered by Quinn *et al.* and has first been described in *Burkholderia cepacia* Pal6 species. He found that this microorganism is able to use phosphonoalanine (**24**) as sole source for phosphorus, carbon, nitrogen and energy⁸⁴ by a two-step biodegradation pathway (scheme 13).



Scheme 13: Degradation pathway of Pn-Ala (**24**) by PPH.

First a transaminase converts phosphonoalanine (**24**), the only yet known substrate for this route, to phosphonopyruvate (**23**). Then the P-C bond cleavage is performed by PPH. For this very substrate specific mechanism, a metal ion is needed, the highest activities are found in the presence of Ni^{2+} , Co^{2+} or Mg^{2+} . The enzyme belongs to the phosphoenolpyruvate (PEP) mutase/isocitrate lyase superfamily and the amino acid sequence shows 40% similarity with PEP mutase.^{66,85,86}

The third known hydrolase belonging to this group is phosphonoacetate hydrolase, opening up another route for the degradation of 2-AEP (**1**). It was first identified and named by Quinn *et al.*⁸⁷ Nature certainly developed several degradation pathways for this phosphonic acid due to its natural abundance. After transamination by PhnW, the formed intermediate (PnAA, **25**) is oxidized by PhnY and finally the actual hydrolytic C-P bond cleavage step is catalyzed by PhnA to give acetate and P_i (scheme 14). PhnA is a metal ion (Mn^{2+} , Fe^{2+} or Zn^{2+}) dependent hydrolase which belongs to the alkaline phosphatase superfamily.^{77,88}



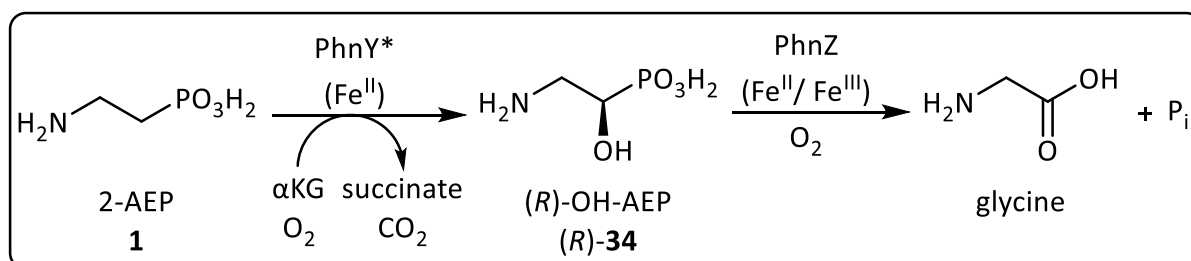
Scheme 14: Degradation pathway of 2-AEP (**1**) via PnAA (**25**) and PnAc (**35**).

For long time it was believed that phosphonoacetate (**35**) is a purely synthetic compound, until Quinn and McMullan discovered that *Pseudomonas fluorescens* sp. 23F is able to use this phosphonate as sole phosphorus and carbon source, followed by identification of a locus in *Sinorhizobium meliloti* sp. 1021, which encodes the catabolism of **1** to P_i by PhnW, PhnY and PhnA.⁸⁹

1.6.5 Oxidative P-C bond cleavage

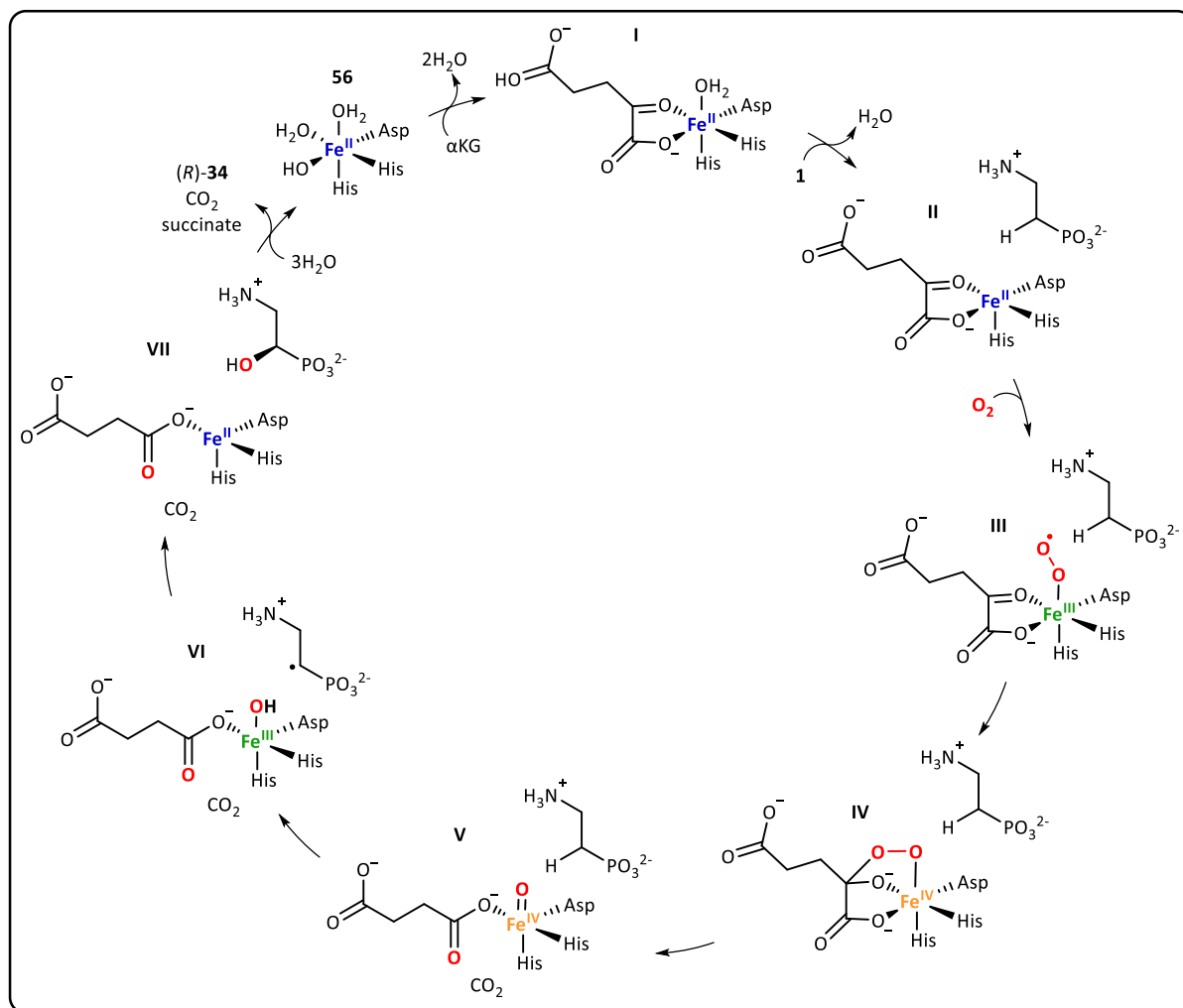
The third known mechanism for C-P bond cleavage is the oxidative pathway, which was discovered latest of all three pathways. Martinez identified the genes involved in this pathway during screenings of metagenomic, marine DNA libraries and named them PhnY (not to be confused with the NAD⁺ dependent dehydrogenase PhnY, thus it was later renamed PhnY*) and PhnZ.⁹⁰⁻⁹²

PhnY*, is an α -ketoglutarate/non-heme Fe^{II}-dependent dioxygenase, which performs a stereospecific hydroxylation of the α -carbon of **1** to form the intermediate (*R*)-**34** (scheme 15).



Scheme 15: Degradation pathway of 2-AEP (**1**) by the oxidative cleavage route.

After α -ketoglutarate (α KG) and O_2 are bound to the active site- Fe^{II} (**56**, scheme 16), molecular oxygen is reduced to superoxide (**I-III**). Subsequent oxidative decarboxylation of α -ketoglutarate to succinate produces an $Fe^{IV}=O$ moiety (**IV-V**). This species is able to attack the α -hydrogen of **1**, to form a radical and Fe^{III} -OH (**VI**). Finally, in a radical reaction, (*R*)-**34** is formed (**VII**).^{67,93}

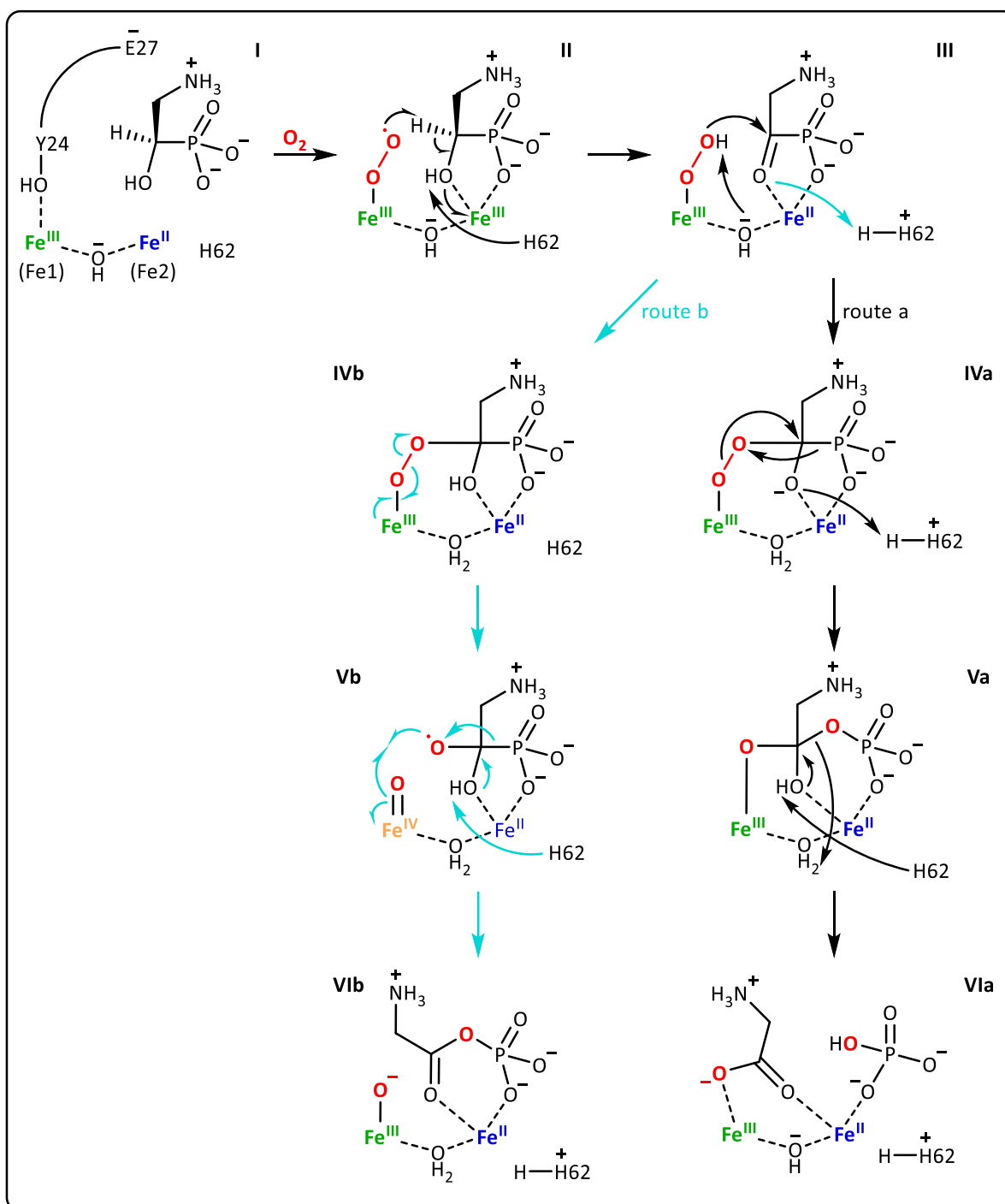


Scheme 16: Proposed mechanism for PhnY*.

PhnZ belongs to the HD superfamily of phosphohydrolases and is a mixed valence (Fe^{II}/Fe^{III}) diiron-dependent oxygenase. There are several other known members of this enzyme family, but only one, the mammalian enzyme *myo*-inositol monooxygenase (MIOX), has been functionally characterized. PhnZ is responsible for the oxidative C-P bond cleavage of (*R*)-**34**, to yield glycine and inorganic phosphate. The mechanism is still not fully elucidated, the first assumption was that PhnZ is a monooxygenase, as MIOX, but recent experimental and computational studies suggest that it is a dioxygenase (scheme 17).^{66,94–96}

In the presence of substrate (*R*)-**34**, a conformational change occurs to allow interaction with PhnZ. Also, a single electron transfer (SET) from Fe1 to Fe2 upon O₂ binding takes place (not shown). A subsequent abstraction of the α -hydrogen next to phosphorus is predicted to be the rate limiting step. The His-62 side chain presumably acts as general base in this reaction and the acylphosphonate intermediate is formed through an electron transfer to the Fe2 (**I-III**). Currently two different mechanisms are discussed. In both cases the bridging hydroxyl, which acts as a base, subtracts the hydrogen from hydroperoxide, giving it the ability to attack the acylphosphonate. Then, either a Criegee-like intermediate (**IVa**) is formed (route a) or an unusual fragmentation is predicted to occur due to the additionally proton transfer (turquoise arrow) from His-62 (**IVb**) (route b). In the latter case a substrate alkoxy radical and a ferryl species are formed (**Vb**). The phosphonyl group can subsequently attack the oxygen radical and a single electron from the alkoxy radical can be taken up by the ferryl species (**Vlb**).

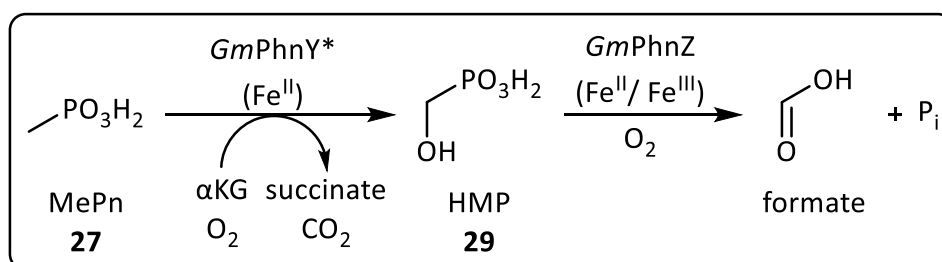
It was found by experimental and computational studies, that the inverse heterolytic C-P bond cleavage pathway (route a) has a lower energy barrier and is thus more likely to take place. This mechanism is also triggered by His-62, which here acts as a general acid. The phosphonyl group directly attacks the more electrophilic, proximal oxygen of the peroxide and the distal oxygen gets bound to the α -carbon of the substrate (**IVa**). The so formed orthoester (**Va**) rapidly collapses to give glycine an P_i (**VIa**).^{66,94-96}



Scheme 17: Proposed mechanism for oxidative cleavage of the P-C bond in (R)-**34** by PhnZ.

Recently, a closely related degradative pathway was found in *Gimesia maris* DSM8797. This microorganism was shown to use both 2-AEP (**1**) and methylphosphonic acid (**27**) as phosphorus source. Zechel and coworkers demonstrated that the degradation of **27** is performed by an oxidative pathway using the enzymes *GmPhnY** and *GmPhnZ1*. *GmPhnY** conserves all residues that are necessary for an α -ketoglutarate/non-heme Fe^{II}-dependent

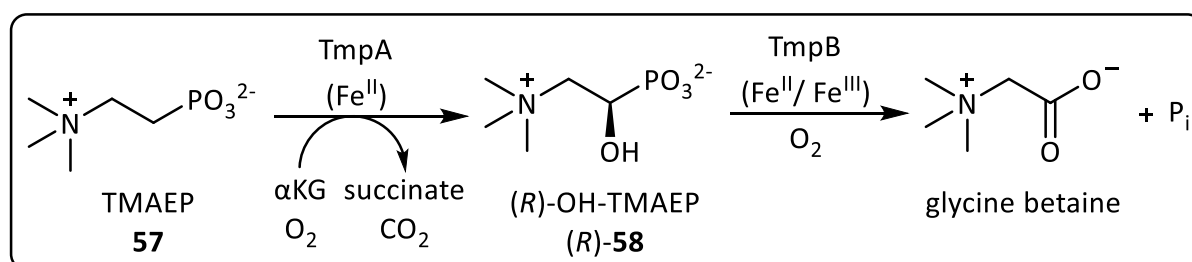
dioxygenase and its sequence is to 36% identical with that of PhnY*. *GmPhnY** converts **27** to hydroxymethylphosphonic acid (HMP, **29**) (scheme 18). *GmPhnZ1* has a similar percentage of sequence similarity to PhnZ. Furthermore, all of the essential active site residues are conserved, except for Tyr-24 and Glu-27, which block O₂ binding in the absence of substrate. *GmPhnZ1* finally converts **29** to formate and P_i by *GmPhnZ1*.⁹⁵



Scheme 18: Degradation pathway of MePn (27) by the oxidative cleavage route.

Yet another very similar set of enzymes was discovered in 2019 in *Leisingera caerulea*. It is encoded by a two-gene operon, and the encoded enzymes were named TmpA and TmpB.

TmpA was first thought to be a γ -butyrobetaine (γ bb) hydroxylase (BBOX) due to structural similarities. However, no Zn^{II} ion is present in TmpA, which is necessary for all BBOXs. After several other studies it was found that TmpA is an α -ketoglutarate Fe^{II}-dependent oxygenase like PhnY*. This enzyme is highly substrate specific for the hydroxylation of 2-(trimethylammino)ethylphosphonate (TMAEP, **57**), which is natural occurring in phosphonoglycans⁹⁷, to give the trimethylated analog of (*R*)-**34**: (*R*)-OH-TMAEP (**58**) (scheme 19).^{94,98}



Scheme 19: Degradation pathway of TMAEP (57) by TmpA and TmpB.

The genomic synteny of TmpA and TmpB suggest that TmpB uses (*R*)-**58**, formed by TmpA, to perform an oxidative C-P bond cleavage reaction producing a glycine betaine and inorganic phosphate.

TmpB was identified as a HD protein with a diiron cofactor. It has 32% sequence identity to PhnZ and both active sites are structurally very similar (figure 9). In TmpB, the hydroxyl group and one oxygen atom at the phosphorus are coordinated to Fe2 in a bidental fashion, as in PhnZ.^{94,98}

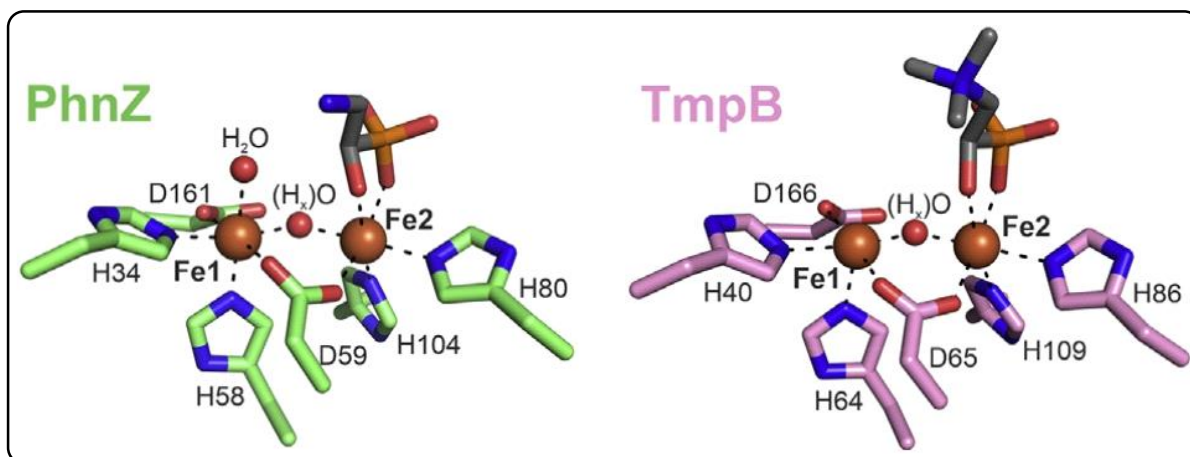


Figure 9: The diiron active site of PhnZ compared to that of TmpB, with (R)-OH-AEP or (R)-OH-TMAEP as substrate, respectively.⁹⁴

However, TmpB is not necessarily an oxygenase. Other enzymes with the same properties have already been identified as phosphohydrolases. Further studies are thus required to determine the exact mode of action of TmpB together with a functional assignment within this structural enzyme superfamily.⁹⁴

2. Aims of the thesis

Due to the natural abundance of phosphonates and their importance as alternative phosphorus source for microorganisms, nature has probably evolved many more biodegradation pathways for phosphonates than those discussed above. A detailed understanding of the already known ones is thus necessary to identify similar genes in other, yet unexplored microorganisms. Studying the underlying biochemical processes of the P-C bond cleavage in known and newly discovered phosphonate degradation pathways will bring us closer to a profound understanding of the global phosphorus cycle. For these mechanistic studies chiral and isotopically labeled compounds are necessary.⁶⁶

Additionally, a detailed understanding of phosphonate degradation pathways will help to improve and design phosphonate-based drugs, which are of special interest in agriculture, medicine and pest control due to their favorable properties and low mammalian toxicities.^{18,21} Thus, methods for their synthesis as pure enantiomers are of high scientific interest. Up to now some synthetic routes for the synthesis of chiral phosphonates are known. However, the disadvantages of these concepts reach from limited substrate scopes, over very complex and expensive methodologies and starting materials, to low stereo- or enantioselectivities.⁹⁹ These drawbacks make many known synthetic routes ineffective for the synthesis of medicinal compounds, since both the stereochemistry and substrate scope are of particular importance when it comes to drug synthesis. Therefore, the development of new methods, especially for the synthesis of the phosphonic acid analogues to the 21 proteinogenic aminocarboxylic acids is of high scientific interest. The high medicinal potential of these compounds stems from their ability to effectively mimic enzymatic transition states. Thus they can potentially act as enzyme inhibitor drugs.³⁸

This work is divided into two parts. On the one hand I worked on the development and improvement of a new general method for the synthesis of the phosphonic acid analogs to the 21 proteinogenic aminocarboxylic acids. This part of my work deals with the synthesis of five compounds, namely (*R*)-phosphaalanine [(*R*)-**20**], (1*R*,2*S*)-phosphaisoleucine [(1*R*,2*S*)-**59**], (*S*)-phosphamethionine [(*S*)-**60**], (*R*)-phosphaarginine [(*R*)-**61**] and (*S*)-phosphaisocysteine [(*S*)-**62**]. In addition, (*R*)-(1-hydroxyethyl)phosphonate as its sodium salt [(*R*)-**63**] should be prepared (figure 10).

On the other hand, enantiopure (*R*)-[1-hydroxy-2-(trimethylammonio)ethyl]phosphonate [(*R*)-**58**] and its isotopically labeled analogs (*R*)-1-[²H]-**58** and (*R*)-1-[¹³C]-1-[²H]-**58** were synthesized as substrates for mechanistic studies of the enzyme TmpB by our collaborators.

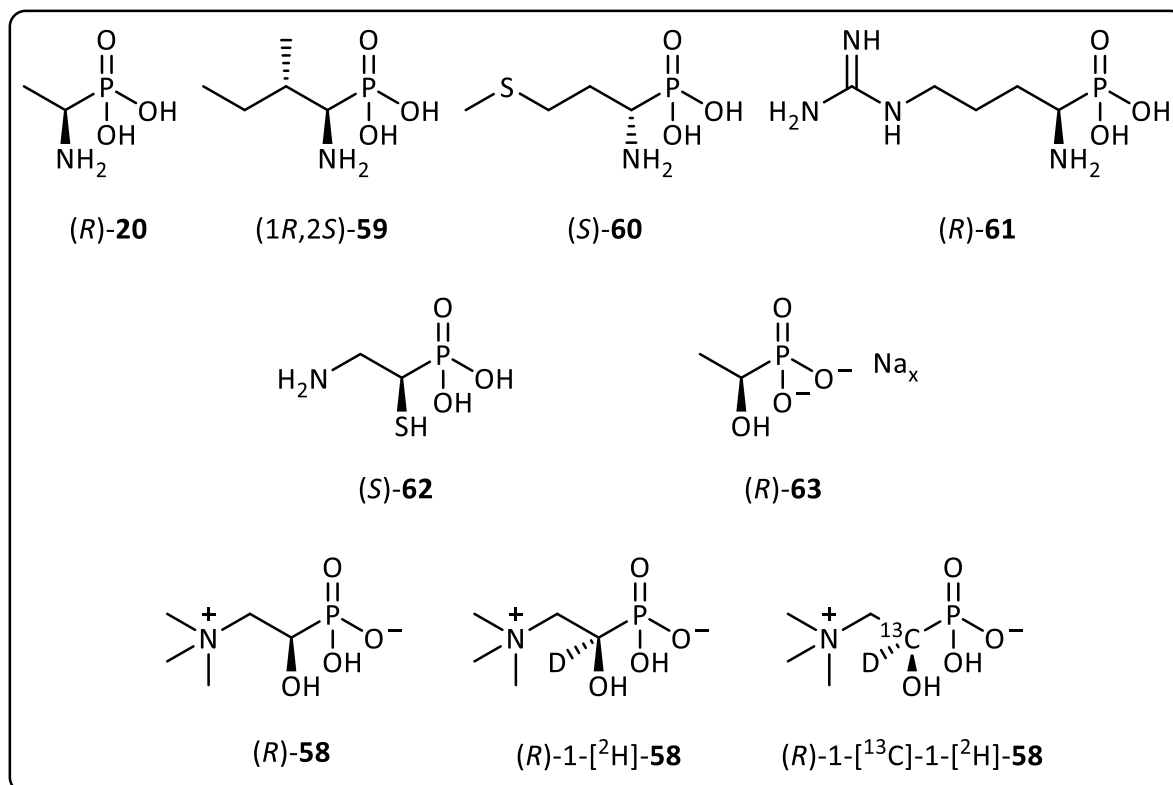


Figure 10: Target compounds of this thesis

3. Results and discussion

3.1 Synthesis of chiral α -aminophosphonic acids

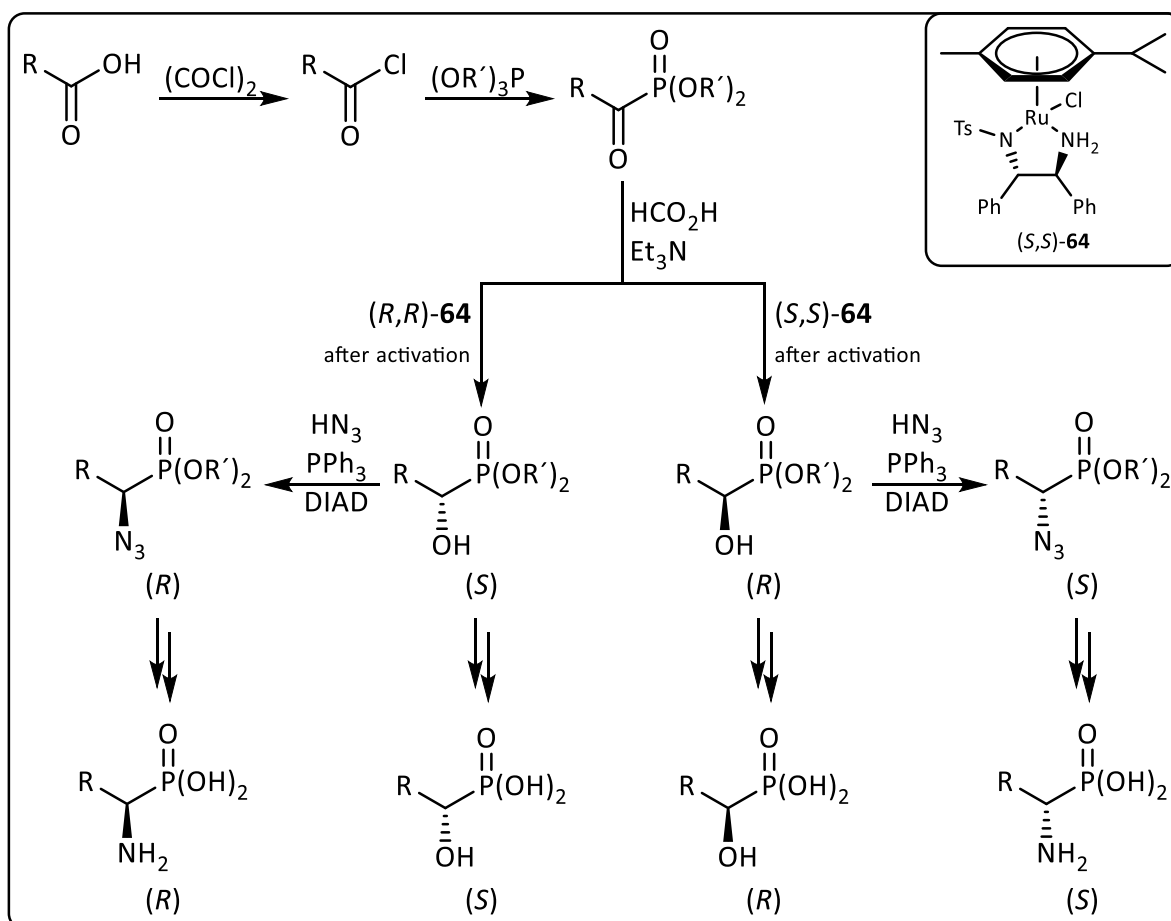
3.1.1 Overview of the new method

The literature known methods for the synthesis of the phosphonic acid analogues to the 21 proteinogenic aminocarboxylic acids all suffer from either one or more severe drawbacks, as mentioned above. While for some compounds there is still no synthesis known to produce them as enantiopure compounds, some other methods are limited to a single target.⁹⁹ Chemo-enzymatic resolutions, in which only one enantiomer is converted, often yielded high ees (above 98%) in the past.¹⁰⁰ However, the maximum yield in this resolution step is 50%. Moreover, enzymes are very substrate specific and the reaction conditions are limited due to their sensitivity.

Therefore, there is still an urgent need for the development of new, general methods, to obtain chiral α -aminophosphonic acid analogues to the 21 proteinogenic amino acids. This purely chemical synthetic route should be tolerant regarding functional groups, of which a high diversity is present in the proteinogenic amino acids. Furthermore, it should make a broad variety of target structures accessible, starting from commercially available, cheap starting materials. In addition, only small adaptations should be required for each α -aminophosphonic acid (e.g. protecting groups), so that the key steps always remain the same and both enantiomers of a compound become accessible by applying the same methodology. Currently, we develop a general synthetic procedure that fulfills all these key points (scheme 20).

First a commercially available carboxylic acid is converted to the corresponding acyl chloride, which is then subjected to a Michaelis-Arbuzov reaction, for phosphorus-carbon bond-formation. Subsequent asymmetric transfer-hydrogenation of the resulting α -ketophosphonate in the presence of a Noyori-type catalyst (**64**) gives α -hydroxyphosphonates of high enantiomeric excess. While the (*R,R*)-catalyst gives the (*S*)-product, the (*S,S*)-catalyst produces the (*R*) enantiomer.¹⁰¹ By global deprotection of these intermediates, α -hydroxyphosphonic acids of high enantiomeric excess can be obtained. For the synthesis of α -amino-phosphonic acids the hydroxyl group is first replaced by an azide in a Mitsunobu reaction under inversion of configuration. This is followed by hydrogenation of the azide to

yield the corresponding amine and final global deprotection to yield the enantiopure α -aminophosphonic acids. In case of labile starting materials, the acyl chloride formation is not possible, and an Abramov reaction can be used as alternative. With this method racemic α -hydroxyphosphonates are formed which can be oxidized *in situ* to the desired α -ketophosphonate intermediates. However, this was not necessary for any of the discussed target compounds.



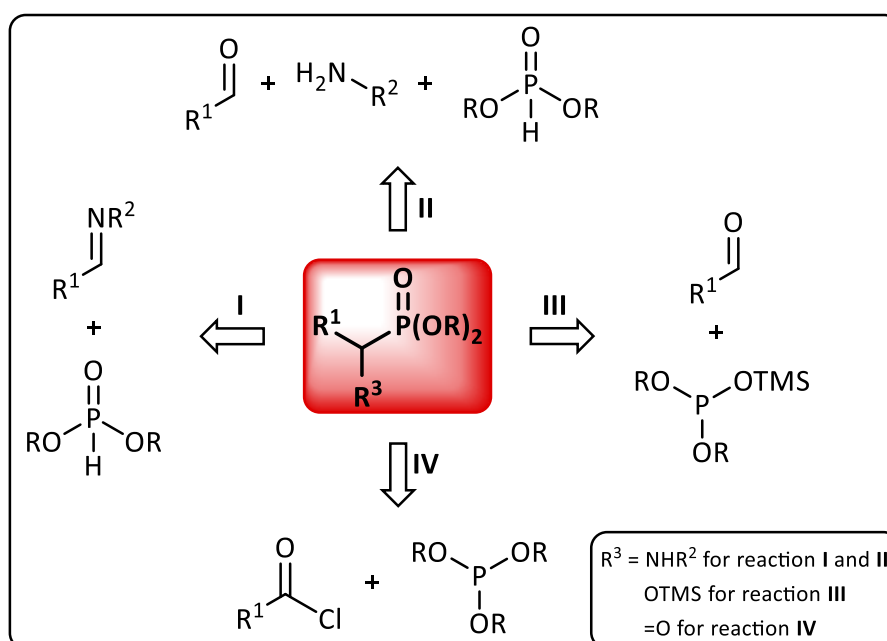
Scheme 20: General scheme of the newly developed method for the synthesis of chiral α -hydroxyphosphonic acids and chiral α -aminophosphonic acids of high ee.

3.1.2 Synthesis of ketophosphonates

Several strategies are currently known for P-C-bond formation (scheme 21). It is possible to use a Pudovik reaction (I) where an aldehyde or imine reacts with a dialkyl phosphite under basic conditions. Another option is the closely related three component Kabachnik-Fields reaction (II), where either an aldehyde or a ketone reacts with an amine and dialkyl phosphite to give the desired product. However, those reactions often need quite harsh conditions and

sometimes the starting materials are not commercially available or very expensive. Both hydrophosphonylations can also be performed under enantio- and diastereoselective conditions, but the obtained *ees* and *des* are - until now - rather low.^{99,102,103} Therefore, these methods are not the best choice for the synthesis of α -chiral phosphonates for enzymatic applications.

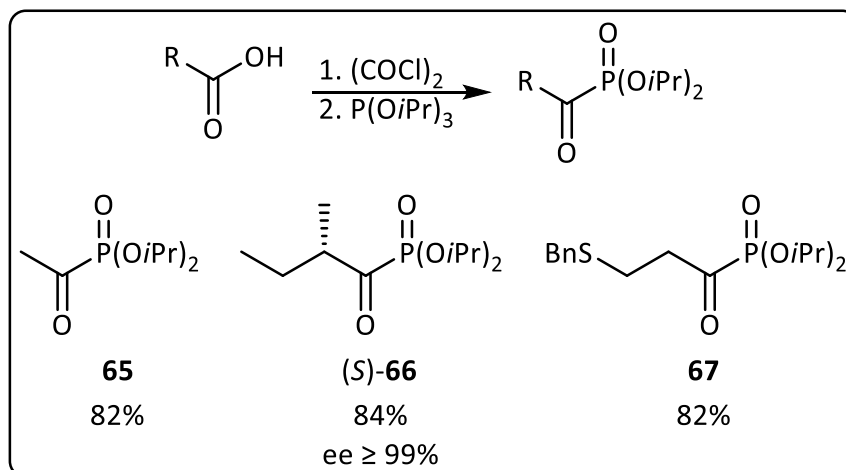
In contrast, the Abramov reaction (III) is a very mild alternative to produce racemic α -hydroxyphosphonates. The only disadvantage of this method is the need for silylated phosphites, where the TMS ether acts as easily transferable protecting group. These compounds can be prepared by reacting dialkyl phosphites with hexamethyldisilazane in the presence of chlorotrimethyl silane.^{104,105}



Scheme 21: Different ways for P-C bond formation: (I) Pudovik, (II) Kabachnick-Fields, (III) Abramov, (IV) Michaelis-Arbuzov reaction.

Another method for the formation of P-C bonds is the Michaelis-Arbuzov reaction (IV), which is used in industry to produce organophosphoryl compounds on a ton scale. Here, a trialkyl phosphite is reacted with either an alkyl or acyl halide to form the C-P bond. Recently, a modified method which works under milder conditions was designed using alcohols instead of halides in the presence of a catalyst.¹⁰⁶ The Michaelis-Arbuzov reaction is easy to handle and a broad variety of cheap starting materials can be used. Therefore, for our new methodology we either started with the conversion of a commercially available carboxylic acid

to its corresponding acyl chloride, followed by an Arbuzov reaction with triisopropyl phosphite or directly with an acyl chloride (scheme 22), in case it was commercially available at a reasonable price.



Scheme 22: General scheme for the formation of α -ketophosphonates and the detailed structures of the synthesized target molecules.

For the synthesis of phosphalaanine we directly started with commercially available acetyl chloride (**98**), for example. The starting material was dissolved in CH_2Cl_2 and $(\text{O}i\text{Pr})_3\text{P}$ was added at 0°C , after stirring at 0°C for 4 h the crude product was obtained which can be used without further purification. Removal of the solvent always has to be performed at room temperature since some ketophosphonates are highly (temperature) sensitive. The product **65** was obtained in 82% yield with a purity of 80 mol%. However, it is possible to further purify this compound by fractional distillation due to its relatively low boiling point (bp = 56°C at 0.1 Torr)¹⁰⁷. As most of the impurities have a very similar bp, a maximal purity of 95 mol% could be achieved.

The first step of the synthesis of (1*R*,2*S*)-phosphaisoleucine [(1*R*,2*S*)-**59**] is the conversion of (*S*)-2-methylbutyric acid [(*S*)-**99**] to the acyl chloride. This was performed under similar conditions as described above. Oxalyl chloride was added at 0°C and the reaction was complete at 25°C after 2 h. Here, the reaction time had to be shortened compared to other target compounds as preliminary experiments showed the stereocenter of (*S*)-**99** to easily racemise under the conditions used for acyl chloride formation at elevated temperatures or during prolonged exposure to the reagents. In this case it is further important to omit the evaporation step due to the low boiling point of the resulting acyl chloride. The crude reaction

mixture has to be used directly for ketophosphonate formation. Thus, the total amount of oxalyl chloride used should be kept very close to one equivalent. After addition of $(O\textit{i}Pr)_3\text{P}$ at 0°C stirring was continued for 2 h. The crude product (*S*)-**66**, which can be used without further purification was obtained in 80% yield and 84 mol% purity with an *ee* of over 99% within a total reaction time of 4 h.

For the synthesis of phosphamethionine, the thiol group of 3-mercaptopropanoic acid (**100**) was first benzylated by a literature known method¹⁰⁸, in which the thiol is deprotonated by KOH in a water/EtOH solution, followed by the addition of benzyl bromide. With this simple method, 3-(benzylthio)propanoic acid (**102**) could be obtained as slightly yellow solid after work-up in a very good yield of 97%. The acyl chloride formation was only performed after this additional protecting step over a period of 20 h at 30°C . The comparably long reaction time needed in this case can be explained by the presence of sulfur in the molecule. After evaporation of all volatiles, the acyl chloride was reacted similarly to the above described procedure to give the crude ketophosphonate **67** in 85% yield and 74 mol% purity, which was again used without further purification.

All other used ketophosphonates were already prepared by other group members and were thus not synthesized during the course of this thesis.

It is possible to store all these ketophosphonates at -25°C for approximately four weeks.

3.1.3 Synthesis of enantiopure α -hydroxyphosphonates

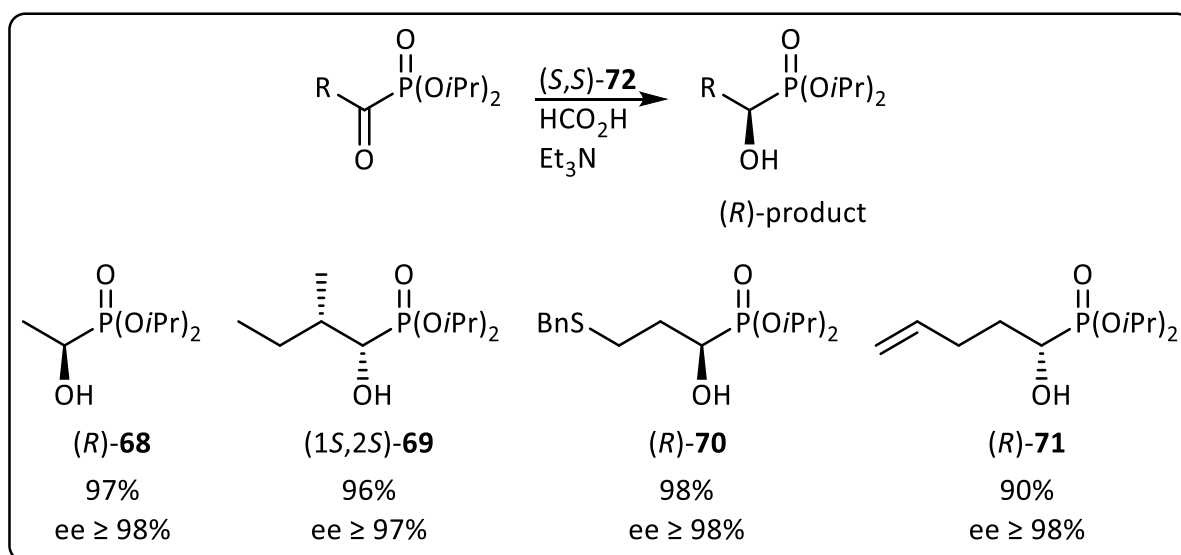
In all cases, the next step was an enantioselective reduction of the obtained ketophosphonates to the corresponding α -hydroxyphosphonate. For this asymmetric transfer hydrogenation a suitable catalyst and a hydride source were required.

The first reported catalysts for homogeneous, asymmetric hydrogenation of olefins date from the late 1960s, although the obtained enantiopurities were still poor. In 1971, the first asymmetric hydrogenation with good *ee* was performed by Kagan, which was a breakthrough in this field. Since then, the used catalysts have been continuously improved by using different chiral ligands and metals, resulting in a broader substrate scope and very good *ees*.¹⁰⁹

Noyori was a pioneer in this area and developed several Ru-containing catalysts for asymmetric transfer hydrogenation. Amongst them (*S,S*)-RuCl[(mesitylene)-TsDPEN], which

was developed in 1995. He prepared this catalyst *in situ* and found that it was able to enantioselectively reduce ketones, dissolved in 2-propanol in the presence of KOH. Transfer hydrogenations of ketones under these conditions are reversible, due to the structural similarity of the hydrogen donor and the product, which are both secondary alcohols. Thus, low substrate concentrations and short exposition times to the catalyst are required.¹¹⁰ However, the enantiopurity as well as the conversion rate are still affected.

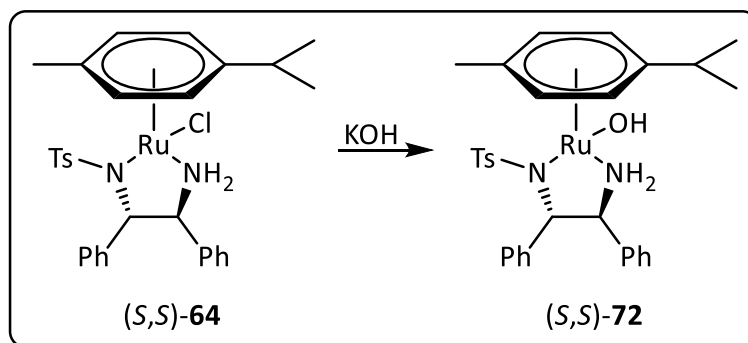
Later, with the new RuCl-DPEN(SO₂Ar)-type catalysts, Noyori introduced the possibility of using a formic acid/Et₃N mixture instead of 2-propanol as the hydrogen donor. This opens up a wide range of applications due to the irreversibility of the hydrogenation step and allows up to 100% conversion.^{111,112} One of these catalysts developed by Noyori is (*R*,R**)-RuCl[(*p*-cymene)-TsDPEN] [(*S,S*)-**64** and (*R,R*)-**64**]. With this catalyst, several groups reported enantioselective reductions of α-ketophosphonates with good yields and outstanding ees.¹¹³ Interestingly, for α-ketophosphonates the opposite face selectivity compared to the reduction of α-ketoesters was observed. The (*R*)-α-hydroxyphosphonates could be obtained by using the activated (*S,S*)-catalyst, while the (*S*)-enantiomers are formed by action of (*R,R*)-catalyst (scheme 23).



Scheme 23: General scheme for the conversion of α-ketophosphonates to enantiopure α-hydroxyphosphonates and detailed results obtained for the synthesized target molecules.

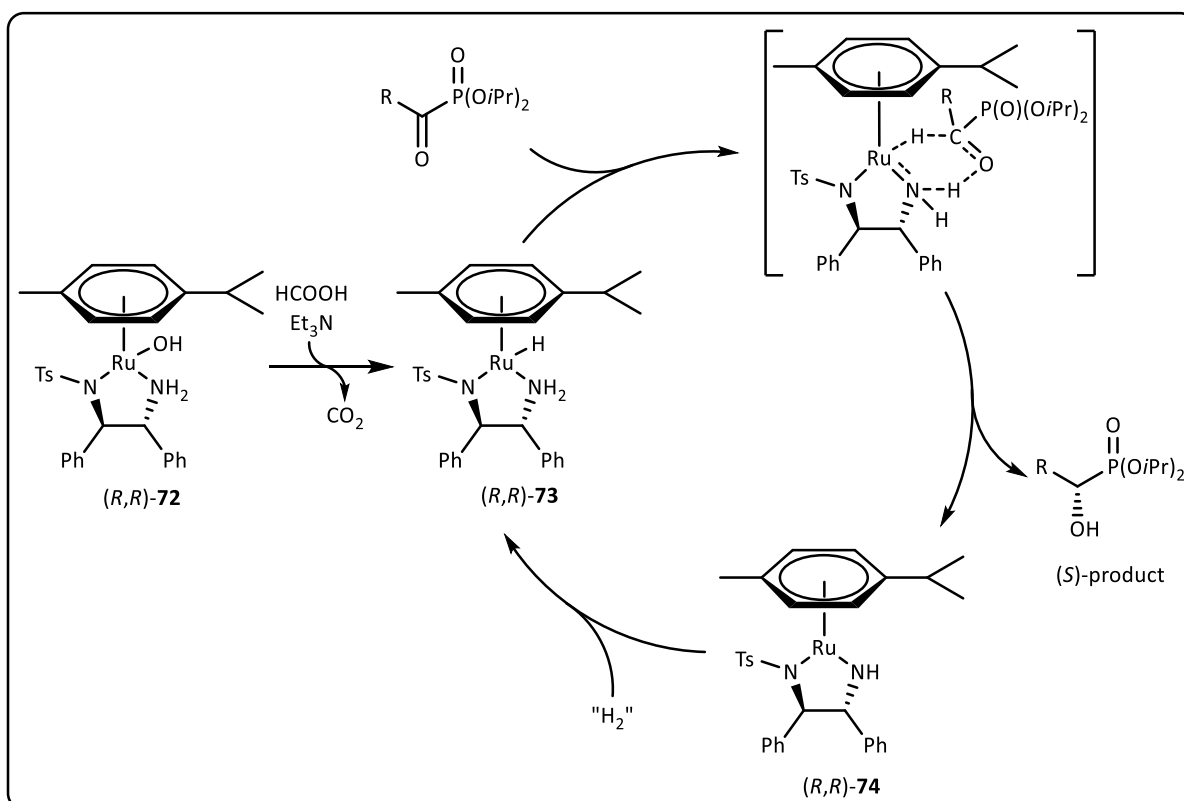
This nowadays moderately priced and commercially available catalyst has to be activated by a base before use (scheme 24). For this purpose (*S,S*)-**64** or (*R,R*)-**64** are dissolved in CH₂Cl₂

and washed with a 0.20 M aqueous potassium hydroxide solution. This leads to the replacement of the Cl ligand by OH, which can be visually traced as the colour of the organic layer changes from brown to deep purple. After work-up, the catalyst can be directly used or stored at 4°C under argon atmosphere for about 7-10 days.



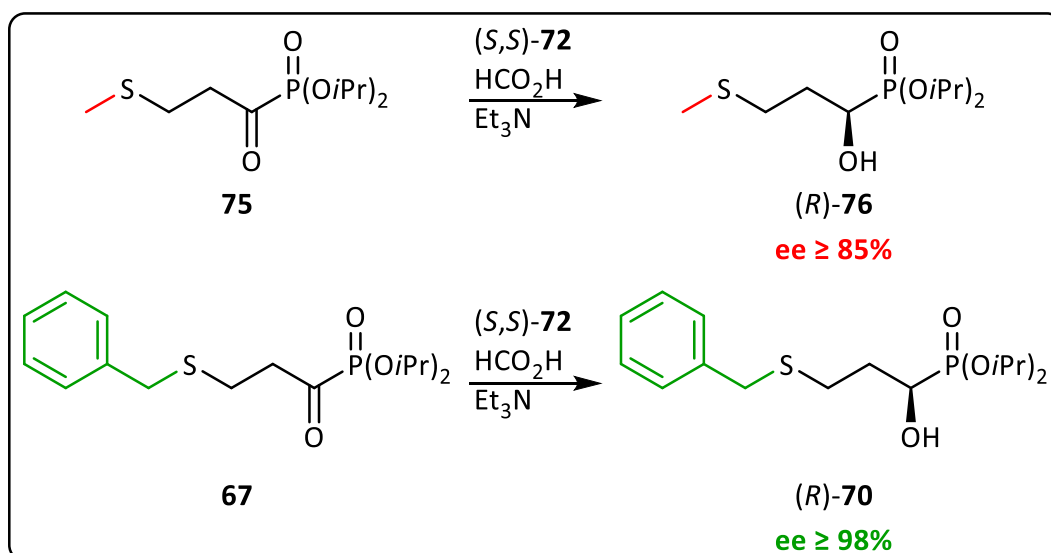
Scheme 24: Activation of the catalyst.

The asymmetric transfer hydrogenation (scheme 25) is carried out under the same conditions for all target compounds, only the total amount of catalyst was adapted depending on the needs of each compound. The formic acid Et₃N mixture was separately prepared under argon atmosphere at 0°C. This mixture was added first to the dissolved starting material, followed by the catalyst solution. All reactions were stirred at 35°C for 18 h. Heating is crucial, because at room temperature no or comparably less conversion was observed. However, in some cases (diisopropyl α -oxo-ethylphosphonate, e.g.) such a long reaction time is not necessary, but for consistencies sake, all reactions were monitored under similar conditions.



Scheme 25: Reaction mechanism of asymmetric transfer hydrogenation of (R,R) - $\text{RuOH}[(p\text{-cymene})\text{-TsDPEN}] [(R,R)\text{-72}]$ with a ketophosphonate.

The required amount of catalyst for full conversion depends strongly on the side chain of the used ketophosphonate, as already mentioned. Very small and simple molecules are converted the best, thus diisopropyl 1-oxo-ethylphosphonate (**65**) only needs 0.01 equivalent (eq.) of catalyst with respect to the ketophosphonate. Compounds with longer and more complex side chains require 0.02 eq. for complete transformation. This is for example the case for the keto-containing intermediates in the synthetic routes towards $(1R,2S)$ -phosphaisoleucine [$(1R,2S)$ -**59**] and (R) -phosphaarginine [(R) -**61**]. Sulfur-containing keto-phosphonates present a special case: comparably high amounts of catalysts are necessary to efficiently reduce them, due to partial catalyst inactivation by the substrate.¹¹⁴ This became obvious both during the synthesis of (S) -phosphamethionine [(S) -**60**] and (S) -phosphaisocysteine [(S) -**62**]. With this in mind, the required amount of 0.05 eq was absolutely acceptable. Catalyst inactivation by sulfur-containing moieties is also the reason why benzyl-protection had to be chosen during the synthesis of (S) -**60** instead of directly using the methylated keto-phosphonate as starting material. Bulkier protecting groups lead to less catalyst poisoning and thus better *ees* (scheme 26).



Scheme 26: Comparison of the effect of methyl and benzyl protecting group on the *ee* of the obtained product.

While reduction of diisopropyl 1-oxo-3-thiomethylpropyl phosphonate (**75**) only gave the respective α -hydroxyphosphonate in 85% *ee*, replacement of the methyl-group by a benzyl-group improved the *ee* to $\geq 98\%$.

The asymmetric transfer hydrogenation gave excellent isolated yields [after purification by medium pressure liquid chromatography (MPLC)] of about 95% (except for phosphoarginine: 90%) in all cases. The *ees* of the products were above 98% in all cases except for one case {(1*S*,2*S*)-diisopropyl 1-hydroxy-2-methylpropyl phosphonate [(1*S*,2*S*)-**69**]: *ee* 97%}.

The *ees* of the obtained α -hydroxyphosphonates could in all cases be determined by means of ^1H and ^{31}P NMR spectroscopy using the chiral solvating agent (*S*)-*tert*-butyl-phenylphosphinothioic acid [(*S*)-**77**] (for a schematic illustration of the concept see figure 11).¹¹⁵ Thus, for comparison, the racemic α -hydroxyphosphonates were also needed. These were easily accessible by reducing the respective α -ketophosphonates in the presence of NaBH_4 in MeOH. It was found that ground NaBH_4 leads to significantly higher yields. The addition of this reagent has to be done carefully, in small portions due to a strong heat development.

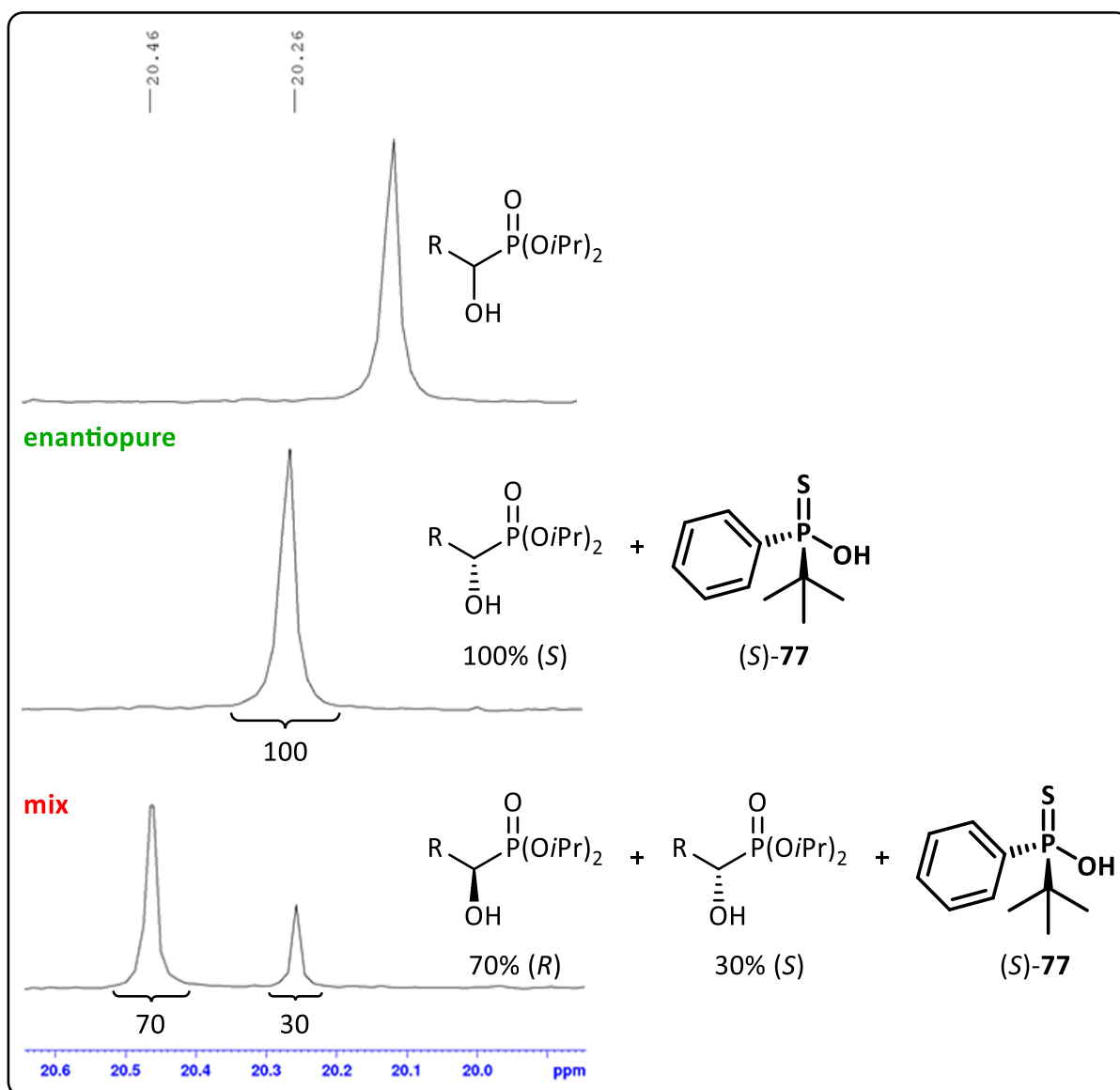


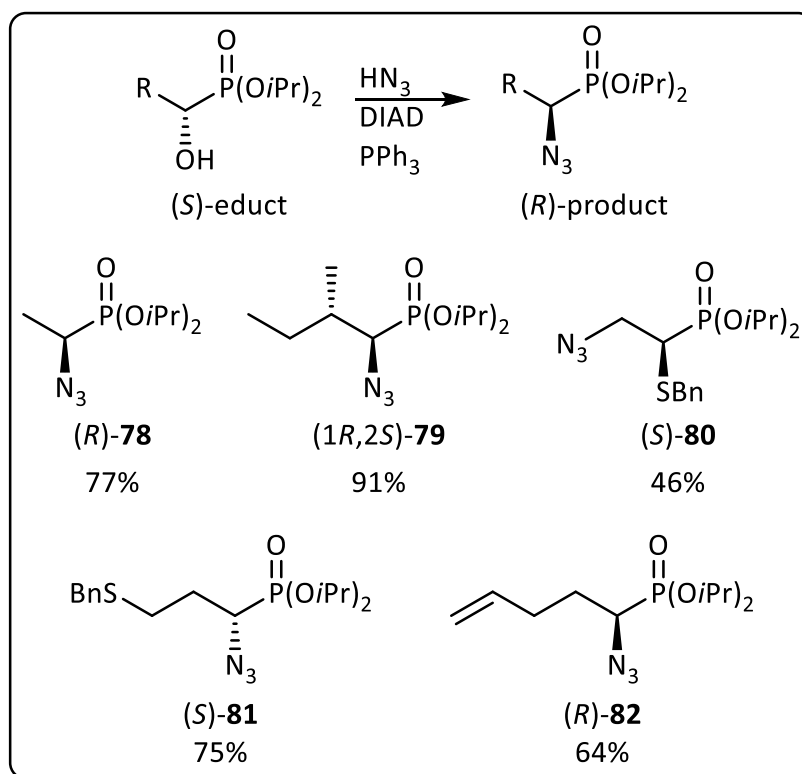
Figure 11: Comparison of the ^{31}P NMR spectra of an enantiopure α -hydroxyphosphonate with (2nd row) and without chiral (1st row) solvating agents, and of a mixture containing both enantiomers of the same compound in the presence of the chiral solvating agent (3rd row).

3.1.4 Synthesis of α -azido-phosphonates by Mitsunobu reaction (with HN_3)

The enantiopure α -hydroxyphosphonates were then further converted to their corresponding azides (scheme 27). For this conversion, a Mitsunobu reaction was chosen due to its high enantioselectivity.¹¹⁶ It is an azodicarboxylate and triphenylphosphine-mediated $\text{S}_{\text{N}}2$ -type reaction, in which primary or secondary alcohols can be replaced by a nucleophile under inversion of configuration.

Several azo-ester compounds are used for this transformation today, depending on the nature of substrate and nucleophile. In this work diethyl azodicarboxylate (DEAD) or diisopropyl azodicarboxylate (DIAD) were used as mentioned for each compound.

A variety of nucleophiles are described in literature e.g. thiols, halogens, alcohols, carboxylic acids, amides and azides, provided these pronucleophiles have a pK_a of around 11 or below.¹¹⁷ This is necessary because the intermediate betaine product has a pK_a of approximately 13 and can therefore only remove the acidic proton of the pronucleophile under these conditions. For the synthesis of α -aminophosphonic acids, HN_3 was the pronucleophile of choice. It is easily deprotonated under the required reaction conditions and sterically only low-demanding. Thus, it usually attacks with high efficiency, leading to high isolated product yields. Despite its inherent health risks, the compound can be handled safely by using it in a well ventilated work-space and in highly diluted toluidic solutions (maximum concentration 1.8 M).



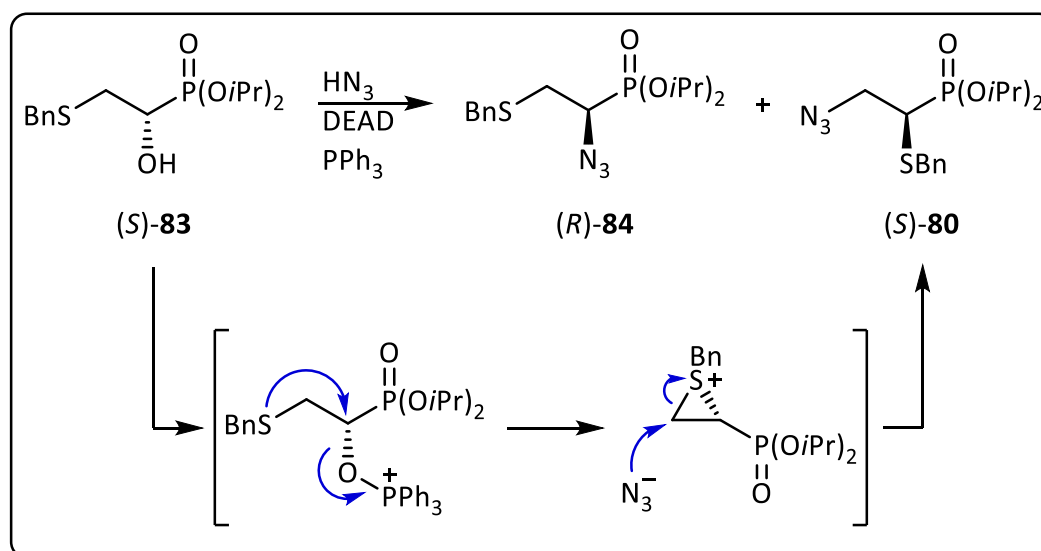
Scheme 27: General scheme for the conversion of α -hydroxyphosphonates to azides and detailed information on the obtained yields for all target compounds.

The Mitsunobu reaction was performed under the same conditions for all target azides. It was important to dry the used α -hydroxyphosphonates by coevaporation of residual water with

toluene, especially if working with low total amounts of substance. Usually, solid triphenylphosphine was directly added to the starting material and the mixture was dissolved in toluene under argon atmosphere. First HN_3 then the specified azodicarboxylate was added at 0°C . After the solution was stirred for 18 h it was quenched with MeOH. The solvent had to be removed at room temperature, as azides are temperature sensitive.

The isolated yields of around 75% were satisfactory for all compounds. However, this step needs to be improved as it gives the lowest yield of all conversions of the entire synthetic pathway towards α -aminophosphonic acids.

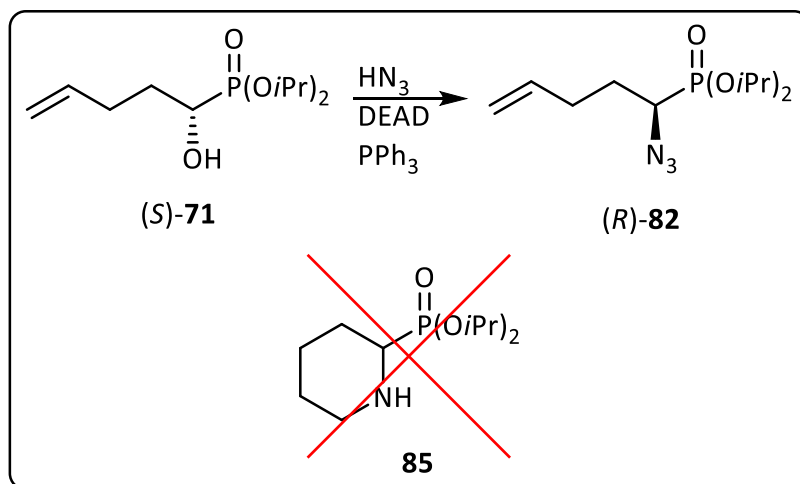
Thus, several solvents were tested for this reaction. THF gave comparably good yields to toluene, while conversion was often incomplete in CH_2Cl_2 , where in some cases the formation of an unknown side product was observed. Mixtures of solvents in different ratios were also tested. However, toluene proved to be the solvent of choice for all synthesized target molecules except for the synthesis of (*S*)-diisopropyl [2-azido-1-(benzylthio)ethyl]phosphonate [(*S*)-**80**], the key intermediate in the synthesis of (*S*)-phosphaisocysteine. As reported, a special rearrangement can occur during the Mitsunobu reaction of (*S*)-**83** (scheme 28). The equilibrium of this rearrangement can be shifted by varying the used solvent composition and azodicarboxylate component.¹⁰⁵



Scheme 28: Mitsunobu reaction of (*R*)-**83**, delivering two products (*S*)-**80** and (*R*)-**84** and the proposed mechanism of this rearrangement step.

Using CH_2Cl_2 as the solvent for this reaction instead of toluene shifts the equilibrium between both possible products significantly to give a ratio of 3:1 in favor of (*S*)-**80**. While (*R*)-**84** has already been analyzed and used for the synthesis of enantiopure (*R*)-phosphacysteine, detailed analytical data for the rearrangement product (*S*)-**80** and enantiopure (*S*)-phosphaisocysteine are still missing and were thus an aim of this thesis. The separation of both components proved difficult despite a seemingly acceptable separation on TLC. Traces of (*R*)-**84** could be found in the rearrangement product even after chromatographic separation. A second chromatographic separation was thus performed, to finally isolate (*S*)-**80** in 46% yield.

Also, the azide intermediate finally leading to phospharginine, proved difficult to purify (scheme 29). The product of this Mitsunobu reaction rearranged both in solution and as pure compound when stored at room temperature after some time. Higher temperatures even accelerated this process. Despite several efforts, the structure of the rearrangement product remained unknown, as it could not be isolated as a pure compound.



*Scheme 29: Synthesis of (*R*)-82 together with a first idea for the possible side-product structure, which was finally ruled out.*

Despite several purification attempts, this side-product could only be obtained with a maximal purity of 76 mol% as judged by ^{31}P NMR ($\delta_{\text{P}} = 22.53$ ppm). Also, a mass spectrum of the unknown compound was recorded: $[\text{M}+\text{H}]^+ = 248.1411$, $[\text{M}+\text{Na}]^+ = 270.1231$. The mass spectrum suggested the loss of N_2 from the azide. In this case, a cyclic product should be formed, containing two additional hydrogen atoms (**85**), or the double bond needs to stay intact, which is unlikely due to the observed proton shift values observed in the ^1H NMR

spectrum (figure 12). The ^1H NMR spectrum only proved that both *i*Pr groups were still intact but did not allow a final structure elucidation.

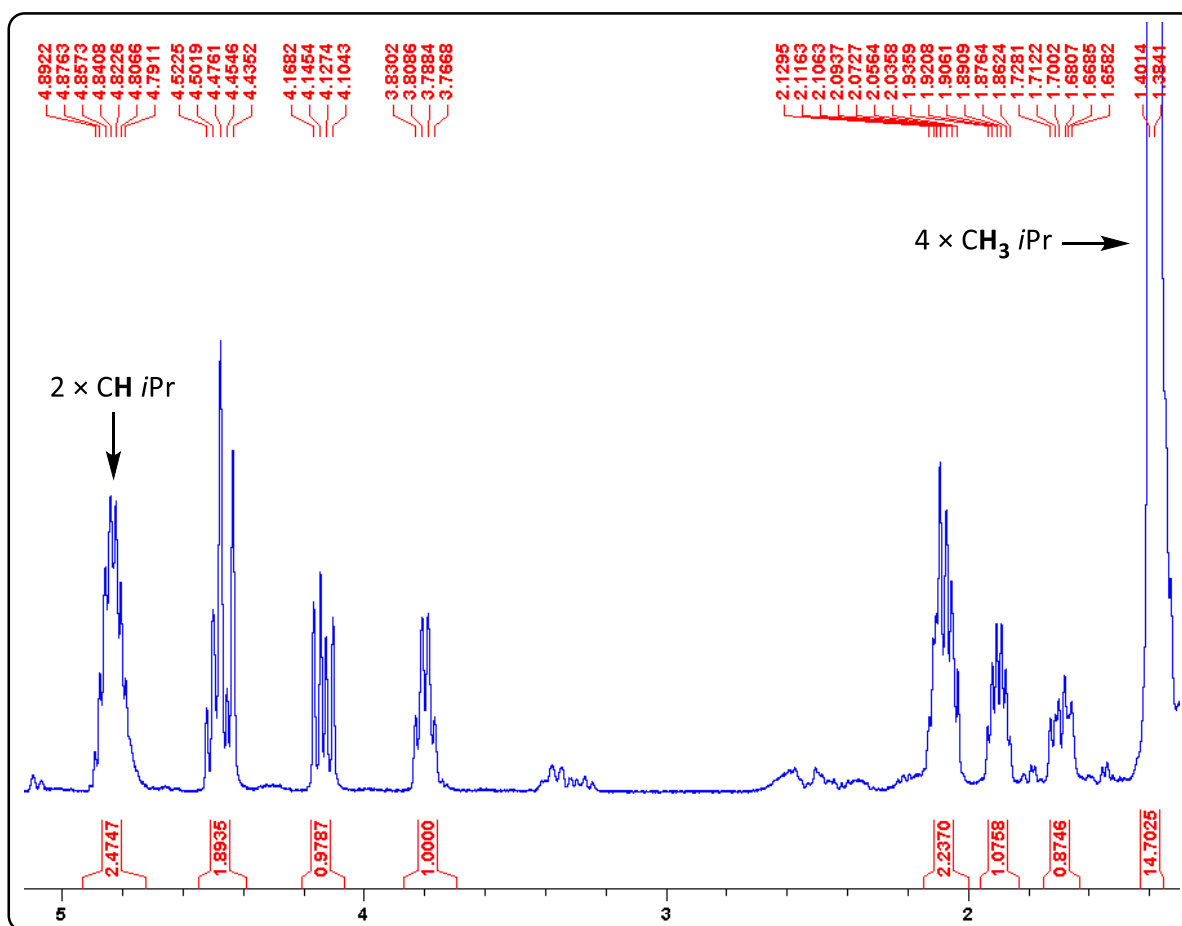
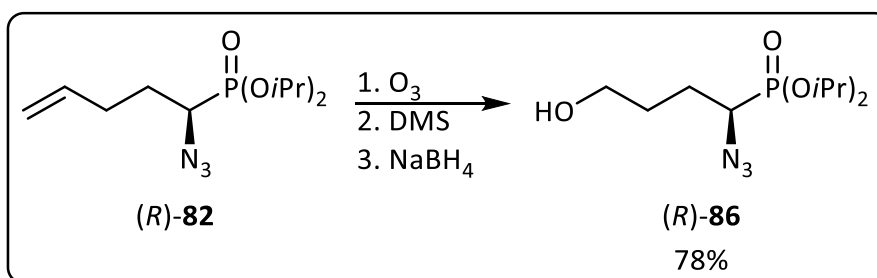


Figure 12: Crude ^1H NMR of the unknown side-product (integrated signals stemming from the unknown compound) formed from (*R*)-**82** upon storage or heating.

3.1.5 Phosphaarginine, additional steps: synthesis of (*R*)-diisopropyl [1-azido-4-bis(*tert*-butoxycarbonyl)guanidino]butylphosphonate [(*R*)-**88**]

During the synthesis of phosphaarginine the azide obtained after the first Mitsunobu reaction has to be further converted in order to reach the desired product. The terminal double bond needs to be first ozonolyzed to give the respective aldehyde and then reduced using NaBH_4 to give the α -azido- δ -hydroxyphosphonate (*R*)-**86** (scheme 30).

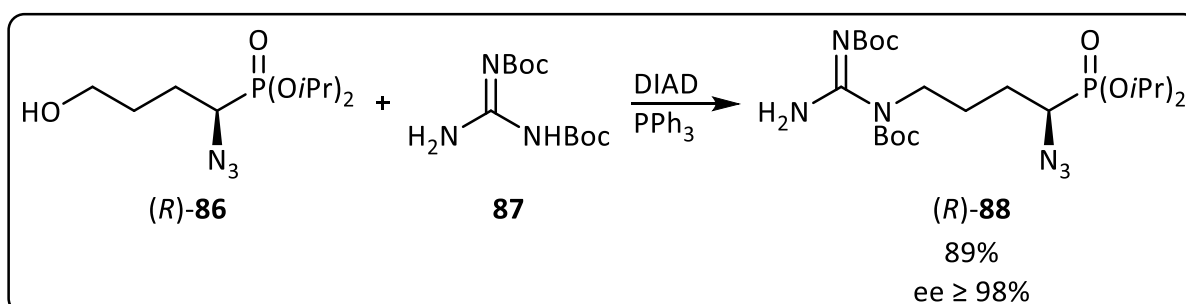


Scheme 30: Ozonolysis and reduction of (R)-82.

For this purpose, the alkene was reacted with ozone at -78°C . After the reaction was finished, O_2 was bubbled through the reaction mixture to remove excess O_3 until the pale blue color disappeared again. Dimethylsulfide (DMS) was used to destroy the formed secondary ozonides and finally give the desired aldehyde.

This aldehyde was then reduced by NaBH_4 dissolved in EtOH, at -35°C . The reaction mixture was allowed to slowly warm to 20°C over 4h; reaction progress was monitored by TLC. The desired product (R)-86 was obtained in 78% yield after work-up and chromatographic purification.

Then, intermediate (R)-86 is coupled with bis(*tert*-butoxycarbonyl)guanidine (87) under Mitsunobu conditions (scheme 31). It was not possible to use the same order for the addition of reagents as described above for the Mitsunobu reactions using hydrazoic acid as pronucleophile. Here, the order of addition of reagents is very crucial for the reaction outcome.



Scheme 31: Synthesis of (R)-88 by Mitsunobu reaction.

An unexpected side reaction occurred, when using the above described sequence for the addition of reagents during the Mitsunobu reaction: bis(*tert*-butoxycarbonyl)guanidine (87) reacted with triphenylphosphine under formation of 89 (figure 13), if both compounds were

mixed before the addition of (*R*)-**86**. First adding DIAD to the starting material also led to the formation of side products.

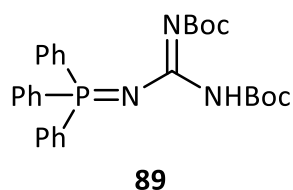


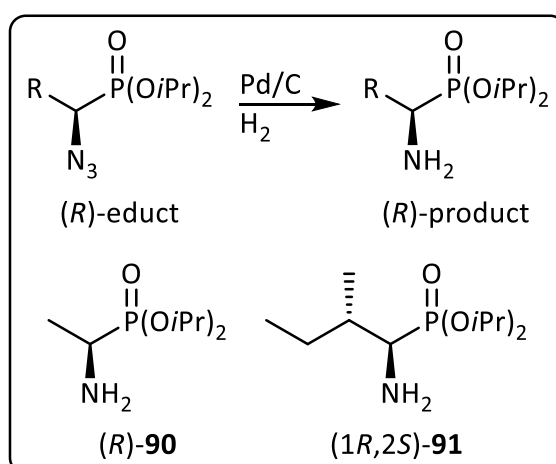
Figure 13: Side product formed by reaction of **87** and Ph_3P .

Thus, the order of addition of the reactants was changed. First DIAD was added to triphenylphosphine, dissolved in toluene under argon atmosphere at 0°C, after 5 minutes (*R*)-**86** was added, followed by the pronucleophile **87**, also dissolved in toluene. Like this, the desired reactivity could be achieved. The reaction mixture was allowed to come to 20°C in the cooling bath and after 4 h of stirring the product (*R*)-**88** was isolated in 89% yield and an *ee* over 98% after chromatographic purification.

All subsequent deprotection steps for the synthesis of (*R*)-phosphaarginine [(*R*)-**61**] are literature known.¹¹⁸

3.1.6 Reduction of azides, synthesis of α -aminophosphonates

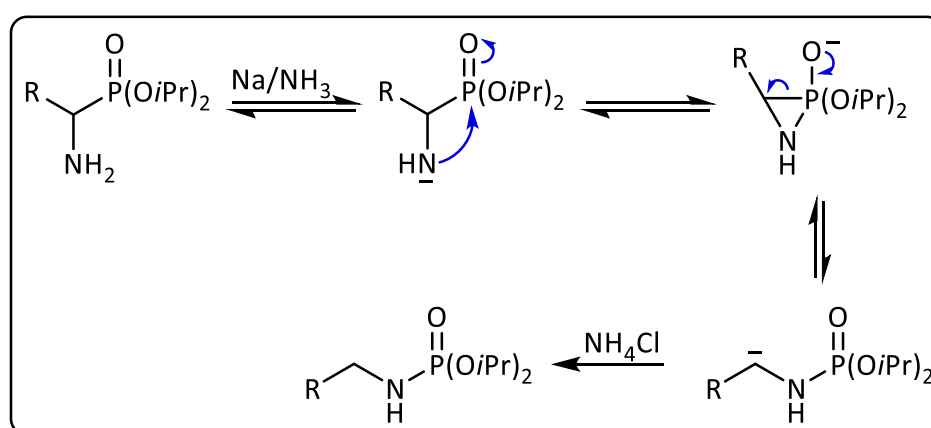
The reduction of the obtained azides to their corresponding α -aminophosphonates was performed by reductive, heterogenous hydrogenation (scheme 32).



Scheme 32: General procedure for reductive hydrogenation of azides and the respective yields for the synthesized target molecules.

For the synthesis of phosphoalanine and phosphoisoleucine the azides (*R*)-**90** or (1*R*,2*S*)-**91** were respectively dissolved in EtOH and Pd on activated charcoal (10 % Pd) was added. The hydrogenation was performed in a Parr apparatus at 3.5 atm H₂ pressure under constant shaking for 3 h. Addition of a drop of concentrated HCl to the reaction mixture sometimes had a positive effect regarding the yield. However, it turned out that (1*R*,2*S*)-diisopropyl (1-azido-2-methylbutyl)phosphonate [(1*R*,2*S*)-**91**] is very sensitive under these conditions (see also deprotection step) and if the acidic solution was shaken at 3.5 atm H₂ pressure the compound decomposed. α -Aminophosphonates are very polar, thus it is not possible to purify the obtained products *via* MPLC and the crude amines were directly used for the next step.

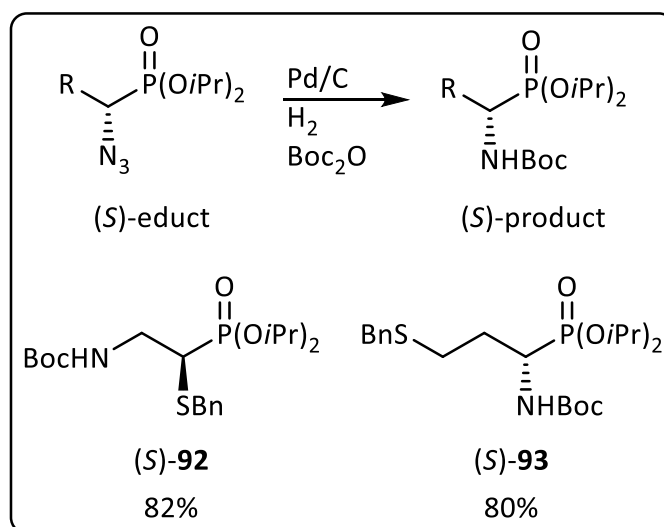
The sulfur containing azides had to be converted to the corresponding amines by a different synthetic route, since the benzyl protecting groups could not be effectively removed by hydrogenation. Catalyst poisoning by the partly obtained free thiol groups, led to incomplete conversion of the azides. Thus, a Birch reduction for removal of the benzyl groups became necessary. In order to avoid an unwanted α -aminophosphonate-phosphoramidate rearrangement (scheme 33) during the harsh basic conditions needed for this step^{119,120}, the azides were first hydrogenated and Boc-protected at ambient pressure. Under these conditions, the benzyl protecting group remains completely intact and can thus be removed in a separate step afterwards.



Scheme 33: General reaction mechanism of the α -aminophosphonates-phosphoramidate rearrangement.

Boc-protection of the product was done *in situ* by addition of Boc₂O to the reaction mixture (scheme 34). This protecting group was selected, since it is cleavable under the same acidic

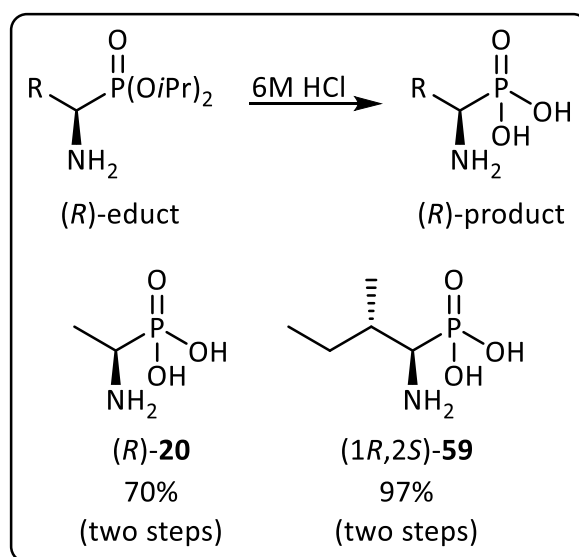
conditions as the isopropyl groups at the phosphorus and thus does not require the introduction of an additional deprotection step.



Scheme 34: General mechanism of one pot reductive hydrogenation and Boc-protection.

3.1.7 Synthesis of α -aminophosphonic acids

The final deprotection of the phosphorus moiety is performed in aqueous 6 M HCl under reflux conditions (scheme 35). After 15 h the solvent can be removed, and the crude α -aminophosphonic acids are obtained as hydrochloride salts. They are then redissolved in water and passed through a cation exchange chromatography column, in H⁺-form to remove impurities and isolate the pure, chiral α -aminophosphonic acids.



Scheme 35: General mechanism of deprotection of α -aminophosphonates and yields for defined products.

The deprotection producing phosphoalanine [(*R*)-**20**] was carried out without any complications. The starting material was dissolved in 6 M HCl and refluxed for 15 h. A relatively high amount of ion exchange resin was necessary in this case (12 ml/mmol) in order to effectively separate the product from remaining impurities. It was possible to eluate the product with water. Crystallization from H₂O/EtOH yielded colorless needles. Over the last two steps (reductive hydrogenation and deprotection) 70% isolated yield were obtained.

To conclude (*R*)-phosphoalanine [(*R*)-**20**], was obtained in excellent purity over 5 reaction steps with an *ee* of over 98% and an overall yield of 42%.

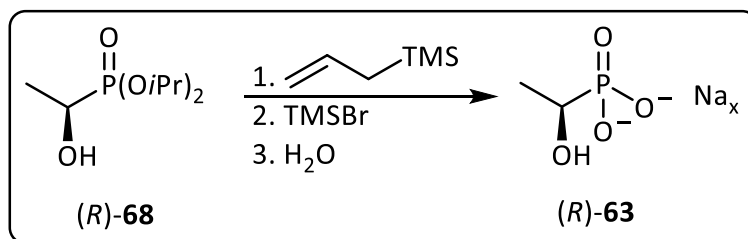
(1*R*,2*S*)-Phosphoisoleucine [(1*R*,2*S*)-**59**] was obtained by the same deprotection. However, it was found, that the reaction temperature is crucial in this case. Using the heating bath at 120°C, as usual for this reaction, leads to partial P-C bond cleavage and thus formation of inorganic phosphate. The problem was solved by lowering the reaction temperature to 100°C. This step needs further improvements regarding temperature and reaction time. For adequate purification 5 ml/mmol ion exchange resin were used and the product was eluted with formic acid (1%, aqueous). It was also possible to elute this compound with water only, but it then spreads over a large number of fractions. In this case crystallization was not possible, the product was obtained as colorless powder in 97% isolated yield over the last two steps.

In conclusion, (1*R*,2*S*)-phosphoisoleucine [(1*R*,2*S*)-**59**] could be synthesized in excellent purity with an *ee* over 97% and an overall yield of 68% in 6 steps starting from (*S*)-2-methylbutyric acid [(*S*)-**99**].

3.1.8 Synthesis of α -hydroxyphosphonic acids

Direct deprotection of α -hydroxyphosphonates without any further functional group manipulation is also possible and gives the respective α -hydroxyphosphonic acids. However, the separation from water soluble impurities by cation exchange chromatography is not as easy as in the case of α -aminophosphonic acids, as there is little retention on the available resins. Thus, the product elutes in the same fractions as the accompanying salts, in case the deprotection of the phosphorus moiety was performed by using 6 M HCl. Therefore, allyltrimethylsilane and trimethylsilyl bromide were used for deprotection (scheme 36). With this concept, methyl protecting groups can be removed at room temperature in 1 h. Isopropyl groups need harsher conditions: they are cleaved at 60°C within a reaction time between 5

and 20 h and ethyl groups require conditions between these two. For the synthesis of 1-hydroxyethylphosphonic acid, allyltrimethylsilane followed by TMSBr was added to the starting material in 1,2-dichloroethane (1,2-DCE) and the reaction was stirred for 5 h before all volatiles were removed.



Scheme 36: Deprotection of α -hydroxyphosphonate (R)-68.

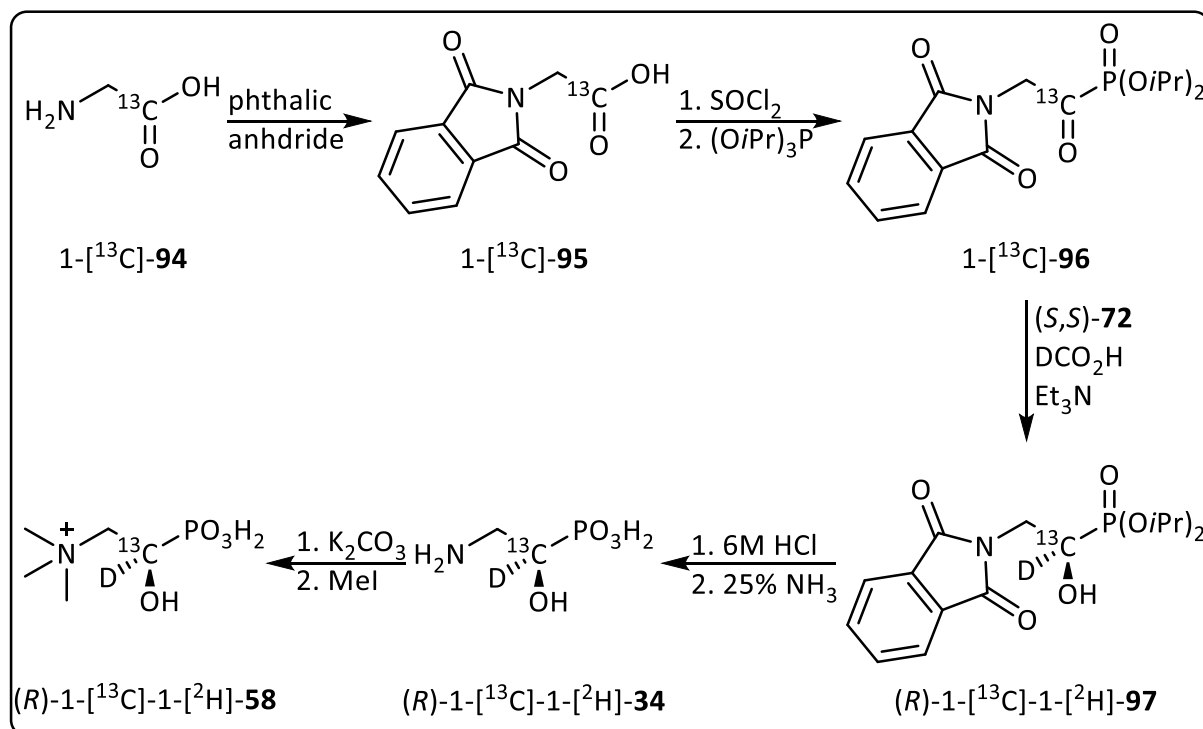
To guarantee the stability of the deprotected compound the pH was adjusted to 7-8 with NaOH immediately after the reaction. (R)-63 was obtained as its sodium salt as powdery colorless solid after lyophilization in 78% yield after 3 steps.

3.2 Synthesis of (R)-[1-hydroxy-2-(trimethylammonio)ethyl]phosphonate (R)-58 and its isotopically labeled analogs (R)-1-[²H]-58 and (R)-1-[¹³C]-1-[²H]-58

Phosphonate degradation pathways in enzymes are far from being fully explored. Mechanistic and kinetic studies of already known enzymes are thus necessary for a better understanding of the underlying degradative pathways. With this knowledge, other, yet unexplored degradation routes can possibly be revealed, and the design of phosphonate-based drugs will become easier. For such mechanistic studies chiral and isotopically labeled compounds are needed. However, they are often associated with expensive starting materials and special chemical techniques.

Being able to use an already established synthetic route, with little adaptations to introduce the isotope-labels at a late stage would be very beneficial. Therefore, during the synthesis of (R)-[1-hydroxy-2-(trimethylammonio)ethyl]phosphonate (R)-58 and its isotopically labeled analogs, we relied on our key strategy using an asymmetric transfer hydrogenation as key step (scheme 37).¹²¹ With this concept, a substrate for mechanistic studies of PhnZ was already synthesized in the deuterated form.¹⁰⁵

Now another phosphonate degrading enzyme shall be studied, namely TmpB. (*R*)-[1-hydroxy-*R*]-[2-(trimethylammonio)ethyl]phosphonate (OH-TMAEP, **58**), the natural substrate for this enzyme, and its labeled analogs (*R*)-1-[²H]-**58** and (*R*)-1-[¹³C]-1-[²H]-**58** are thus needed. In comparison to the synthesis of the already prepared substrate for PhnZ, the synthesis of this trimethylated compound (*R*)-**58** and its deuterated and deuterated/¹³C labeled analogs requires only one additional step. However, this last step proved difficult.



Scheme 37: Overview of the synthetic route for the synthesis of (*R*)-1-[¹³C]-1-[²H]-**58**.

The synthetic route is here described for the deuterated and ¹³C labeled compound; but it can likewise be applied to the synthesis of the deuterated and unlabeled analogs. Following a literature procedure, 1-[¹³C]-**94** was protected as phthalimide and then converted to the corresponding acyl chloride using thionyl chloride. The P-C bond was formed through an Arbuzov reaction and enantioselective reduction was carried out with Noyori's catalyst (*S,S*)-**72**. To obtain the deuterated analog, DCO₂H was used instead of HCO₂H for the asymmetric transfer hydrogenation. This compound cannot be replaced by the cheaper, commercially available compound DCO₂D due to an observed additional incorporation of the acidic deuterium in β-position to the phosphorus atom *via* keto-enol tautomerism. However, DCO₂H could be easily prepared by reaction of commercially available DCO₂Na and dry H₃PO₄.¹⁰⁵

The degree of deuteration for (*R*)-1-[²H]-**97** and (*R*)-1-[¹³C]-1-[²H]-**97** was determined as follows. In the ¹³C NMR [6Jul0219/10] spectrum of the ¹³C-labeled compound, it was possible to clearly distinguish signals from the deuterated and non-deuterated compound (figure 14). The signals from ¹³C-D are highlighted in red (td, 66.67 ppm, *J* = 161.4 Hz, *J* = 22.1 Hz). The signals of the non-deuterated compound ¹³C-H are slightly shifted to lower field (d, 67.06 ppm, *J* = 161.7 Hz) and marked in green.

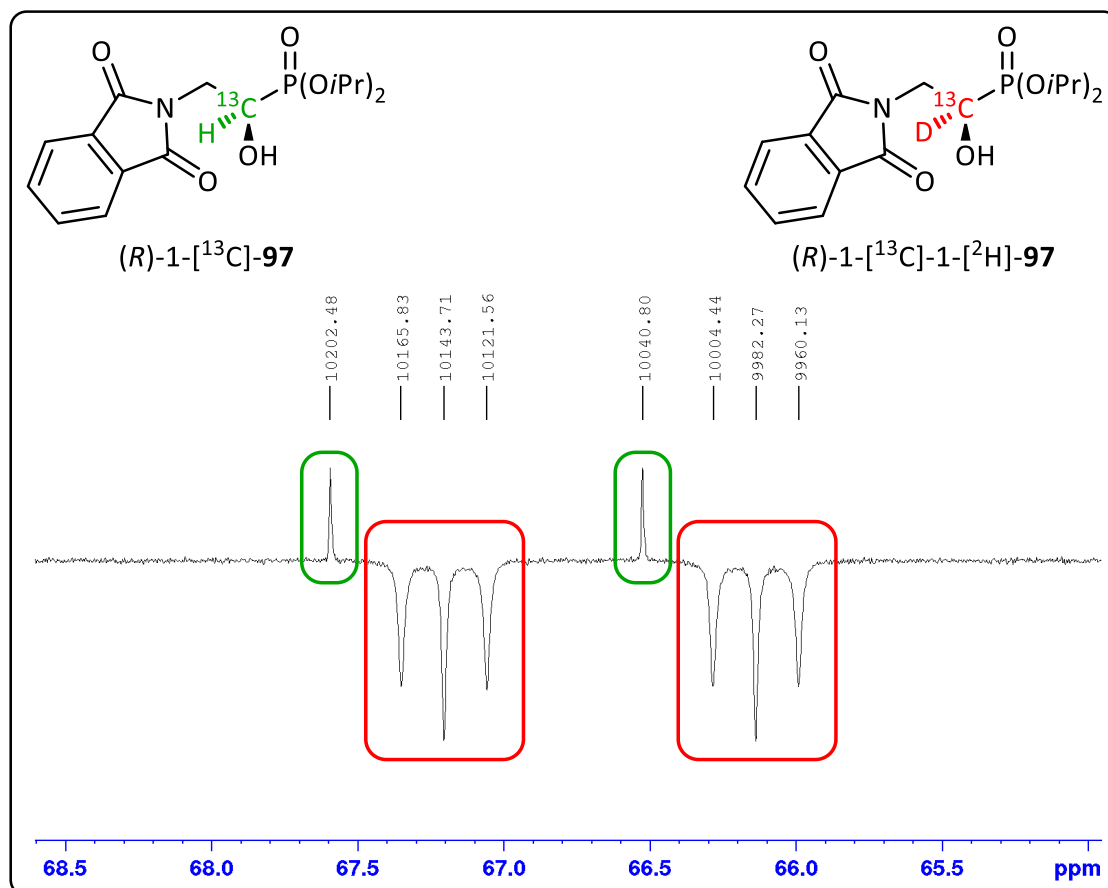


Figure 14: ¹³C NMR of (*R*)-1-[¹³C]-1-[²H]-**97**.

As the signals in the ¹³C NMR cannot be quantified, due to different nature of the carbon atoms (quaternary and tertiary) and too short relaxation times in the performed NMR experiment, additional experiments were necessary.

Therefore, 2D NMR spectra (HSQC, ¹³C-decoupled [6Jul0219/98] and ¹³C-coupled [6Jul0219/101]) were recorded additionally to identify the residual ¹³C-H signal in the ¹H NMR spectrum, where they can be accurately quantified with respect to signals of the desired deuterated product (figure 15).

In the upper picture the ^{13}C -decoupled signals are highlighted in red, while the ^{13}C -coupled signals are marked in light violet. It is clearly visible that the duplet (67.06 ppm, $J = 161.7$ Hz), generated by ^{13}C -H, couples in a region of the ^1H NMR with very low signal intensity. Thus, the spectrum intensity was increased for the respective region and the protons attached to the ^{13}C -atom are highlighted in red (lower picture).

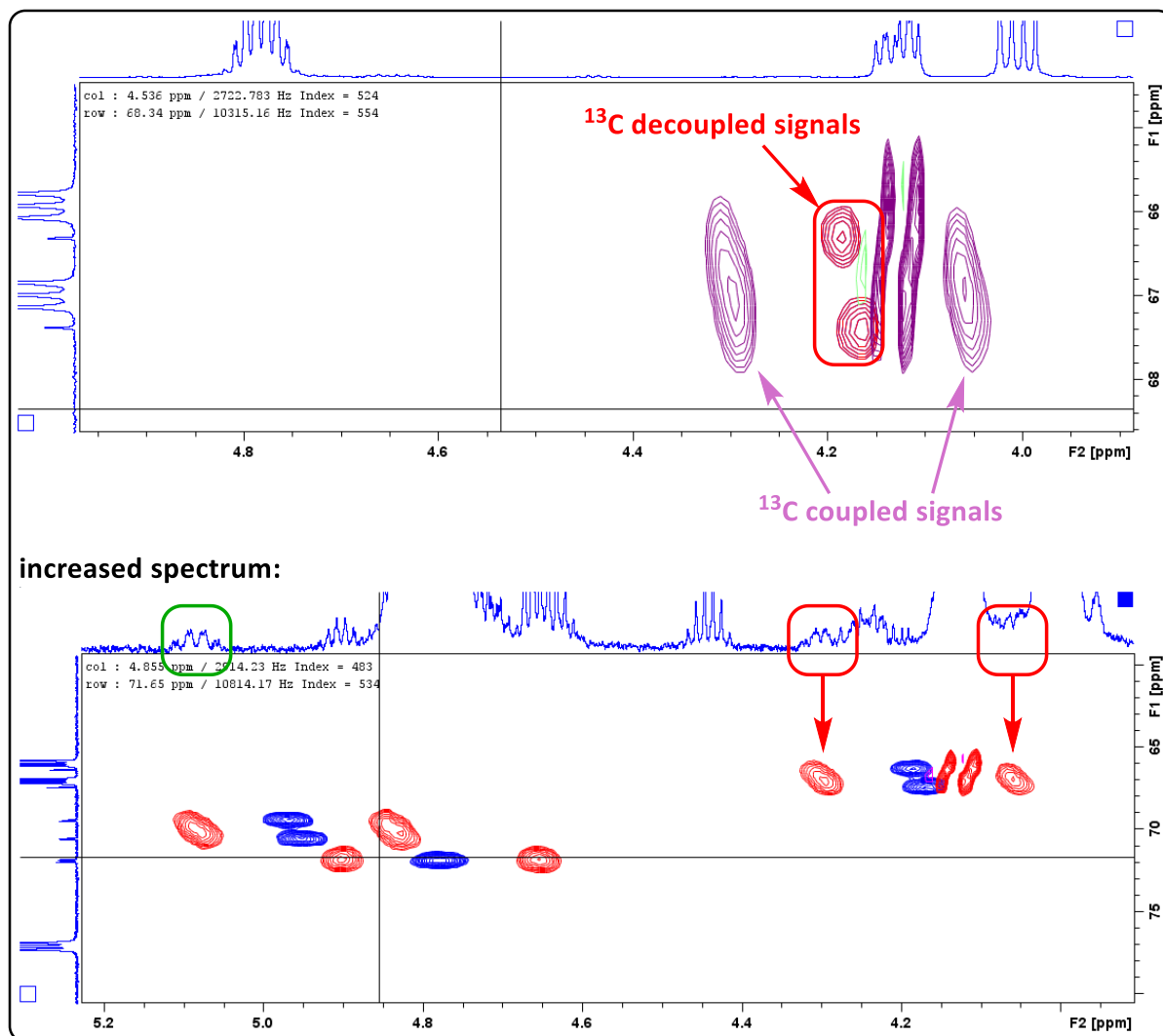


Figure 15: Upper row: HSCQ spectrum of **97** with (red box) and without (marked in violet) ^{13}C -decoupling; lower row: zoom of the relevant region of the ^{13}C -coupled ^1H NMR with increased intensity; the ^{13}C signals of the non-deuterated compound couple in a region of ^1H NMR with very low signal intensity (red boxes).

One half of the signal derived from the non-deuterated compound overlaps with other signals, while the second half is pretty well visible. Comparing the relative intensity of this signal to the intensity of the ^{13}C -satellites of another signal nearby, derived from two protons (marked in green) shows that the absolute amount of the non-deuterated compound is less than 1%.

Thus, the degree of deuterium labeling is $\geq 99\%$, despite the relatively intensive looking signals observed in ^{13}C NMR. The same result was obtained for (*R*)-1-[^2H]-**97**.

Global deprotection was accomplished as described in the literature. First the isopropyl groups were removed with 6M HCl, followed by removal of the phthalimide moieties with an aqueous solution of ammonia (25%). As previously discussed for α -hydroxyphosphonic acids, purification per cation exchange chromatography over Dowex 50W / H^+ -form is possible. The products were obtained in good yields and the specific optical rotations were in agreement to those reported in the literature for the non-labeled compounds. The degree of deuteration for (*R*)-1-[^2H]-**34** was $\geq 98\%$, however, for (*R*)-1-[^{13}C]-1-[^2H]-**34** the deuteration was only $\geq 94\%$

The obtained products (*R*)-(2-amino-1-hydroxyethyl)phosphonic acid [(*R*)-**34**], (*R*)-1-[^2H]-2-amino-1-hydroxyethyl)phosphonic acid {(*R*)-1-[^2H]-**34**} and (*R*)-1-[^{13}C]-1-[^2H]-2-amino-1-hydroxyethylphosphonic acid {(*R*)-1-[^{13}C]-1-[^2H]-**34**} finally needed to be methylated to obtain the required compounds for enzymatic studies on the mechanism of TmpB. The methylation was challenging, although it is often described in the literature. It was optimized using racemic 1-OH-2-AEP and then applied to all three enantiopure (and isotopically labeled) target molecules. MeOH was tested as solvent and a mixture of MeOH/water, as (*R*)-**34** is only partially soluble in pure MeOH. Several bases were tested for the deprotonation of the amine, amongst them NH_3 (25%, aqueous), Et_3N , $(\text{NH}_4)_2\text{CO}_3$, $\text{Ba}(\text{OH})_2$ and K_2CO_3 . Even after heating the reaction mixture only the last one effectively produced the desired product. After 10 minutes of stirring with K_2CO_3 (5 eq.) in MeOH, MeI (4 eq.) was added and stirring was continued at room temperature for at least 24h. The reaction process was easily traceable by ^{31}P NMR. The peaks for the starting material, the intermediate compounds (mono- and dimethylated species) as well as for the product are clearly distinguishable.

While the synthesis itself could be accomplished with good yield after a few optimization cycles, the purification of the product turned out to be very difficult. At the end point of the reaction (judged by ^{31}P NMR), the mixture became turbid again. Thus, the solid and the liquid phase were separated and analyzed independently. Unfortunately, the product was found in the solution as well as in the solid phase, thus the whole suspension had to be used to quantitatively isolate the product. The solvent was removed before the crude product was redissolved in water and acidified to remove carbonate. First, HCl was used for this purpose,

which proved difficult to remove by ion exchange chromatography due to a similar retention of chloride ions and the product on the resin. Thus, during later trials H_2SO_4 was used to acidify. The next step was an extraction with Et_2O , to remove excess MeI . Other tested solvents proved less effective for this purpose.

Several different ion exchanging resins were tested in order to remove potassium cations, as well as iodide and sulfate anions from the product. Using a cation exchanger, the envisaged strategy involved retaining the product on the resin, while no retention for anions is expected. Thus, the product should be easily separable from the latter. However, using the cationic resin Dowex 50W / H^+ , the product could not be recovered, even by using high concentrations of formic acid as eluent. So, a different strategy was tested, using the anion exchanging resin Dowex Monosphere-550A/ OH^- . Like this, it was possible to obtain the pure salt-free product, although in poor to medium yield. It was found that approximately half of the product was not retained on the column and eluted directly with the first fractions alongside the potassium ions. The remaining compound could be eluted in salt free form from the resin with formic acid, giving 58% (*R*)-**58**, 46% (*R*)-1- ^{2}H -**58** and 44% (*R*)-1- ^{13}C -1- ^{2}H -**58**. Using a higher amount of ion exchanger did not solve the problem, neither did changing the pH of the sample before applying it to the column. However, we found that applying those impure fractions again to the same type of resin is a practicable work-around. Like this it was possible to isolate additional product-containing fractions. Other tested anion exchanging resins such as Amberlite Cl^- conditioned with ammonium acetate buffer, gave the same result with even lower overall isolated yields. By applying this procedure, it was possible to reisolate (*R*)-**58**, (*R*)-1- ^{2}H -**58** and (*R*)-1- ^{13}C -1- ^{2}H -**58** in an overall yield of 80%, 58% and 55%, respectively.

Attempts to first remove chloride and iodide ions by precipitation with AgNO_3 in order to improve the reproducibility of the performed ion exchange chromatography were made. Unfortunately, the remaining Ag^+ -ions were found in all product containing fractions. In order to determine the isoelectric point of **58**, an acidimetric titration was performed (figure 16). The idea behind this experiment was that possibly the ion exchange chromatographic separation could be improved by adjusting the pH of the product solution to the isoelectric point before application to the resin. Therefore, about 1.65 mg of the sample and 0.2 mL of 0.1 M HCl were combined and titrated with 0.1 M NaOH. This showed the first proton of the

phosphonate group to be strongly acidic ($pK_a < 2.5$) and the pK_a value of the second phosphonic acid proton to be 6.19.

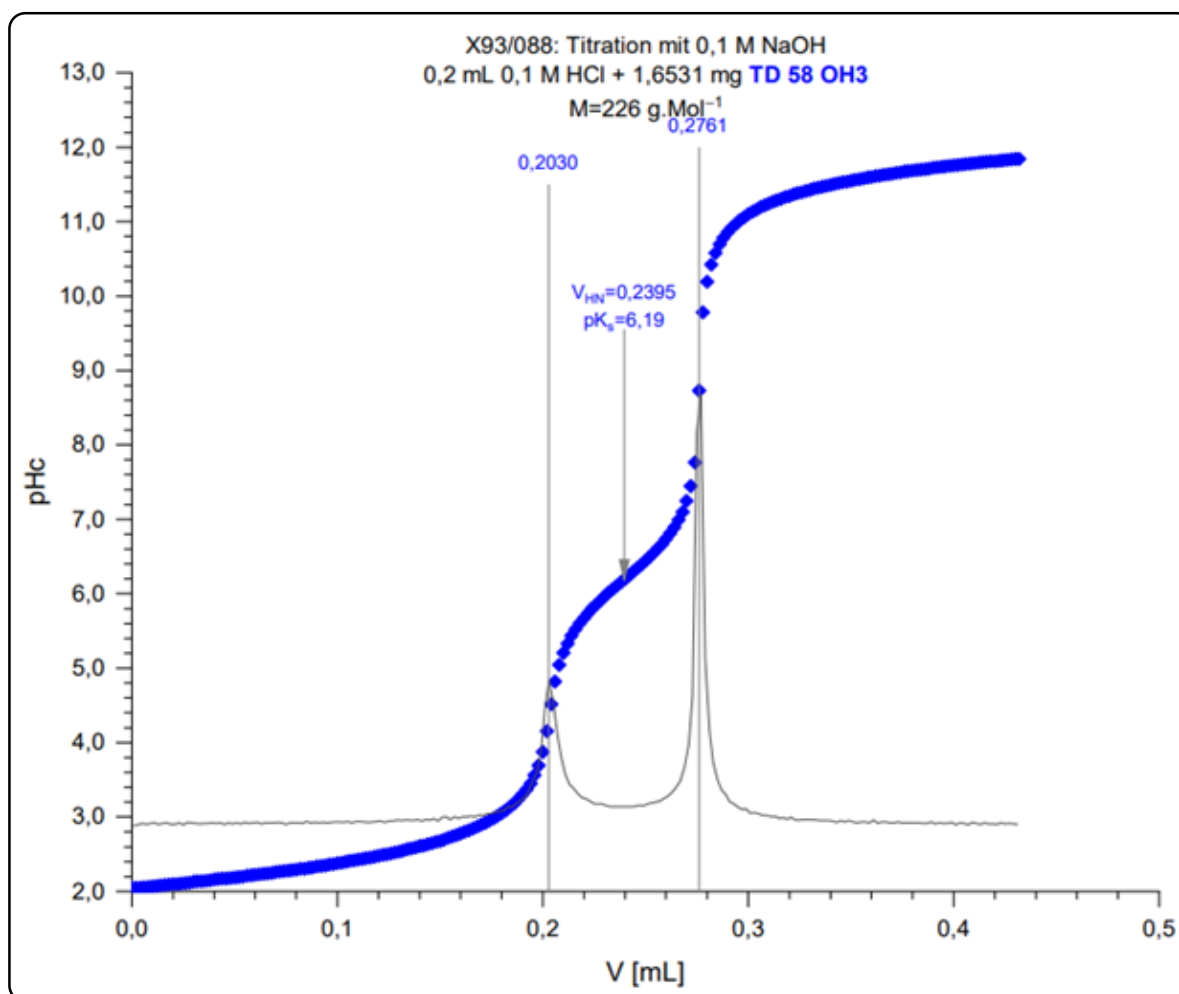


Figure 16: Titration curve of (R)-58.ⁱ

However, adjusting the pH of the crude product containing solution to 6.2 did not improve the separation process.

Finally, varying yields after purification had to be accepted. In order to obtain the highest possible yield, especially in the case of the precious, isotopically labeled compounds, several chromatographic separations had to be performed. The products were crystallized from H₂O/EtOH to give colorless highly hygroscopic needles with varying content of crystal water.

Combustion analysis was performed for all target molecules as final proof of the removal of all accompanying ions. However, this proofed difficult, due to the hygroscopic character of

ⁱ This analysis was done by Johannes Theiner.

these compounds. The samples were especially tested for their content of several standard ions (e.g. sodium, potassium, iodide, sulfate). Satisfyingly, none of these inorganic compounds were detected. All three compounds were pure to elemental analysis and only contained a varying degree of crystal water, depending on the respective sample as can be seen below (table 1). This result was further underpinned by X-ray crystallography (see experimental part).

Table 1: content of crystal water determined by combustion analysis.

compound		C	H	N	O
(R)-58	found	26.37	8.45	6.06	45.20
	calc.	32.79	7.71	7.65	34.94
	calc. + 2.5 H ₂ O	26.32	8.39	6.14	45.57
(R)-58	found	32.19	7.70	7.97	35.21
	calc.	32.79	7.71	7.65	34.94
	calc. + 0.1 H ₂ O	32.47	7.74	7.57	35.47
(R)-1-[²H]-58	found	31.51	7.65	7.72	35.69
	calc.	32.61	7.66	7.61	34.75
	calc. + 0.25 H ₂ O	31.83	7.75	7.42	36.04
(R)-1-[¹³C]-1-[²H]-58	found	31.06	7.50	7.61	35.91
	calc.	32.44	7.62	7.57	34.57
	calc. + 0.35 H ₂ O	31.36	7.74	7.32	36.35

A special phenomenon was observed in the ³¹P NMR spectrum of the target compounds. The ³¹P signal was found to be a pseudo-triplet with relative signal intensities of 1:1:1 (figure 17). The reason for this splitting in the trimethylated compounds is not clear but has been observed alike for TMAEP (**57**) and OH-TMAEP (**58**) in the literature. There, three options were discussed: maybe this signal splitting is due to *I* = 1 of the ¹⁴N nucleus on C2, which is three bonds away from phosphorus, or maybe the methylation effects the dynamics of rotation around the C1-C2 bond. Or it could be derived from a through-space interaction of the phosphonate ion with the trimethylammonium ion.⁹⁸

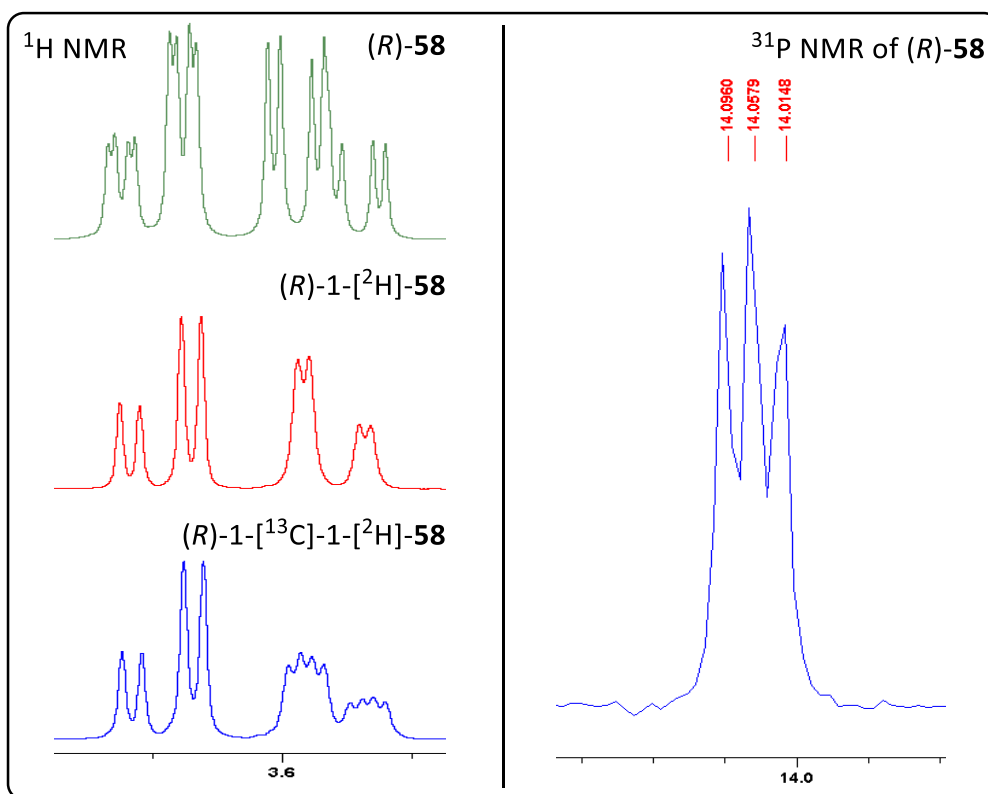


Figure 17: Left side: a comparison of the ^1H NMR signals of the CH_2 -group in β -position to the phosphorus with different coupling patterns depending on the isotope labeling; right side: ^{31}P NMR of (R)-58 with unexpected signal splitting.

4. Experimental part

4.1 General experimental part

Chemicals:

HN_3 was obtained by reaction of NaN_3 and H_2SO_4 according to Wolff.¹²²

DCO_2H was obtained by reaction of deuterated DCO_2Na with H_3PO_4 according to Stankovic.¹⁰⁵

All other chemicals were bought from ABCR, Acros, Fluka, Sigma-Aldrich or TCL and were used without any further purification.

Thin layer chromatography (TLC):

Thin layer chromatography was carried out using Merck silica gel 60 F₂₅₄ glass plates (coating 0.25 mm thick) and spots were visualized either by

- UV light (254 nm)
- iodine
- dipping the plate in Cer-Ammonium-Molybdate (CAM) solution [23 g $(\text{NH}_4)_6\text{Mo}_7\text{O}_{24} \times 4 \text{H}_2\text{O}$, 1 g $\text{Ce}(\text{SO}_4)_2 \times 4 \text{H}_2\text{O}$ in 500 mL 10% aqueous H_2SO_4], followed by heating with a heat gun
- or dipping the plate in ninhydrin solution [0.2% ninhydrin in ethanol (98%)], followed by heating with a heat gun

as specified within the respective procedure.

Compound purification:

Medium pressure liquid chromatography (MPLC):

Chromatographic purification of target compounds was either performed manually or carried out on a fully automated Biotage Isolera Prime flash purification system using KP-Sil separation cartridges 10-100 g (depending on the total amount of substance), filled with Merck silica gel 60 (230-400 mesh).

Ion exchange chromatography (IEC):

Ion exchange chromatography was performed manually, the separations were either carried out using Dowex 50W × 8 /H⁺-form (cation exchanger) or Dowex Monosphere-550A-OH⁻-form (anion exchanger) as specified.

Compound analysis:

NMR spectra:

NMR spectra were either recorded on a Bruker BioSpin AV III HD 700 (¹H: 700.40 MHz, ¹³C: 176.12 MHz), AV III 600 (¹H: 600.25 MHz, ¹³C: 150.93 MHz, ³¹P: 242.99 MHz), AV NEO 400 (¹H: 400.27 MHz, ³¹P: 162.03 MHz) or AV NEO NanoBay 400 (¹H: 400.13 MHz, ³¹P: 161.98 MHz)

The recorded spectra were referenced to the following solvent (residual) peaks:

¹H NMR spectra: CDCl₃: CHCl₃, δ_H = 7.26 ppm

D₂O: HOD, δ_H = 4.79 ppm

toluene-d₈: (C₆D₅)CHD₂, δ_H = 2.08 ppm

¹³C NMR spectra: CDCl₃, δ_C = 77.16 ppm

³¹P NMR spectra: external H₃PO₄ (85% aqueous solution), δ_P = 0.00 ppm.

Mass spectra:

Mass spectra were recorded on a Bruker maXis UHR-TOF (instrument type: Qq-TOF), the samples were ionized by electrospray ionization (ESI).

IR spectra:

Were recorded on a Bruker Vertex 70 IR spectrometer in ATR mode.

X-ray crystallography:

Data were recorded on a Bruker D8 Venture diffractometer at 100.0 K. Olex2¹²³ was used and the structure was solved with XS¹²⁴ structure solution program with direct methods and for refinement XL¹²⁴ refinement package with least squares minimalization was used.

Specific optical rotations:

Optical rotations were determined using a Perkin-Elmer 341 polarimeter in a 1 dm cell, at 20°C and the [α]_D values are given in 10⁻¹ deg cm² g⁻¹.

4.2 General procedures

Several general procedures have been optimized and applied to the synthesis of the described target compounds with small alterations.

4.2.1 General procedure A – Ketophosphonate synthesis via acyl chloride formation and subsequent Arbuzov reaction

The required carboxylic acid is dissolved in CH₂Cl₂ (1.5 mL/mmol, final concentration: 0.66 M) and the solution is cooled to 0°C under argon-atmosphere before dropwise addition of oxalyl chloride (1.10 eq.). The cooling bath is removed, and stirring is continued at 25-30°C for 2-20 h (compound-specific, see below). All volatiles are removed under reduced pressure and the crude acyl chloride is again dissolved in CH₂Cl₂ (1.5 mL/mmol, final concentration: 0.66 M). (O*i*Pr)₃P (1.05 eq.) is added dropwise at 0°C and the mixture is stirred at 0 or 25°C for 1.5-4 h as specified. The solvent is removed *in vacuo* at room temperature to give the desired crude ketophosphonate, which can either be used directly for the next step without purification or stored for approximately four weeks at -25°C.

4.2.2 General procedure B – Synthesis of (±)-α-hydroxyphosphonates by reduction with NaBH₄

NaBH₄ (2 eq.) is grinded in a mortar and added to the crude ketophosphonate (obtained by **general procedure A**) in MeOH (1-3 mL/mmol, final concentration: 1.00 M - 0.33 M) in small portions (strong heat development!) at 0°C. The cooling bath is removed after 1 h and stirring is continued at room temperature for 15-18 h. The reaction is quenched by addition of H₂O (2 mL/mmol). Methanol is removed *in vacuo* and the product is extracted with EtOAc (3 × 1.5 mL/mmol). The combined organic layers are dried (Na₂SO₄), filtered and the solvent removed under reduced pressure to give the crude racemic α-hydroxyphosphonate of interest, which can be purified by MPLC.

4.2.3 General procedure C – Activation of Noyori-catalyst for asymmetric transfer hydrogenation

(*R,R*)- or (*S,S*)-RuCl[(*p*-cymene)-TsDPEN] is dissolved in CH₂Cl₂ (1 mL/100 mg, final concentration: 0.16 M; for smaller amounts than 100 mg: 1 mL) and the resulting solution is washed with potassium hydroxide (aqueous solution, 0.20 M, 1 eq.) in a syringe, upon which the organic layer turns from orange to deep purple. The organic layer is separated, and the

aqueous phase is washed with CH₂Cl₂ (2 × 0.5 mL). The combined organic layers are dried (CaH₂), the solution filtered over a plug of cotton wool and the solid residue is again washed with CH₂Cl₂ (2 × 0.5 mL). The combined filtrates can be directly used for the catalytic transfer hydrogenation (see **general procedure D**).

4.2.4 General procedure D – Synthesis of (*R*)- and (*S*)- α -hydroxyphosphonates via catalytic transfer hydrogenation

A mixture of formic acid (4.40 eq.) and Et₃N (2.60 eq.) is added dropwise to a solution of crude α -ketophosphonate (obtained by **general procedure A**) dissolved in CH₂Cl₂ (2 mL/mmol, final concentration: 0.50 M) under argon atmosphere at 0°C. Then the catalyst solution containing either (*R,R*)- or (*S,S*)-RuOH[(*p*-cymene)-TsDPEN] (0.01-0.05 eq., compound specific, received by **general procedure C**) is added. The resulting reaction mixture is stirred at 35°C for 18 h before removal of the solvent under reduced pressure to give the crude (*R*)- or (*S*)- α -hydroxyphosphonate that can be purified as specified for each compound. [The (*R,R*)-catalyst gives the (*S*)- α -hydroxyphosphonate while the (*S,S*)-catalyst produces the respective (*R*)-hydroxyphosphonate].

4.2.5 General procedure E – Synthesis of α -azido-phosphonates by Mitsunobu reaction (with HN₃)

The respective α -hydroxyphosphonate (obtained by **general procedure B** or **D**) is dried by coevaporation of residual water with toluene (1 mL/mmol). Ph₃P (1.44 eq.) is added and the mixture is dissolved in dry toluene (4 mL/mmol, final concentration: 0.25 M) under argon atmosphere. HN₃ (1.8 eq., solution in toluene, 1.75 M), followed by the specified azodicarboxylate (DEAD, solution in toluene, 40 wt%; or DIAD 98% purity, 1.44 eq.) is added at 0°C. The reaction is quenched by addition of MeOH (2 mL/mmol) after stirring at room temperature for 18 h and stirring is continued for 10 minutes. The solvent is removed *in vacuo* at room temperature to give the crude azide which is purified manually.

4.2.6 General procedure F – Synthesis of (protected) α -aminophosphonates by reductive hydrogenation of azides

The respective α -azidophosphonate (obtained by **general procedure E**) is dissolved in EtOH (3 mL/mmol, final concentration: 0.33 M) and Pd on activated charcoal (10% Pd, 20 mg/mmol) is added. The hydrogenation is performed in a Parr apparatus at 3.5 atm H₂ pressure under

constant shaking for 3 h. Subsequently the mixture is filtered over Celite® (moistened with ethanol) and the solvent is removed under reduced pressure, to yield the desired crude amine, which can be used for the next step without further purification.

If desired, the obtained amine can be directly Boc-protected by addition of Boc₂O (1.3 eq) to the hydrogenation mixture. The reaction mixture is then degassed and the hydrogenation performed at ambient pressure (using a H₂-filled balloon) over 20 h. In this case, the obtained crude products can be purified by MPLC as specified below.

4.2.8 General procedure G – Deprotection of α -aminophosphonates

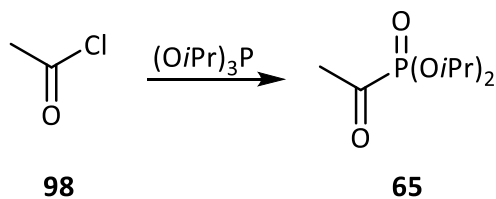
α -Aminophosphonates (obtained by **general procedure F**) are suspended in aqueous HCl (6 M, 10 mL/mmol) and refluxed (120°C oil-bath temperature) for 15 h before removal of the solvent under reduced pressure. The obtained residue is redissolved in H₂O (2 mL/mmol) and again concentrated to dryness before purification by ion exchange chromatography (Dowex 50W \times 8 /H⁺-form) with water or formic acid (1%, aqueous) as eluent. Ninhydrin positive fractions are pooled and the solvent is removed *in vacuo*. The solid residue is crystallized from H₂O/EtOH, to yield the desired α -aminophosphonic acid.

4.2.9 General procedure H – Deprotection of α -hydroxyphosphonates

The desired α -hydroxyphosphonic acid (obtained by **general procedure B** or **D**) is dissolved in dry 1,2-DCE (2 mL/mmol, final concentration: 0.5 M) under argon atmosphere. Subsequently, allyltrimethylsilane (4 eq.), followed by TMSBr (6 eq.) is added and the mixture is stirred at 20-60°C for 1-24 h as specified below. All volatiles are removed under reduced pressure, the residue is redissolved in 1,2-DCE (2 mL/mmol) and again concentrated to dryness. The crude product is taken up in H₂O (2 mL/mmol) and the pH-value is immediately adjusted to 7-8 with aqueous NaOH (0.5-1 M). The product is obtained as its sodium-salt after lyophilization.

4.3 Synthesis of (*R*)-phosphaalanine [(*R*)-**20**]

4.3.1 Diisopropyl 1-Oxoethylphosphonate (**65**)

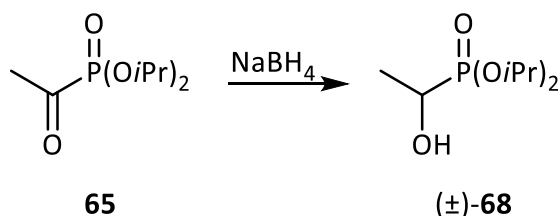


α -Ketophosphonate **65** was obtained in sufficient purity for all subsequent steps by **general procedure A**, starting from commercially available acetyl chloride (**98**, 1.65 g, 1.5 mL, 21.02 mmol) and (*iPrO*)₃P at 0 °C within 4 h. A small sample was purified by fractional distillation (heated to 120 °C, 5 Torr) for analytical purposes.

¹H NMR (400.13 MHz, CDCl₃, [42Aug1120/400], TD 80 Fr 4): δ_{H} = 4.84-4.73 (m, 2H, 2 \times CH *iPr*), 2.47 (d, J = 4.9 Hz, 3H, CH₃-C), 1.37 (d, J = 6.2 Hz, 12H, 4 \times CH₃ *iPr*) ppm.

³¹P NMR (161.98 MHz, CDCl₃, [42Aug1120/401], TD 80 Fr 4): δ_{P} = 4.45 (s, 2 mol%, unknown impurity), -3.34 (s, 4 mol%, unknown impurity), -4.40 (s, 95 mol%, product) ppm.

4.3.2 (\pm)-Diisopropyl (1-hydroxyethyl)phosphonate [(\pm)-**68**]



Ketophosphonate **65** (0.743 g, 3.57 mmol) was dissolved in methanol (final concentration 0.5 M) and reduced according to **general procedure B** over a period of 15 h. The crude product was purified by MPLC [R_{f} (*n*-heptane:EtOAc, 1:3) = 0.31, gradient: 18 \rightarrow 100% EtOAc] to give (\pm)-1-hydroxyphosphonate **68** (0.55 mg, 2.62 mmol, 74%,) as colorless oil.

¹H NMR (700.40 MHz, CDCl₃, [7Aug1920/10], TD 84 nT3): δ_{H} = 4.79-4.71 (m, 2H, 2 \times CH *iPr*), 3.95 (qd, J = 7.0 Hz, J = 3.5 Hz, 1H, CH), 2.68 (broad s, 1H, OH), 1.41 (dd, J = 17.3 Hz, J = 7.0 Hz, 3H, CH₃-CH-P), 1.35 (d, J = 6.3 Hz, 3H, CH₃ *iPr*), 1.35-1.33 (m, 9H, 3 \times CH₃ *iPr*) ppm.

¹³C NMR (176.12 MHz, CDCl₃, [7Aug1920/11], TD 84 nT3): δ_{C} = 71.35 (d, J = 7.1 Hz, CH *iPr*), 71.14 (d, J = 7.3 Hz, CH *iPr*), 64.41 (d, J = 162.9 Hz, CH-P), 24.31 (d, J = 3.5 Hz, CH₃ *iPr*), 24.25 (d,

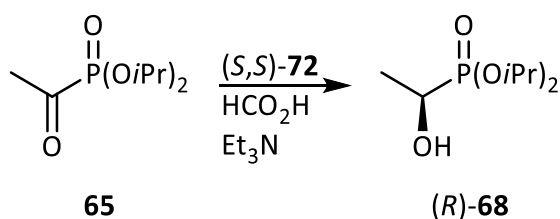
$J = 3.5$ Hz, CH₃ *i*Pr), 24.16 (d, $J = 4.9$ Hz, CH₃ *i*Pr), 24.13 (d, $J = 4.9$ Hz, CH₃ *i*Pr), 17.41 (s, CH₃-CH(OH)-P) ppm.

³¹P NMR: (161.98 MHz, CDCl₃, [42Aug1820/571], TD 84 nT3): $\delta_P = 23.73$ (s) ppm.

HRMS calculated for C₈H₁₉O₄P (210.21 g/mol): [M+Na]⁺ 233.0910; found: [M+Na]⁺ 233.0912.

IR (ATR, TD 84): $\nu = 3305, 2980, 1379, 1216, 1107, 980, 891, 634$ cm⁻¹.

4.3.3 (*R*)-Diisopropyl (1-hydroxyethyl)phosphonate [(*R*)-**68**]



General procedure D was used to convert ketophosphonate **65** (978 mg, 4.70 mmol) to (*R*)-**68** (0.956 mg, 4.55 mmol, 97%). The product was obtained as colorless oil after MPLC [R_f (*n*-heptane:EtOAc, 1:3) = 0.31, gradient: 18 → 100% EtOAc]. The used catalyst (*S,S*)-RuOH[(*p*-cymene)-TsDPEN] [(*S,S*)-**(72)**, 0.01 eq.] was obtained by **general procedure C**.

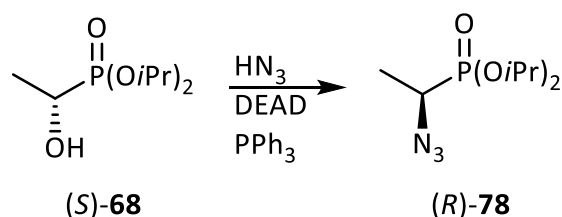
The spectroscopic data were identical to those reported for (\pm)-**68**.

Specific optical rotation: $\alpha_D^{20} = -10.1$ (c 0.97, acetone).

³¹P NMR with chiral solvating agent (161.98 MHz, toluene-*d*₈, [42Aug3120/171], TD 84 + Shift): $\delta_P = 94.42$ [J 0.54, chiral solvating agent (*S*)-**77**], 24.34 [J 0.46, complex of chiral solvating agent with (*R*)-**68**], 24.14 [J 0.003, complex of chiral solvating agent with (*S*)-**68**] → $ee \geq 98\%$.

(*S*)-**68** (1.25 mg, 5.95 mmol, 98%) can be obtained similarly by using (*R,R*)-**72** (0.01 eq) as catalyst. The purity of the product was 98 mol% and of sufficient purity for the subsequent reactions.

4.3.4 (*R*)-Diisopropyl (1-azidoethyl)phosphonate [(*R*)-78]



(*S*)-**68** (764 mg, 3.64 mmol) was converted to the corresponding α -azido phosphonate (*R*)-**78** (656 mg, 2.82 mmol, 77%) by **general procedure E**, using DEAD as azoester. The product was isolated as colorless oil after column chromatography [R_f ($\text{CH}_2\text{Cl}_2:\text{Et}_2\text{O}$, 9:1) = 0.69, solvent ratio used for purification: $\text{CH}_2\text{Cl}_2:\text{Et}_2\text{O}$ = 95:5%].

^1H NMR (400.27 MHz, CDCl_3 , PR1.4.3, [41Mar2919/180]): δ = 4.85-4.72 (m, 2H, 2 \times CH *i*Pr), 3.47 (qd, J = 7.4 Hz, 12.0 Hz, 1H, CH-P), 1.44 (dd, J = 16.9 Hz, J = 7.4 Hz, 3H, $\text{CH}_3\text{-CH(OH)-P}$), 1.37 (d, J = 6.2 Hz, 9H, CH_3 *i*Pr), 1.36 (d, J = 6.2 Hz, 3H, CH_3 *i*Pr) ppm.

^{13}C NMR (150.92 MHz, CDCl_3 , PR1.4.3, [61Apr1719/110]): δ = 72.06 (d, J = 7.3 Hz, CH *i*Pr), 71.98 (d, J = 7.1 Hz, CH *i*Pr), 52.91 (d, J = 159.3 Hz, CH-P), 24.47 (d, J = 3.6 Hz, CH_3 *i*Pr), 24.44 (d, J = 3.7 Hz, CH_3 *i*Pr), 24.28 (d, J = 4.6 Hz, CH_3 *i*Pr), 24.27 (d, J = 4.9 Hz, CH_3 *i*Pr), 14.32 (d, J = 1.4 Hz, $\text{CH}_3\text{-CH-P}$) ppm.

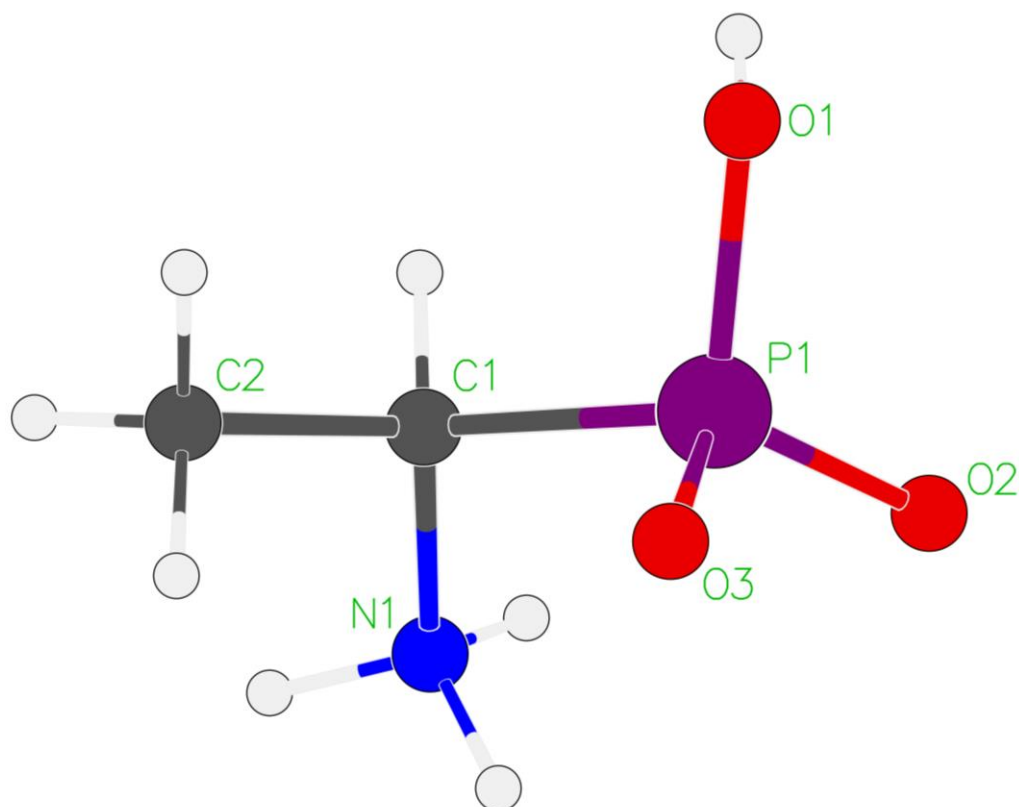
^{31}P NMR (162.02 MHz, CDCl_3 , TD 83 nT, [41Aug1820/491]): δ = 20.67 (s) ppm.

HRMS calculated for $\text{C}_8\text{H}_{18}\text{N}_3\text{O}_3\text{P}$ (235.22 g/mol): $[\text{M}+\text{Na}]^+$ 258.0983; found: $[\text{M}+\text{Na}]^+$ 258.0984.

IR (ATR, TD 83): ν = 2982, 2092, 1380, 1232, 1105, 979, 891, 619 cm^{-1} .

Specific optical rotation: α_D^{20} = -9.9 (c 1.01, acetone).

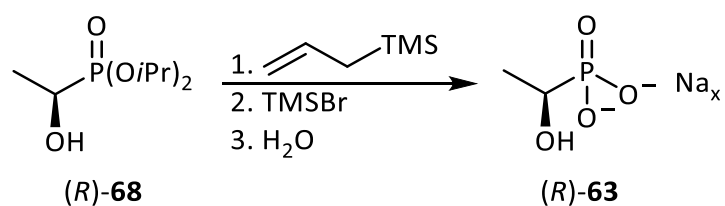
Crystal structure analysis:



This analysis confirmed the absolute configuration, the relevant data can be found in the appendix.

Specific optical rotation: $\alpha_D^{20} = -4.7$ (c 0.70, H₂O).

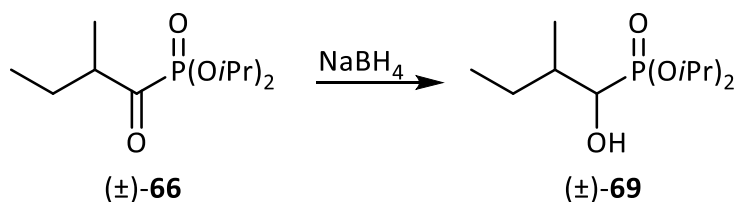
4.3.6 (*R*)-(1-hydroxyethyl)phosphonate as its sodium salt [(*R*)-**63**]



(*R*)-**68** (300 mg, 1.43 mmol) was deprotected using **general procedure H**, with a stirring time of 5 h at 60°C to give (*R*)-**63** (243 mg, quant.)ⁱⁱ as colorless solid after lyophilization.

ⁱⁱ The yield was determined by ³¹P-NMR, by addition of an internal standard [2-AEP (**1**)]. The concentration was 5.8 μmol (*R*)-**63**/mg lyophilizate.

4.4.2 (±)-Diisopropyl (1-hydroxy-2-methylbutyl)phosphonate [(±)-69]



(±)-66 (2.56 g, 10.23 mmol) was reduced by **general procedure B**, using a reaction concentration of 1.0 M and a stirring time of 18 h, to give (±)-69 (2.00 g, 7.93 mmol, 77%) as colorless oil after MPLC purification [R_f (*n*-heptane:EtOAc, 1:3) = 0.57, gradient: 18 → 100% EtOAc)].

¹H NMR (700.40 MHz, CDCl₃, [7Sep0320/10], KS 1210): δ_H = 4.79-4.72 (m, 2H, 2 × CH *i*Pr), 3.78-3.72 (m, 1H, CH-P), 2.12 (m, 1H, OH), 1.88-1.79 (m, 1H, CH-CH-P), 1.45 (ABXP system; A-part: m, 1.59-1.53; B-part: m, 1.41-1.29; 2H, CH₂) 1.34 (d, J = 6.2 Hz, 12H, 4 × CH₃ *i*Pr), 1.04 (d, J = 6.9 Hz, 3H, CH₃-CH), 0.92 (t, J = 7.4 Hz, 3H, CH₃-CH₂) ppm.

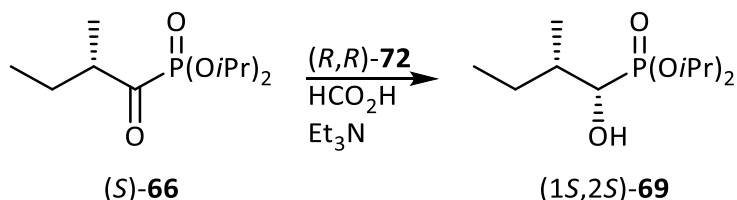
¹³C NMR (176.12 MHz, CDCl₃, [7Jul2920/11], KS 1210): δ_C = 71.44 (d, J = 157.4 Hz, CH-P), 71.14 (d, J = 7.2 Hz, CH *i*Pr), 71.11 (d, J = 7.3 Hz, CH *i*Pr), 36.43 (d, J = 2.1 Hz, CH-CH-P), 26.82 (d, J = 12.3 Hz, CH₂), 24.32 (d, J = 2.9 Hz, CH₃ *i*Pr), 24.31 (d, J = 3.1 Hz, CH₃ *i*Pr), 24.15 (d, J = 4.7 Hz, 2C, 2 × CH₃ *i*Pr), 14.19 (d, J = 4.8 Hz, CH₃-CH-CH), 11.79 (s, CH₃-CH₂) ppm.

³¹P NMR: (161.98 MHz, CDCl₃, [42Jul2820/261], KS 1210): δ_P = 23.58 (s) ppm.

HRMS calculated for C₁₁H₂₅O₄P (252.29 g/mol): [M+Na]⁺ 275.1388; found: [M+Na]⁺ 275.1392.

IR (ATR, KS 1210): ν = 3315, 2978, 1385, 1209, 1105, 979, 886, 626 cm⁻¹.

4.4.3 (1*S*,2*S*)-Diisopropyl (1-hydroxy-2-methylbutyl)phosphonate [(1*S*,2*S*)-69]



(*S*)-66 (650 mg, 2.60 mmol) was reduced following **general procedure D**, using (*R,R*)-RuOH[(*p*-cymene)-TsDPEN] (0.02 eq.), obtained by **general procedure C** In this case the reaction was

HRMS calculated for C₅H₁₄NO₃P (167.14 g/mol): [2M+H]⁺ 335.1501; found: [2M+H]⁺ 335.1499.

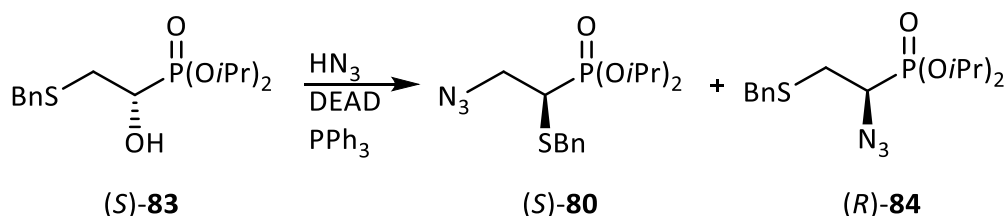
IR (ATR, TD 89): $\nu = 2881, 1610, 1525, 1176, 1058, 926, 815, 730 \text{ cm}^{-1}$.

Elemental analysis for C₅H₁₄NO₃P (% calculated/% found): C (35.93/35.60), H (8.44/8.56), N (8.39/8.09), O (28.72/28.96), P (18.53/18.35).

Specific optical rotation: $\alpha_D^{20} = -8.7$ (c 1.08, H₂O).

4.5 Synthesis of (*S*)-phosphaisocysteine [(*S*)-**62**]

4.5.1 (*S*)-Diisopropyl [2-azido-1-(benzylthio)ethyl]phosphonate [(*S*)-**80**] and (*R*)-diisopropyl [1-azido-2-(benzylthio)ethyl]phosphonate [(*R*)-**84**]



(*S*)-**80** and (*R*)-**84** were obtained in admixture with each other, starting from (*S*)-**83** (354 mg, 1.07 mmol) by following **general procedure E**. In this case CH₂Cl₂ was used as solvent and DEAD as azoester, to obtain a mixture of (*S*)-**80** (174 mg, 0.49 mmol, 46 %) and (*R*)-**84** (116 mg, 0.32 mmol, 30 %). The isomers could be separated by 2 subsequent column chromatographic separation steps [R_f (CH₂Cl₂:Et₂O, 9:1) = (*S*)-**80**: 0.44 (*R*)-**84**: 0.53, solvent ratio used for purification: CH₂Cl₂:Et₂O = 95:5%].

(*S*)-**80**:

¹H NMR (*S*)-**80** (700.40 MHz, CDCl₃, [7Aug2620/10], TD 60): $\delta_H = 7.38\text{-}7.37$ (m, 2H, 2 × CH arom), 7.34-7.31 (m, 2H, 2 × CH arom), 7.28-7.25 (m, 1H, 2 × CH arom), 4.77 (symm m, 2H, 2 × CH *i*Pr), 4.00 (ABP-System; A-Part: dd, $J_{AB} = 13.0$ Hz, $J_{AP} = 1.3$ Hz; B-Part: d, $J_{AB} = 13.0$ Hz, 2H, CH₂ Bn), 3.65 (ddd, $J_{XA} = 13.0$ Hz, $J_{XP} = 11.4$ Hz, $J_{XB} = 4.5$ Hz, 1H, CH-P), 3.09 (ABXP-System; A-Part: ddd, 3.4, $J_{AX} = 13.0$ Hz, $J_{AB} = J_{AP} = 8.5$ Hz; B-Part: ddd, 2.74, $J_{BP} = 17.2$ Hz, $J_{AB} = 8.5$ Hz, $J_{BX} = 4.5$ Hz, 2H, CH₂-CH-P), 1.34 (d, $J = 6.1$ Hz, 3H, CH₃), 1.33 (d, $J = 6.6$ Hz, 3H, CH₃), 1.32 (d, $J = 6.8$ Hz, 3H, CH₃), 1.31 (d, $J = 6.2$ Hz, 3H, CH₃) ppm.

¹³C NMR (*S*)-**80** (176.12 MHz, CDCl₃, [7Aug2620/11], TD 60): $\delta_C = 137.13$ (s, C arom), 129.47 (s, 2C, 2 × CH arom), 128.77 (s, 2C, 2 × CH arom), 127.59 (s, CH arom), 72.27 (d, $J = 7.3$ Hz, CH *i*Pr),

71.86 (d, $J = 7.3$ Hz, CH *i*Pr), 51.82 (d, $J = 2.9$ Hz, $\underline{\text{C}}\text{H}_2\text{-CH-P}$), 40.55 (d, $J = 148.3$ Hz, CH-P), 37.12 (d, $J = 3.0$ Hz, CH_2 Bn), 24.36 (d, $J = 3.2$ Hz, CH_3), 24.26 (d, $J = 3.7$ Hz, CH_3), 24.06 (d, $J = 5.2$ Hz, CH_3), 23.97 (d, $J = 5.6$ Hz, CH_3) ppm.

^{31}P NMR (*S*)-**80** (161.98 MHz, CDCl_3 , [41Aug2520/521], TD 60): $\delta_{\text{P}} = 20.09$ (s) ppm.

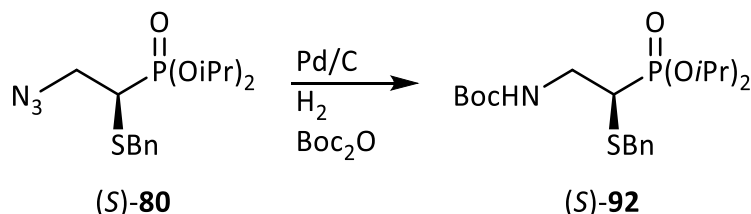
HRMS calculated for $\text{C}_{15}\text{H}_{24}\text{N}_3\text{O}_3\text{PS}$ (357.41 g/mol): $[\text{M}+\text{Na}]^+$ 380.1174; found: $[\text{M}+\text{Na}]^+$ 380.1172.

IR (*R*)-**80** (ATR, TD 60): $\nu = 2979, 2931, 2097, 1380, 1245, 1105, 978, 704$ cm^{-1} .

Specific optical rotation (*S*)-**80**: $\alpha_{\text{D}}^{20} = -28.8$ (c 0.97, acetone).

^{31}P NMR with chiral solvating agent (161.98 MHz, toluene- d_8 , [42Aug3120/161], TD 60 + Shift): $\delta_{\text{P}} = 95.31$ [f 0.54, chiral solvating agent (*S*)-**77**], 20.21 [f 0.46, complex of chiral solvating agent with (*S*)-**80**], [peak from complex of chiral solvating agent with (*R*)-**80** not detected] $\rightarrow ee \geq 99\%$.

4.5.2 (*S*)-*tert*-Butyl [2-(benzylthio)-2-(diisopropoxyphosphoryl)ethyl]carbamate [(*S*)-**92**]



The reduction and simultaneous Boc-protection of (*S*)-**80** (153 mg, 0.43 mmol) was performed following **general procedure F** to yield (*S*)-**92** (153 mg, 0.35 mmol, 82 %) as colorless solid.

Attempts to obtain a completely pure sample of (*S*)-**92** by flash column chromatography failed. (Solvent used: $\text{CH}_2\text{Cl}_2\text{:Et}_2\text{O}$, 4:1) due to an unknown impurity with the same R_f value. The given ^1H - and ^{13}C -spectroscopic data represent the signals which have been tentatively assigned to the product from a sample of approximately 89 mol% purity (judged by ^{31}P NMR).

^1H NMR (600.25 MHz, CDCl_3 , [61Oct0120/10], TD 102): $\delta_{\text{H}} = 7.39\text{-}7.34$ (m, 2H, CH arom), 7.32-7.27 (m, 2H, CH arom), 7.25-7.22 (m, 1H, CH arom), 5.18 (s, 1H, NH), 4.81-4.66 (m, 2H, 2 \times CH *i*Pr), 3.92 (AB-system; A-part: br d, $J_{\text{AB}} = 13.3$ Hz; B-part: d, $J_{\text{AB}} = 13.3$ Hz, 2H, CH_2 Bn), 3.61-3.50

(m, 1H, CH-P), 3.04 (ABXP-System; A-part: m, 3.46-3.34; B-part: ddd, 2.66, $J_{AB} = 16.5$ Hz, $J_{BP} = J_{XB} = 6.5$ Hz, 2H, $\underline{\text{CH}}_2\text{-CH-P}$), 1.43 (s, 9H, 3 \times CH₃ Boc), 1.328 (d, $J = 6.0$ Hz, 3H, CH₃ *i*Pr), 1.326 (d, $J = 6.2$ Hz, 3H, CH₃ *i*Pr), 1.31 (d, $J = 6.1$ Hz, 3H, CH₃ *i*Pr), 1.25 (d, $J = 6.1$ Hz, 3H, CH₃ *i*Pr) ppm.

¹³C NMR (150.93 MHz, CDCl₃, [61Oct0120/11], TD 102): $\delta_c = 155.83$ (s, $\underline{\text{C}}\text{O}$ Boc), 137.44 (s, C arom), 129.44 (s, 2C, 2 \times CH arom), 128.72 (s, 2C, 2 \times CH arom), 127.47 (s, CH arom), 79.47 (s, $\underline{\text{C}}(\text{CH}_3)_3$), 72.01 (d, $J = 7.0$ Hz, CH *i*Pr), 71.78 (d, $J = 7.0$ Hz, CH *i*Pr), 40.39 (s, CH₂ Bn), 40.11 (d, $J = 147.3$ Hz, CH-P), 36.33 (d, $J = 3.8$ Hz, $\underline{\text{C}}\text{H}_2\text{-CH-P}$), 28.52 (s, 3C, 3 \times CH₃ Boc), 24.31 (d, $J = 3.1$ Hz, CH₃ *i*Pr), 24.27 (d, $J = 3.7$ Hz, CH₃ *i*Pr), 24.07 (d, $J = 5.0$ Hz, CH₃ *i*Pr), 23.90 (d, $J = 5.3$ Hz, CH₃ *i*Pr) ppm.

³¹P NMR: (162.02 MHz, CDCl₃, [41Sep2520/331], TD 102 Fr 28-47): $\delta_p = 22.21$ (s, 89 mol%, product), 21.80 (s, 11 mol%, unknown impurity) ppm.

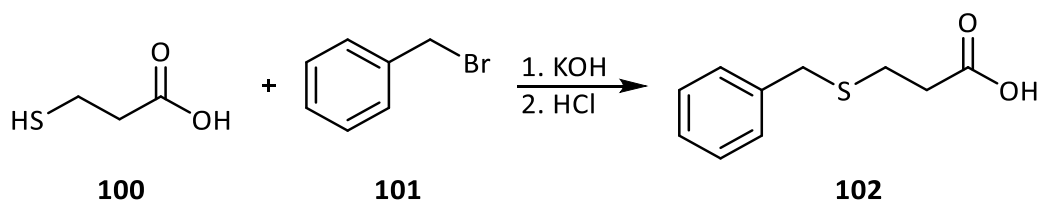
HRMS calculated for C₂₀H₃₄NO₅PS (431.53 g/mol): [M+Na]⁺ 454.1793; found: [M+Na]⁺ 454.1784.

IR (ATR, TD 102): $\nu = 3336, 2978, 2927, 1700, 1523, 1228, 1169, 978$ cm⁻¹.

Specific optical rotation: $\alpha_D^{20} = -25.6$ (*c* 0.50, acetone).

4.6 Synthesis of (*S*)-phosphamethionine[(*S*)-**60**]

4.6.1 3-(Benzylthio)propanoic acid (**102**)¹⁰⁸



A solution of KOH (4.76 g, 84.79 mmol) in H₂O (6 mL) was added to **100** (3.00 g, 28.26 mmol), dissolved in EtOH (15 mL). After 30 minutes of stirring, benzyl bromide (**101**, 5.32 g, 31.09 mmol) was added and the mixture was refluxed for 3.5 h. EtOH was removed under reduced pressure and the remaining aqueous phase was acidified with conc. HCl (37 %) to pH 1. The resulting solution was extracted with Et₂O (3 \times 15 mL), the combined organic layers were washed with H₂O (2 \times 20 mL), dried (Na₂SO₄) and filtered. The solvent was removed *in vacuo* to yield **102** (5.37 g, 27.36 mmol, 97%) as slightly yellow solid.

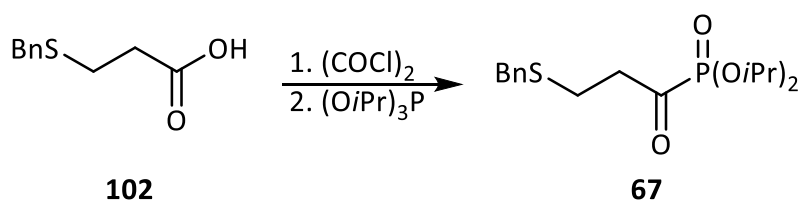
¹H NMR (700.40 MHz, CDCl₃, [7Sep0320/20], TD 91): δ_H = 10.60 (broad s, 1H, OH), 7.34-7.23 (m, 5H, 5 × CH arom), 3.74 (s, 2H, CH₂ Bn), 2.69 (dd, *J* = 7.3 Hz, *J* = 7.2 Hz, 2H, CH₂-CO), 2.59 (dd, *J* = 7.3 Hz, *J* = 7.2 Hz, 2H, CH₂-S) ppm.

¹³C NMR (176.12 MHz, CDCl₃, [7Sep0320/21], TD 91): δ_C = 176.84 (s, CO), 138.06 (s, C arom), 128.98 (s, 2C, 2 × CH arom), 128.75 (s, 2C, 2 × CH arom), 127.32 (s, CH arom), 36.51 (s, CH₂ Bn), 34.22 (d, *J* = 2.1 Hz, CH₂-CO), 25.98 (s, CH₂-S) ppm.

HRMS calculated for C₁₀H₁₂O₂S (196.26 g/mol): [M+Na]⁺ 219.0456; found: [M+Na]⁺ 219.0445.

IR (ATR, TD 91): ν = 2904, 1696, 1412, 1265, 1194, 920, 698, 656 cm⁻¹.

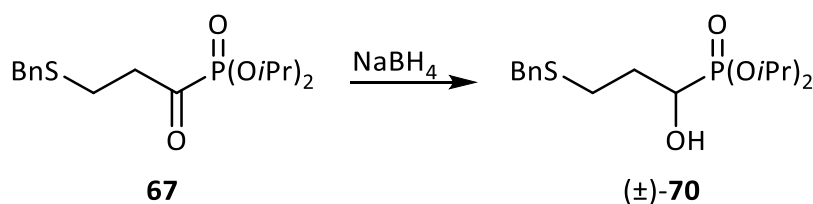
4.6.2 Diisopropyl [3-(benzylthio)propanoyl]phosphonate (**67**)



Acyl chloride formation by **general procedure A**, starting from **102** (5.00 g, 25.48 mmol), was complete after 20 h at 30°C. The subsequent reaction with (OiPr)₃P was performed at 25°C for 4 h to give ketophosphonate **67** as colorless oil of sufficient purity for the subsequent reactions.

³¹P NMR (162.03 MHz, CDCl₃, [42Sep0120/251], TD 92): δ_P = 17.98 (s, 2 mol%, unknown impurity), 17.68 (d, *J* = 26.1 Hz, 6 mol%, unknown impurity), 9.07 (s, 5 mol%, unknown impurity), 5.59 (s, 3 mol%, unknown impurity), 4.45 (s, 7 mol%, unknown impurity), -2.57 (d, *J* = 26.1 Hz, unknown impurity), -3.33 (s, 3 mol%, unknown impurity), -4.70 (s, 74 mol% product) ppm.

4.6.3 (±)-Diisopropyl [3-(benzylthio)-1-hydroxypropyl]phosphonate [(±)-70]



Ketophosphonate **67** (699 mg, 2.03 mmol) was reduced by **general procedure B** (reaction concentration 0.33 M) to give (±)-**70** (550 mg, 1.59 mmol, 78%) as colorless oil after MPLC [R_f (*n*-heptane:EtOAc, 1:3) = 0.38, gradient: 18 → 100% EtOAc] within 15 h.

¹H NMR (600.25 MHz, CDCl₃, [61Sep1120/220], ET 1): δ_{H} = 7.32-7.22 (m, 5H, 5 × CH arom), 4.75 (spt, J = 6.2 Hz, 1H, CH *i*Pr), 4.73 (spt, J = 6.2 Hz, 1H, CH *i*Pr), 3.97-3.94 (ddd, J = 4.5 Hz, 3.4 Hz, 9.7 Hz, 1H, CH-P), 3.72 (AB-system, J_{AB} = 13.8 Hz, 2H, CH₂ Bn), 2.76 (broad s, 1H, OH), 2.63 (ABXX'-System; A-Part: ddd, J_{AB} = 13.2 Hz, J_{AX} = 5.1 Hz, $J_{\text{AX}'}$ = 7.7 Hz; B-Part: ddd, J_{AB} = 13.2 Hz, J_{AX} = 15.6 Hz, $J_{\text{AX}'}$ = 7.9 Hz, CH₂-S), 2.01-1.88 (ABXX'P-system: m, 2H, CH₂-CH(OH)-P), 1.330 (d, J = 6.3 Hz, 6H, 2 × CH₃), 1.327 (d, J = 6.2 Hz, 6H, 2 × CH₃) ppm.

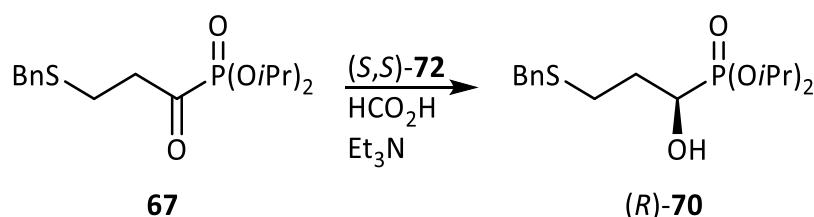
¹³C NMR (150.93 MHz, CDCl₃, [61Sep1120/221], ET 1): δ_{C} = 138.42 (s, C arom), 129.01 (s, 2C, 2 × CH arom), 128.67 (s, 2C, 2 × CH arom), 127.16 (s, CH arom), 71.50 (d, J = 7.2 Hz, CH *i*Pr), 71.36 (d, J = 7.3 Hz, CH *i*Pr), 66.97 (d, J = 163.0 Hz, CH-P), 36.21 (s, CH₂ Bn), 30.87 (d, J = 1.4 Hz, CH₂-S), 27.68 (d, J = 15.4 Hz, CH₂-CH-P), 24.30 (d, J = 3.5 Hz, CH₃), 24.27 (d, J = 3.6 Hz, CH₃), 24.18 (d, J = 4.7 Hz, CH₃), 24.17 (d, J = 4.8 Hz, CH₃) ppm.

³¹P NMR: (161.98 MHz, CDCl₃, [42Sep1120/261], ET 1): δ_{P} = 22.71 (s) ppm.

HRMS calculated for C₁₆H₂₇O₄PS (346.42 g/mol): [M+Na]⁺ 369.1265; found: [M+Na]⁺ 369.1241.

IR (ATR, ET 1): ν = 3276, 2979, 2929, 1726, 1380, 1220, 986, 629 cm⁻¹.

4.6.4 (*R*)-Diisopropyl [3-(benzylthio)-1-hydroxypropyl]phosphonate [(*R*)-**70**]



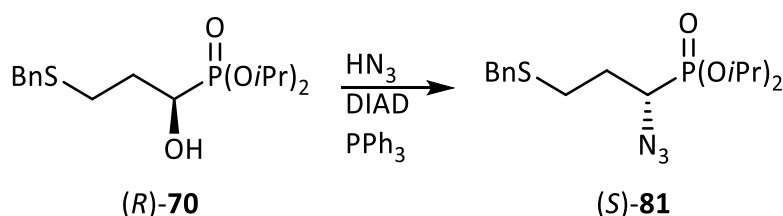
Ketophosphonate **67** (350 mg, 1.02 mmol) was reduced by **general procedure D**, using (*S,S*)-RuOH[*p*-cymene]-TsDPEN] as catalyst, obtained by **general procedure C** (0.05 eq.). This yielded (*R*)-**70** (346 mg, 1.00 mmol, 98%) as colorless oil after MPLC [R_f (*n*-heptane:EtOAc, 1:3) = 0.38, gradient: 18 → 100% EtOAc].

The spectroscopic data were identical to those reported for (\pm)-**70**.

Specific optical rotation: $\alpha_D^{20} = -29.6$ (c 0.85, CH₂Cl₂).

³¹P NMR with chiral solvating agent (161.98 MHz, toluene-*d*₈, [42Sep1120/251], ET 1 + Shift): $\delta_P = 95.95$ [J 0.73, chiral solvating agent (*S*)-**77**], 23.30 [J 0.27, complex of chiral solvating agent with (*R*)-**70**], 23.48 [J 0.002, complex of chiral solvating agent with (*S*)-**70**] → $ee \geq 98\%$.

4.6.5 (*S*)-Diisopropyl [1-azido-3-(benzylthio)propyl]phosphonate [(*S*)-**81**]



The transformation of (*R*)-**70** (260 mg, 0.75 mmol) to the colorless oil (*S*)-**81** (209 mg, 0.56 mmol, 75%) was accomplished following **general procedure E**, using DIAD as azoester. The product was purified by column chromatography [R_f (CH₂Cl₂:Et₂O, 4:1) = 0.81, solvent ratio used for purification: 95:5%]

¹H NMR (600.25 MHz, CDCl₃, [61Sep1820/120], ET 9): $\delta_H = 7.34$ -7.23 (m, 5H, 5 × CH arom), 4.79 (spt, $J = 6.2$ Hz, 1H, CH *i*Pr), 4.77 (spt, $J = 6.2$ Hz, 1H, CH *i*Pr), 3.71 (AB-system; $J_{AB} = 13.7$ Hz, 2H, CH₂ Bn), 3.63 (ddd, $J_1 = J_2 = 11.4$ Hz, $J_3 = 3.2$ Hz, 1H, CH-P), 2.56 (ABXX'P-System; A-part: dddd, $J_{AB} = 13.4$ Hz, $J_2 = 7.6$ Hz, $J_3 = 4.6$ Hz, $J_4 = 1.3$ Hz; B-part: m, 2.54-2.47, 2H, CH₂-S), 2.01-1.88 (ABX₂X'P-System; A-part: m, 2.05-1.98; B-part: m, 1.88-1.80, 2H, CH₂-CH-P), 1.364

^1H - and ^{13}C -spectroscopic data represent the signals which have been tentatively assigned to the product from a sample of approximately 83 mol% purity (judged by ^{31}P NMR).

^1H NMR (600.25 MHz, CDCl_3 , [61Oct0120/20], ET 20): δ_{H} = 7.30-7.21 (m, 5H, CH arom), 4.74-4.65 (m, 2H, 2 \times CH *i*Pr), 4.63 (d, J = 10.0 Hz, 1H, NH), 4.03 (tdd, J = 18.1 Hz, J = 10.4 Hz, J = 3.5 Hz, 1H, CH-P), 3.71 (s, 2H, CH_2 Bn), 2.49 (ABXX'P-System; A-part: m, 2.55-2.51; B-part: m, 2.48-2.43, 2H, CH_2 -S), 1.90 (ABXX'X''P-System; A-Part: m, 2.12-2.05; B-Part: m, 1.75-1.67, 2H, CH_2 -CH-P), 1.42 (s, 9H, 3 \times CH_3 Boc), 1.32 (d, J = 6.1 Hz, 6H, 2 \times CH_3 *i*Pr), 1.30 (d, J = 7.2 Hz, 3H, CH_3 *i*Pr), 1.28 (d, J = 6.9 Hz, 3H, CH_3 *i*Pr) ppm.

^{13}C NMR (150.93 MHz, CDCl_3 , [61Oct0120/121], ET 20): δ_{C} = 155.83 (d, J = 7.1 Hz, NCO Boc), 138.41 (s, C arom), 129.00 (s, 2C, 2 \times CH arom), 128.63 (s, 2C, 2 \times CH arom), 127.11 (s, CH arom), 80.10 (s, $\text{C}(\text{CH}_3)_3$), 71.51 (d, J = 7.3 Hz, CH *i*Pr), 71.33 (d, J = 6.9 Hz, CH *i*Pr), 47.13 (d, J = 157.8 Hz, CH-P), 36.33 (s, CH_2 Bn), 30.85 (d, J = 4.1 Hz, CH_2 -S), 28.43 (s, 3C, 3 \times CH_3 Boc), 27.77 (d, J = 14.3 Hz, CH_2 -CH-P), 24.29 (d, J = 3.4 Hz, CH_3 *i*Pr), 24.23 (d, J = 3.5 Hz, CH_3 *i*Pr), 24.06 (d, J = 5.4 Hz, CH_3 *i*Pr), 24.02 (d, J = 5.7 Hz, CH_3 *i*Pr) ppm.

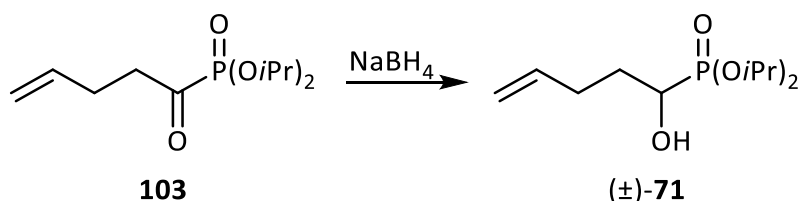
^{31}P NMR: (161.98 MHz, CDCl_3 , [42Sep2920/461], ET 20): δ_{P} = 22.42 (s, 83 mol% purity) ppm.

HRMS calculated for $\text{C}_{21}\text{H}_{36}\text{NO}_5\text{PS}$ (445.55 g/mol): $[\text{M}+\text{H}]^+$ 446.2130; found: $[\text{M}+\text{H}]^+$ 446.2127.

IR (ATR, ET 20): ν = 3249, 2974, 1708, 1520, 1374, 1236, 1167, 992 cm^{-1} .

4.7 Synthesis of (*R*)-phosphaarginine [(*R*)-**61**]ⁱⁱⁱ

4.7.1 (\pm)-Diisopropyl (1-hydroxy-pent-4-en-1-yl)phosphonate [(\pm)-**71**]



103^{iv} (3.15 g, 12.69 mmol) was dissolved (final concentration 0.4 M) and reduced following **general procedure B**. After a total stirring time of 18 h, (\pm)-**71** (2.30 g, 9.17 mmol, 72 %) was

ⁱⁱⁱ This substance was synthesized in cooperation with Kristof Braunsteiner.

^{iv} Obtained from Braunsteiner, using **general procedure A**.

obtained as colorless oil after purification by MPLC [R_f (*n*-heptane:EtOAc, 1:1) = 0.17, gradient: 18 → 100% EtOAc].

$^1\text{H NMR}$ (600.25 MHz, CDCl_3 , [61May2920/590], KB069 2nd Fr. 21-28 dry HCP): $\delta_{\text{H}} = 5.87\text{--}5.77$ (m, 1H, $-\text{CH}=\text{}$), 5.10-4.99 (m, 2H, $=\text{CH}_2$), 4.79-4.72 (m, 2H, $2 \times \text{CH } i\text{Pr}$), 3.80 (ddd, $J_{\text{HP}} = 10.2$ Hz, $J_{\text{XA}} = 4.6$ Hz, $J_{\text{XB}} = 3.6$ Hz, 1H, CH-P), 2.28 (ABX₂X'P-System; A-part: m, 2.39-2.31; B-part: m, 2.24-2.15, 2H, $\text{CH}_2\text{-CH}=\text{CH}_2$), 1.97 (broad s, 1H, OH), 1.80 (ABX₂X'P-System; A-part: m, 1.89-1.81; B-part: m, 1.80-1.71, 2H, $\text{CH}_2\text{-CH-P}$), 1.346 (d, $J = 4.2$ Hz, 3H, CH_3), 1.343 (d, $J = 4.6$ Hz, 3H, CH_3), 1.336 (d, $J = 4.2$ Hz, 3H, CH_3), 1.33 (d, $J = 4.6$ Hz, 3H, CH_3) ppm.

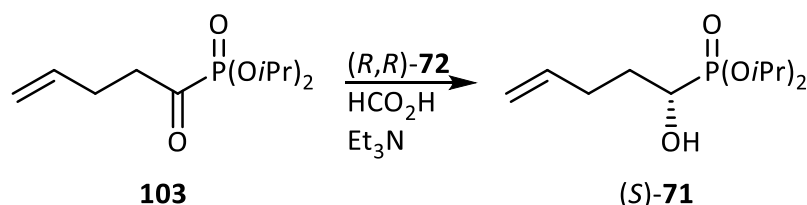
$^{13}\text{C NMR}$ (150.93 MHz, CDCl_3 , [61May2920/592], KB069 2nd Fr. 21-28 dry HCP): $\delta_{\text{C}} = 137.74$ (s, $-\text{CH}=\text{}$), 115.67 (s, $\text{CH}_2=\text{}$), 71.35 (d, $J = 7.1$ Hz, $\text{CH } i\text{Pr}$), 71.22 (d, $J = 7.3$ Hz, $\text{CH } i\text{Pr}$), 67.67 (d, $J = 161.6$ Hz, CH-P), 30.64 (s, $-\text{CH}_2\text{-CH}=\text{}$), 29.93 (d, $J = 13.7$ Hz, $\text{CH}_2\text{-CH-P}$), 24.30 (d, $J = 3.7$ Hz, CH_3), 24.27 (d, $J = 3.7$ Hz, CH_3), 24.18 (d, $J = 4.7$ Hz, CH_3), 24.17 (d, $J = 4.5$ Hz, CH_3) ppm.

$^{31}\text{P NMR}$: (242.99 MHz, CDCl_3 , [61May2920/591], KB069 2nd Fr. 21-28 dry HCP): $\delta_{\text{P}} = 23.28$ (s) ppm.

HRMS calculated for $\text{C}_{11}\text{H}_{23}\text{O}_4\text{P}$ (250.27 g/mol): $[\text{M}+\text{Na}]^+ 273.1232$; found: $[\text{M}+\text{Na}]^+ 273.1225$.

IR (ATR, KB 075): $\nu = 3307, 2979, 2936, 1641, 1385, 1219, 1105, 979$ cm^{-1} .

4.7.2 (*S*)-Diisopropyl (1-hydroxy-pent-4-en-1-yl)phosphonate [(*S*)-**71**]



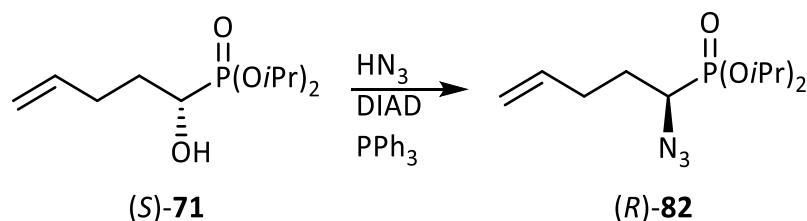
General procedure D was used to convert ketophosphonate **103** (1.08 g, 4.34 mmol) to the desired hydroxyphosphonate (*S*)-**71** (982 mg, 3.92 mmol, 90%) in the presence of (*R,R*)- $\text{RuOH}[(p\text{-cymene})\text{-TsDPEN}]$ (obtained by **general procedure C**, 0.02 eq.). The product was isolated as colorless oil after chromatographic purification [R_f (*n*-heptane:EtOAc, 1:1) = 0.17, gradient: 18 → 100% EtOAc].

The spectroscopic data were in agreement to those reported for (\pm)-**71**.

Specific rotation: $\alpha_D^{20} = +5.9$ (c 0.53, CH_2Cl_2).

^{31}P NMR with chiral solvating agent (242.99 MHz, CDCl_3 , [61May2920/30], KB070 Fr.21-29 dry w. shift): $\delta_P = 95.28$ [J 0.37, chiral solvating agent (*S*)-77], 23.38 [J 0.004, complex of chiral solvating agent with (*R*)-71], 23.24 [J 0.62, complex of chiral solvating agent with (*S*)-71 $\rightarrow ee \geq 98\%$].

4.7.3 (*R*)-diisopropyl (1-azidopent-4-en-1-yl)phosphonate [(*R*)-82]



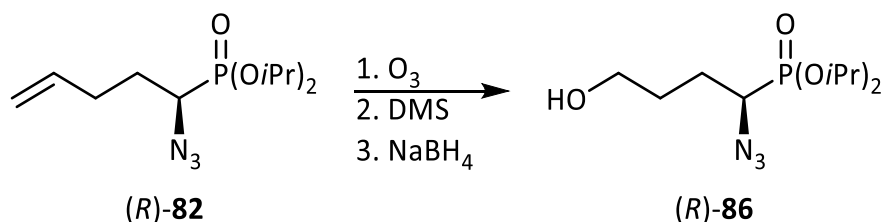
(*S*)-71 (931 mg, 3.72 mmol) was converted to (*R*)-82 (658 mg, 2.39 mmol, 64%) following **general procedure E**, using DIAD as azoester. The product was isolated after MPLC [R_f (CH_2Cl_2 : Et_2O , 9:1) = 0.52, solvent ratio used for purification: 95:5%] as colorless oil in 78 mol% purity, which was sufficient for the subsequent step. Thus, no further purification was attempted.

^1H NMR (tentatively assigned signals, 400.24 MHz, CDCl_3 , [41Sep3020/340], TD 104 Fr 8-14): $\delta_H = 5.85$ -5.70 (m, 1H, $-\text{CH}=\text{}$), 5.14-5.00 (m, 2H, $\text{CH}_2=\text{}$), 4.88-4.70 (m, 2H, $2 \times \text{CH } i\text{Pr}$), 3.40-3.33 (td, $J = 11.7$ Hz, 3.7 Hz, 1H, $\text{CH}-\text{P}$), 2.26 (ABX₂X'P-System; A-part: m, 2.40-2.30; B-part: m, 2.25-2.12, 2H, $\text{CH}_2-\text{CH}=\text{CH}_2$), 1.82 (ABX₂X'P-System; A-part: m, 1.99-1.86; B-part: m, 1.81-1.63, 2H, $\text{CH}_2-\text{CH}-\text{P}$), 1.36 (broadened d, $J = 6.0$ Hz, 12H, $4 \times \text{CH}_3$) ppm.

^{31}P NMR: (162.02 MHz, CDCl_3 , [41Sep2920/341], TD 104 nS2): $\delta_P = 22.53$ (s, 7 mol%, unknown impurity), 20.28 (s, 78 mol%, product), 19.71 (s, 7.5 mol%, unknown impurity), 19.67 (s, 7.5 mol%, unknown impurity) ppm.

HRMS calculated for $\text{C}_{11}\text{H}_{22}\text{N}_3\text{O}_3\text{P}$ (275.29 g/mol): $[\text{M}+\text{Na}]^+$ 298.1296; found: $[\text{M}+\text{Na}]^+$ 298.1289.

4.7.4 (*R*)-Diisopropyl (1-azido-4-hydroxybutyl)phosphonate [(*R*)-**86**]



(*R*)-**82** (482 mg, 1.75 mmol) was dissolved in a 1:1 mixture of MeOH and CH₂Cl₂ (8 + 8 mL) and the resulting solution was cooled to –78°C. O₃ (flow: 100 N/h, O₃ level: 70%) was bubbled through the reaction mixture until the solution turned pale blue (5 minutes). Then, O₂ was bubbled through the mixture until the blue color disappeared again. Dimethylsulfide (120 mg, 0.14 mL, 1.93 mmol, 1.1 eq.) was added and the cooling bath was removed. The reaction mixture was allowed to come to 20°C for 20 minutes. Subsequently, the solution was again cooled to –35°C and NaBH₄ (132 mg, 3.50 mmol, 2 eq.), dissolved in EtOH (2 mL), was added. The reaction mixture was allowed to warm up in the cooling bath to 20°C over a period of 4 h, before the solvent was evaporated *in vacuo* at room temperature. The residue was redissolved in EtOAc (15 mL), washed with a saturated aqueous NaHCO₃ solution (3 × 15 mL). The combined aqueous phases were extracted with EtOAc (2 × 10 mL). The combined organic layers were dried (Na₂SO₄), filtered and concentrated to dryness. The crude product was purified by MPLC [*R_f* (*n*-heptane:EtOAc, 1:1) = 0.09, gradient: 18 → 100% EtOAc] to give (*R*)-**86** (383 mg, 1.37 mmol, 78%) as colorless oil.

¹H NMR (700.40 MHz, CDCl₃, [7Oct0920/60], TD 107 Fr 47-70): δ_H = 4.84-4.74 (m, 2H, 2 × CH *i*Pr), 3.70 (dd, *J* = 6.2 Hz, *J* = 5.5 Hz, 2H, CH₂-OH), 3.43-3.39 (ddd, *J* = 3.5 Hz, *J* = 10.4 Hz, *J* = 11.8 Hz, 1H, CH-P), 1.93 (ABX₂X'-P-System; A-part: m, 2.05-1.93; B-part: m, 1.93-1.80, 2H, CH₂-CH-P), 1.80-1.66 (m, 1H, CH₂-CH₂-OH), 1.63 (broad s, 1H, OH), 1.37 (d, *J* = 6.2 Hz, 9H, 3 × CH₃), 1.36 (d, *J* = 6.0 Hz, 3H, CH₃) ppm.

¹³C NMR (176.12 MHz, CDCl₃, [7Oct0920/61], TD 107 Fr 47-70): δ_C = 72.00 (d, *J* = 7.4 Hz, CH *i*Pr), 71.95 (d, *J* = 7.2 Hz, CH *i*Pr), 62.22 (s, CH₂-OH), 57.81 (d, *J* = 156.7 Hz, CH-P), 29.80 (d, *J* = 12.7 Hz, CH₂-CH-P), 25.53 (s, CH₂-CH₂-OH), 24.31, (d, *J* = 3.7 Hz, 2C, 2 × CH₃), 24.15 (d, *J* = 4.7 Hz, 2C, 2 × CH₃) ppm.

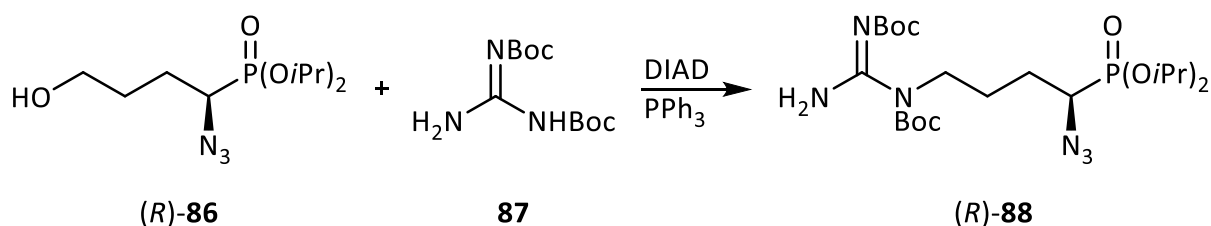
³¹P NMR: (162.02 MHz, CDCl₃, [41Oct0920/191], TD 107 Fr 47-70): δ_P = 20.13 (s) ppm.

HRMS calculated for $C_{10}H_{22}N_3O_4P$ (279.28 g/mol): $[M+Na]^+$ 302.1246; found: $[M+Na]^+$ 302.1241.

IR (ATR, TD 107): $\nu = 3406, 2941, 2101, 1451, 1379, 1234, 985 \text{ cm}^{-1}$.

Specific optical rotation: $\alpha_D^{20} = -46.9$ (c 0.55, acetone).

4.7.5 (*R*)-Diisopropyl [1-azido-4-bis(*tert*-butoxycarbonyl)guanidino]butylphosphonate [(*R*)-**88**]



(*R*)-**86** (300 mg, 1.08 mmol) was dried by coevaporation of residual water with toluene (1 mL) and then dissolved in toluene (4 mL) under argon atmosphere. Meanwhile, DIAD (365 mg, 0.36 mL, 1.80 mmol, 1.66 eq.) was added to a solution of Ph_3P (473 mg, 1.80 mmol, 1.66 eq.) in dry toluene (5 mL) under argon atmosphere at 0°C. After 5 minutes the solution of (*R*)-**86** was added, followed by dropwise addition of *N,N'*-bis(*tert*-butoxycarbonyl)guanidine¹²⁵ (**87**, 0.341 mg, 1.32 mmol, 1.22eq.), dissolved in toluene (4 mL). The reaction mixture was allowed to come to 20°C in the cooling bath and stirring was continued for 4 h. The solvent was removed in *vacuo* at room temperature and the residue was purified by flash column chromatography [R_f (*n*-heptane:EtOAc, 1:1) = 0.54, solvent ratio used for purification: 2:1], to yield (*R*)-**88** (499 mg, 0.96 mmol, 89%) as colorless oil.

¹H NMR (700.40 MHz, $CDCl_3$, [7Oct0620/70], TD 108): $\delta_H = 9.39$ (broad s, 1H, NH), 9.20 (broad s, 1H, NH), 4.85-4.71 (m, 2H, 2 × CH *iPr*), 3.95 (symm m, 2H, CH_2 -NBoc), 3.48 (ddd, $J_{HP} = J_2 = 11.5$, $J_3 = 3.0$ Hz, 1H, CH-P), 1.97-1.78 (m, 2H, CH_2 - CH_2 -NBoc), 1.77-1.60 (m, 2H, CH_2 -CH-P), 1.53 (s, 9H, 3 × CH_3 Boc), 1.49 (s, 9H, 3 × CH_3 Boc), 1.36 (d, $J = 6.4$ Hz, 9H, 3 × CH_3 *iPr*), 1.35 (d, $J = 7.2$ Hz, 3H, CH_3 *iPr*) ppm.

¹³C NMR (176.12 MHz, $CDCl_3$, [7Oct0620/71], TD 108): $\delta_C = 163.95$ (s, C_q -NH₂), 160.66 (s, C=O), 155.11 (s, C=O), 84.08 (s, $C(CH_3)_3$), 78.91 (s, $C(CH_3)_3$), 71.90 (d, $J = 7.3$ Hz, CH *iPr*), 71.81 (d, $J = 7.1$ Hz, CH *iPr*), 57.52 (d, $J = 157.1$ Hz, CH-P), 43.84 (s, CH_2 -NBoc), 28.44 (s, 3C, 3 × CH_3 Boc),

28.18 (s, 3C, 3 × CH₃ Boc), 26.11 (d, *J* = 13.6 Hz, CH₂-CH-P), 25.93 (s, CH₂-CH₂-NBoc), 24.34 (d, *J* = 3.4 Hz, CH₃ *i*Pr), 24.33 (d, *J* = 3.5 Hz, CH₃ *i*Pr), 24.17 (d, *J* = 4.8 Hz, 2C, 2 × CH₃ *i*Pr) ppm.

³¹P NMR: (162.02 MHz, CDCl₃, [41Sep2520/41], ET 18 Fr 46-67): δ_P = 20.17 (s) ppm.

HRMS calculated for C₂₁H₄₁N₆O₇P (520.57 g/mol): [M+Na]⁺ 521.2853; found: [M+Na]⁺ 521.2849.

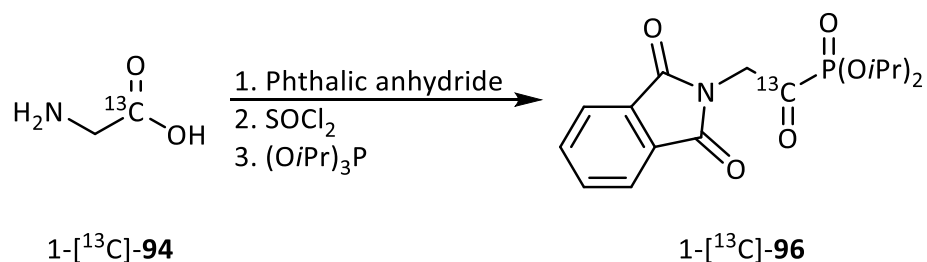
IR (ATR, TD 108): ν = 3398, 2978, 2102, 1711, 1610, 1509, 1373, 1246, 1141, 983 cm⁻¹.

Specific optical rotation: α_D²⁰ = -44.0 (*c* 0.5, acetone).

³¹P NMR with chiral solvating agent (161.98 MHz, toluene-*d*₈, [42Oct2820/231], TD 108 + Shift): δ_P = 95.82 [*f* 0.75, chiral solvating agent (*S*)-**77**], 20.23 [*f* 0.25, complex of chiral solvating agent with (*R*)-**88**], 20.27 [*f* 0.002 complex of chiral solvating agent with (*S*)-**88**] → *ee* ≥ 98%.

4.8 Synthesis of (*R*)-[1-hydroxy-2-(trimethylammonio)ethyl]phosphonate (*R*)-**58** and its isotopically labeled analogs (*R*)-1-[²H]-**58** and (*R*)-1-[¹³C]-1-[²H]-**58**

4.8.1 1-[¹³C]-Diisopropyl [2-(1,3-dioxoisindolin-2-yl)acetyl]phosphonate {1-[¹³C]-**96**}

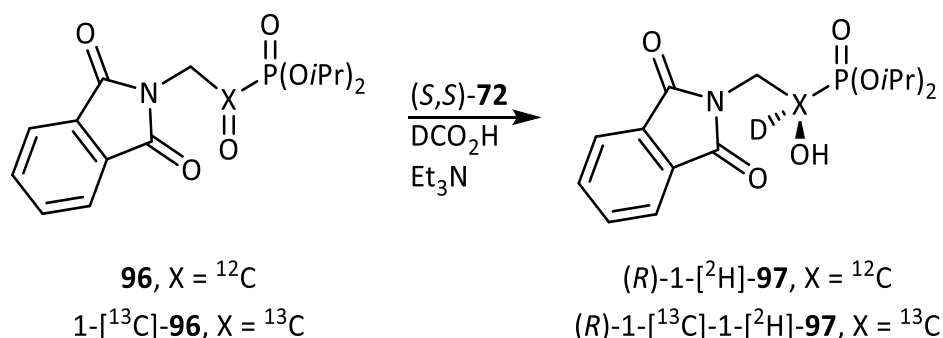


Ketophosphonate 1-[¹³C]-**96** was obtained by adapting a literature known method, starting from [1-¹³C]-glycine ([1-¹³C]-**94**, 99% ¹³C, Sigma Aldrich).¹²¹

¹H NMR (400.24 MHz, CDCl₃, [41Aug1020/120], TD 79): δ_H = 7.90-7.86 (m, 2H, 2 × CH arom), 7.77-7.73 (m, 2H, 2 × CH arom), 4.91 (t, *J* = 3.8, 2H, CH₂), 4.89-4.78 (m, 2H, 2 × CH *i*Pr), 1.41 (d, *J* = 6.2, 6H, 2 × CH₃), 1.40 (d, *J* = 6.2, 6H, 2 × CH₃) ppm.

³¹P NMR (242.99 MHz, CDCl₃, [41Aug1020/121], TD 79): δ_P = -5.84 (d, *J* = 176.7 Hz, 89 mol%) ppm.

4.8.3 (*R*)-1-[²H]- Diisopropyl [2-(1,3-dioxoisindolin-2-yl)-1-hydroxyethyl]phosphonate {(*R*)-1-[²H]-**97**} and (*R*)-1-[¹³C]-1-[²H]- diisopropyl [2-(1,3-dioxoisindolin-2-yl)-1-hydroxyethyl]phosphonate {(*R*)-1-[¹³C]-1-[²H]-**97**}



The deuterated (*R*)-hydroxyphosphonate {(*R*)-1-[²H]-**97**} (544 mg, 1.53 mmol, 72%) was synthesized starting from ketophosphonate 1-[²H]-**96**¹²¹ (751 mg, 2.12 mmol) by **general procedure D**, using (*S,S*)-RuOH[(*p*-cymene)-TsDPEN] (**general procedure C**, 0.04 eq.) as catalyst and 3 eq. DCO₂H (0.30 mg, 0.25 mL, 6.36 mmol).¹⁰⁵ It was obtained as colorless solid after MPLC [*R*_f (*n*-heptane:EtOAc, 1:1) = 0.17, gradient: 12 → 100% EtOAc]

¹H NMR (600.25 MHz, CDCl₃, [61Sep0420/190], TD 96): δ_H = 7.84-7.81 (m, 2H, 2 × CH arom), 7.71-7.68 (m, 2H, 2 × CH arom), 4.80-4.69 (m, 2H, 2 × CH *i*Pr), 4.02 (ABP-System; A-Part: dd, *J*_{AB} = 14.4 Hz, *J*_{AP} = 8.4 Hz; B-Part: dd, *J*_{AB} = 14.4 Hz, *J*_{BP} = 6.2 Hz, 2H, CH₂), 3.91 (broad d, *J* = 4.4 Hz, 1H, OH), 1.36 (d, *J* = 6.2, 3H, CH₃), 1.31 (d, *J* = 6.2, 3H, CH₃), 1.30 (d, *J* = 6.0, 3H, CH₃), 1.27 (d, *J* = 6.2, 3H, CH₃) ppm.

¹³C NMR (150.93 MHz, CDCl₃, [61Sep0420/191], TD 96): δ_C = 168.54 (s, 2C, 2 × CO), 134.13 (s, 2C, 2 × CH arom), 132.17 (s, 2C, 2 × C arom), 123.45 (s, 2C, 2 × CH arom), 71.99 (d, *J* = 7.1 Hz, CH *i*Pr), 71.81 (d, *J* = 7.5 Hz, CH *i*Pr), 65.96 (td, *J*_{CP} = 161.8 Hz, *J*_{CD} = 21.8 Hz, CD), 39.93 (d, *J* = 7.6 Hz, CH₂), 24.21 (d, *J* = 6.3 Hz, CH₃), 24.18 (d, *J* = 6.5 Hz, CH₃), 24.02 (d, *J* = 5.0 Hz, CH₃), 23.94 (d, *J* = 5.0 Hz, CH₃) ppm.

³¹P NMR (161.98 MHz, CDCl₃, [42Sep0320/461], TD 96 nT): δ_P = 18.93 (s).

HRMS calculated for C₁₆H₂₁DNO₆P (356.33 g/mol): [M+Na]⁺ 379.1145; found: [M+Na]⁺ 379.1140.

IR (ATR, TD 96): ν = 3263, 2980, 1707, 1392, 1219, 1085, 981, 710 cm⁻¹.

Specific optical rotation: $\alpha_D^{20} = -21.2$ (c 1.05, CH_2Cl_2).

Degree of deuteration: $^1\text{H-NMR}$: $\delta_{\text{H}} = 4.23\text{-}4.20$ ppm (m, CH-P, non-deuterated compound, $\int 0.0087$), 4.02 ppm (ABP-System deuterated compound, CH_2 , $\int 2.0000$) \rightarrow degree of deuteration $\geq 99\%$.

In analogy, the reduction of (*R*)-1- ^{13}C]-**96** (713 mg, 2.01 mmol) was accomplished following the same procedure, but using 4.4 eq of DCO_2H (412 mg, 34 mL, 8.84 mmol) instead of HCO_2H . The product, (*R*)-1- ^{13}C]-1- ^{2}H]-**97** (515 mg, 1.44 mmol, 72%), was obtained as colorless solid after MPLC [R_f (*n*-heptane:EtOAc, 1:1) = 0.17, gradient: 12 \rightarrow 100% EtOAc].

$^1\text{H NMR}$ (600.27 MHz, CDCl_3): $\delta_{\text{H}} = 7.86\text{-}7.82$ (m, 2H, CH arom), 7.73-7.69 (m, 2H, CH arom), 4.76 (sym. m, 2H, CH *i*Pr), 4.04 (ABXP-System; A-Part: ddd, $J_{\text{AB}} = 14.6$ Hz, $J_{\text{AP}} = 6.8$ Hz, $J_{\text{AX}} = 4.9$ Hz; B-Part: dd, $J_{\text{AB}} = 14.6$ Hz, $J_{\text{BP}} = 7.4$ Hz, 2H, CH_2), 3.01 (dd, $J = 5.5$ Hz, $J = 2.7$ Hz, 1H, OH), 1.36 (d, $J = 6.2$ Hz, 3H, CH_3), 1.33 (d, $J = 6.1$ Hz, 3H, CH_3), 1.32 (d, $J = 6.2$ Hz, 3H, CH_3), 1.31 ppm (d, $J = 6.2$ Hz, 3H, CH_3) ppm.

$^{13}\text{C NMR}$ (150.93 MHz, CDCl_3): $\delta_{\text{C}} = 168.8$ (s, 2 C, $2 \times \text{C}=\text{O}$), 134.4 (s, 2C, $2 \times \text{CH}$ arom), 132.2 (s, 2C, $2 \times \text{C}$ arom), 123.7 (s, 2C, $2 \times \text{CH}$ arom), 72.1 (d, $J = 7.2$ Hz, CH *i*Pr of C(OH)**D**-P), 72.0 (d, $J = 7.3$ Hz, CH *i*Pr of C(OH)**D**-P), 70.7 (d, $J = 7.5$ Hz, CH *i*Pr of C(OH)**H**-P), 69.6 (d, $J = 7.5$ Hz, CH *i*Pr of C(OH)**H**-P), 67.1 (d, $J = 161.7$ Hz, C(OH)**H**-P), 66.7 (td, $J = 161.5$ Hz, $J = 22.2$ Hz, C(OH)**D**-P), 40.2 (dd, $J = 37.9$ Hz, $J_{\text{C}} = 7.2$ Hz, CH_2), 24.34 (d, $J = 7.0$ Hz, CH_3), 24.32 (d, $J = 7.1$ Hz, CH_3), 24.2 (d, $J = 4.9$ Hz, CH_3), 24.1 ppm (d, $J = 4.8$ Hz, CH_3) ppm.

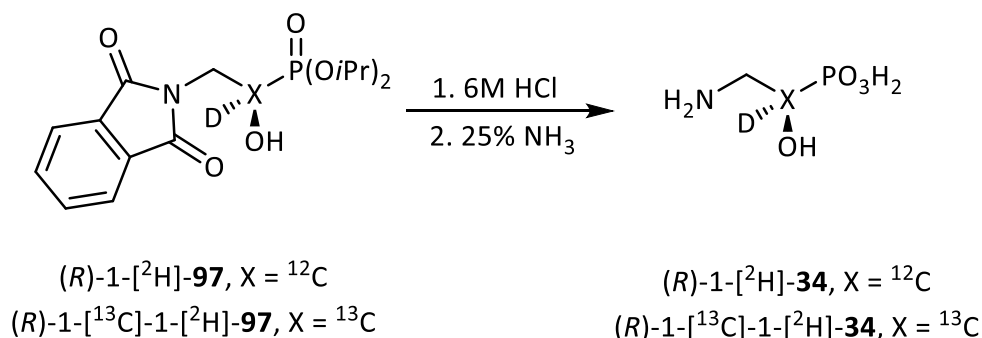
$^{31}\text{P NMR}$ (162.03 MHz, CDCl_3): $\delta_{\text{P}} = 18.93$ ppm (d, $J = 161.5$ Hz) ppm.

Specific optical rotation: $\alpha_D^{20} = -19.4$ ($c = 0.54$, CH_2Cl_2)

Degree of deuteration: $^1\text{H-NMR}$: $\delta_{\text{H}} = 4.31\text{-}4.27$ ppm (m, ^{13}CH -P, non-deuterated compound, $\int 0.0099$), 4.04 ppm (ABXP-System deuterated compound, CH_2 , $\int 2.0000$) \rightarrow degree of deuteration $\geq 99\%$.

Chiral stationary phase HPLC (Lux-Cellulose 1, Chiracel OD-H, 250×4.6 mm, *n*-heptane + 0.1% *i*PrOH/*i*PrOH, 85:15): R_{T} (*R*)-1- ^{13}C]-1- ^{2}H]-**97** = 7.24 min ($\int 99.44$), R_{T} (*S*)-1- ^{13}C]-1- ^{2}H]-**97** = 8.68 min ($\int 0.60$) $\rightarrow ee \geq 99\%$, chemical purity $\geq 99\%$.

4.8.4 (*R*)-1-[²H]--(2-amino-1-hydroxyethyl)phosphonic acid {(*R*)-1-[²H]-**34**} and (*R*)-1-[¹³C]-1-[²H]--(2-amino-1-hydroxyethyl)phosphonic acid {(*R*)-1-[¹³C]-1-[²H]-**34**}



In analogy to the literature described synthesis of (*R*)-**34**,¹²¹ global deprotection of 1-[²H]-(*R*)-**97** was performed by **general procedure F**, followed by dissolving the crude residue (after evaporation of the solvent) in NH₃ (aqueous, 25%, 10 mL/mmol) and stirring the resulting mixture at 60°C for 24 h. Afterwards, the solvent was removed under reduced pressure, the crude product was redissolved in H₂O (2 mL/mmol) and again concentrated to dryness. The glassy residue was purified by ion exchange chromatography using Dowex 50W /H⁺-form (see **general procedure F**, 15 mL moist resin/mmol) and water as eluent. This yielded (*R*)-1-[²H]-**34** (69 mg, 0.49 mmol, 95%) as colorless crystals after recrystallization from water/EtOH.

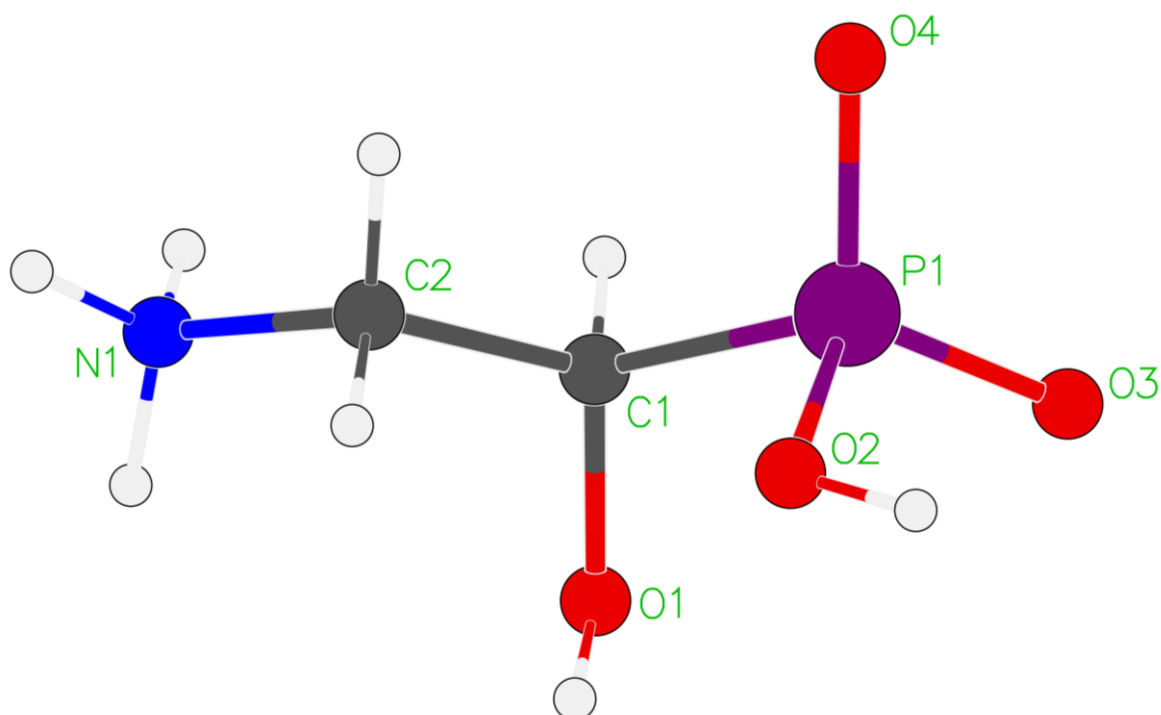
¹H NMR (600.25 MHz, D₂O, [61Sep1020/130], TD 99): δ_H = 3.96 (td, *J* = 10.1 Hz, *J* = 3.3 Hz, CH-P impurity), 3.26 (ABP-System; A-part: dd, *J*_{AB} = 13.3 Hz, *J*_{AP} = 6.4 Hz; B-part: dd, *J*_{AB} = 13.3 Hz, *J*_{BP} = 6.2 Hz, 2H, CH₂) ppm.

¹³C NMR (150.93 MHz, D₂O, [61Sep1020/131], TD 99): δ_C = 64.94 (td, *J*_{CP} = 155.4 Hz, *J*_{CD} = 21.5 Hz, CD), 41.32 (d, *J* = 8.9 Hz, CH₂) ppm.

³¹P NMR (162.02 MHz, D₂O, [41Sep0820/111], TD 99): δ_P = 14.97 (s) ppm.

Elemental analysis for C₂H₇DNO₄P (% calculated/ % found): C (16.91/16.84), H (5.67/5.75), N (9.86/9.69), O (45.05/44.78), P (21.80/21.98).

Crystal structure analysis:



This analysis confirmed the absolute configuration of the non-isotopically labeled compound, the relevant atom distances and angles can be found in the appendix.

Specific optical rotation: $\alpha_D^{20} = -33.6$ (c 0.92, H₂O); lit. value of non-deuterated compound:¹²¹ $\alpha_D^{20} = -36.8$ (c 0.99, H₂O).

Degree of deuteration: ¹H-NMR: $\delta_H = 3.96$ ppm (td, CH-P, non-deuterated compound, $J_{0.0128}$), 3.26 (ABP-System deuterated compound, CH₂, $J_{2.0000}$) → degree of deuteration ≥ 98%.

Analogously (*R*)-1-[¹³C]-1-[²H]-**34** (185 mg, 1.29 mmol, 90%) was obtained starting from (*R*)-1-[¹³C]-1-[²H]-**97** (514 mg, 1.43 mmol).

¹H NMR (600.25 MHz, D₂O, [61Sep1020/140], TD 100): $\delta_H = 3.96$ (tdd, $J = 140.1$ Hz, $J = 10.1$ Hz, $J = 3.3$ Hz, ¹³CH-P impurity), 3.26 (ABP¹³C-System; A-part: dd, $J_{AB} = 13.3$ Hz, $J_{AP} = 6.3$ Hz; B-part: ddd, $J_{AB} = 13.3$ Hz, $J_{BP} = 5.8$ Hz, $J_{^{13}CB} = 5.4$ Hz, 2H, CH₂) ppm.

¹³C NMR (150.93 MHz, D₂O, [61Sep1020/141], TD 100): $\delta_C = 64.84$ (td, $J_{CP} = 155.2$ Hz, $J_{CD} = 21.5$ Hz, CD), 41.30 (dd, $J_{CD} = 9.0$ Hz, $J_{CC} = 36.8$ Hz, CH₂) ppm.

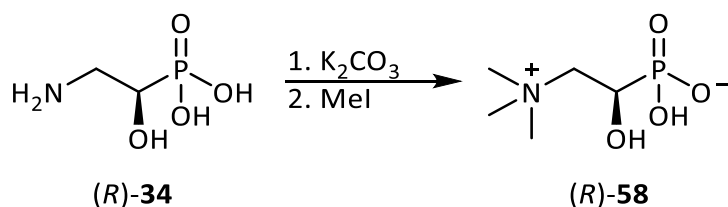
³¹P NMR (161.98 MHz, D₂O, [42Sep0820/81], TD 100): δ_P = 14.95 (d, *J* = 155.2 Hz) ppm.

Elemental analysis for C¹³CH₇DNO₄P (% calculated/ % found): C (16.79/16.72), H (5.63/5.80), N (10.30/9.58), O (44.73/44.72), P (21.65/21.82).

Specific optical rotation: α_D²⁰ = -33.2 (*c* 0.78, H₂O), lit. value of non-deuterated, non ¹³C-labeled compound¹²¹: α_D²⁰ = -36.8 (*c* 0.99, H₂O).

Degree of deuteration: ¹H-NMR: δ_H = 3.96 ppm (tdd, ¹³CH-P, non-deuterated compound, [0.0524], 3.26 (ABP-System deuterated compound, CH₂, [2.0000]) → degree of deuteration ≥ 94%.

4.8.5 (*R*)-[1-Hydroxy-2-(trimethylammino)ethyl]phosphonate [(*R*)-**58**]



K₂CO₃ (2347 mg, 16.98 mmol, 5 eq.) was added to a suspension of (*R*)-**34**¹²¹ (479 mg, 3.40 mmol) in MeOH (14 mL/mmol). After 10 minutes of stirring, MeI (1928 mg, 13.58 mmol, 0.85 mL, 4 eq.) was added and stirring was continued for 48 h. The solvent was removed *in vacuo* and the residue was taken up in H₂O (1 mL/mmol). Subsequently, the solution was acidified with conc. H₂SO₄ to a final pH 1 and the resulting mixture was stirred for 1 h. The solvent was removed under reduced pressure and the crude residue was dissolved in water and extracted with Et₂O (3 × 1.5 mL/mmol). The aqueous phase was concentrated to dryness. Purification of the crude, salt-containing mixture was done by anion exchange chromatography over Dowex Monosphere-550A-OH⁻-form, using formic acid (5%, aqueous) as eluent. The product containing ninhydrine positive fractions [*R*_f (*i*PrOH/H₂O/NH₃ (25%), 6:3:1) = 0.08] were pooled and concentrated. The obtained solid was recrystallized from H₂O/EtOH to yield (*R*)-**58** (501 mg, 2.72 mmol, 80%) as colorless needles.

¹H NMR (600.25 MHz, D₂O, [61Oct2720/40], TD 98 Umk): δ_H = 4.33 (ddd, *J* = 11.4 Hz, *J* = 10.1 Hz, *J* = 1.3 Hz, 1H, CH-P), 3.62 (ABXP-System; A-Part: ddd, *J*_{AB} = 14.2 Hz, *J*_{AP} = 4.6 Hz, *J*_{AX} = 1.3 Hz; B-Part: ddd, *J*_{AB} = 14.2 Hz, *J*_{BX} = 10.1 Hz, *J*_{BP} = 3.0 Hz, 2H, CH₂), 3.24 (s, 9H, 3 × CH₃) ppm.

^{13}C NMR (150.93 MHz, D_2O , [61Oct2720/41], TD 98 Umk): δ_{C} = 68.06 (td, J = 12.7 Hz, J = 2.3 Hz, CH_2), 64.17 (d, J = 151.7 Hz, CH), 53.97 (s, CH_3), 53.95 (s, CH_3), 53.92 (s, CH_3) ppm.

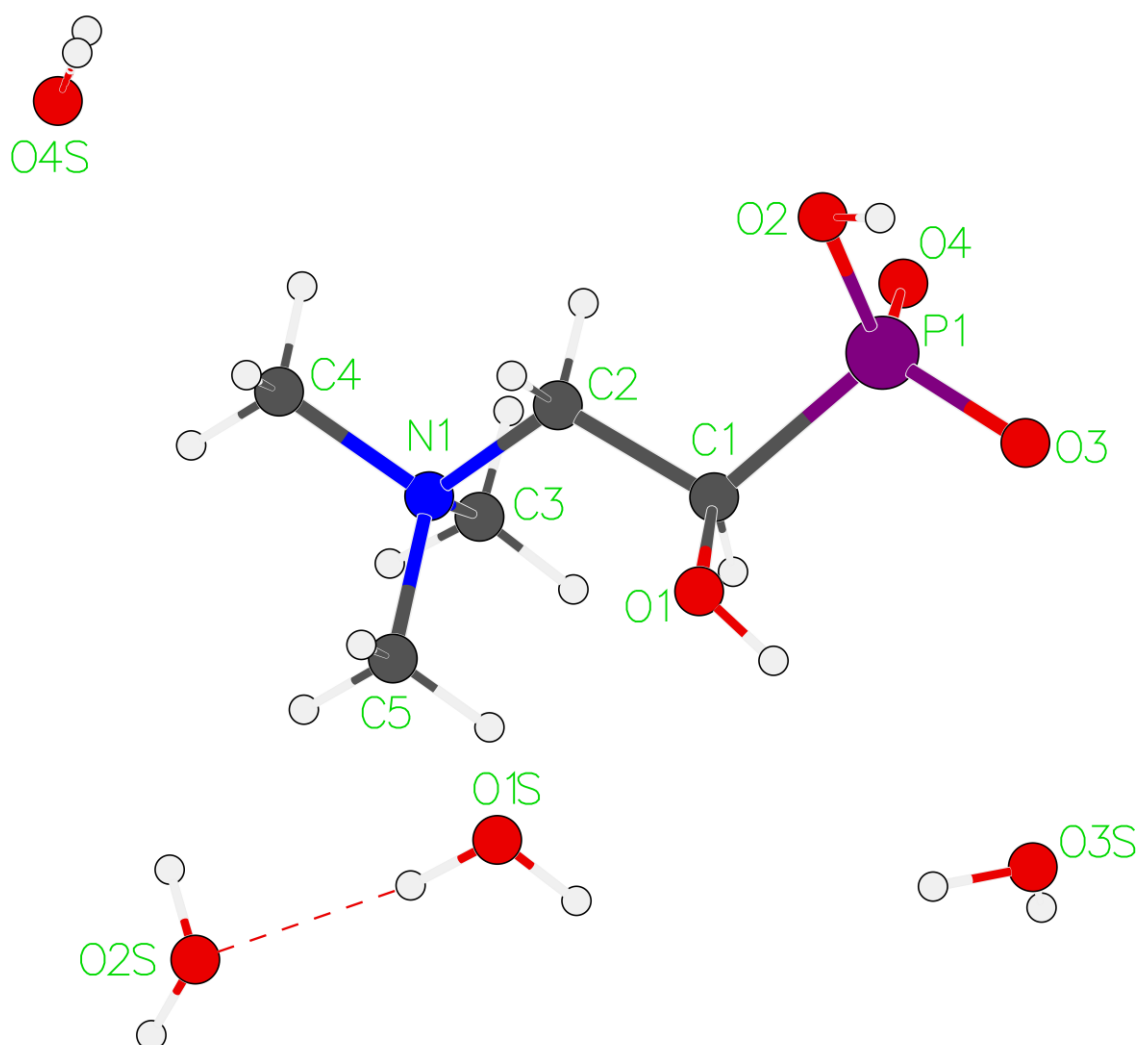
^{31}P NMR (161.98 MHz, D_2O , [42Oct2320/151], TD 98 Umk): δ_{P} = 14.05 (t, J = 6.2 Hz)⁹⁸ ppm.

HRMS calculated for $\text{C}_5\text{H}_{14}\text{NO}_4\text{P}$ (183.14 g/mol): $[\text{M}+\text{H}]^+$ 184.0739; found: $[\text{M}+\text{H}]^+$ 184.0730.

IR (ATR, TD 58): ν = 3160, 2337, 1599, 1478, 1248, 1084, 967, 914 cm^{-1} .

Elemental analysis for $\text{C}_5\text{H}_{14}\text{NO}_4\text{P} \times 2.5 \text{H}_2\text{O}$ (% calculated/ % found): C (26.32/26.37), H (8.39/8.45), N (6.14/6.06), O (45.57/45.20), P (13.57/13.44).

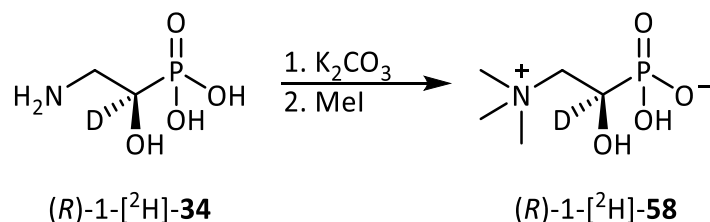
Crystal structure analysis:



X-ray crystallographic analysis confirmed the amount of co-crystallized water which was been determined by combustion analysis. Detailed data can be found in the appendix.

Specific optical rotation: $\alpha_D^{20} = -29.0$ (c 0.91, D_2O).

4.8.6 (*R*)-1-[2H]-[1-hydroxy-2-(trimethylammonio)ethyl]phosphonic acid {(*R*)-1-[2H]-**58**}



(*R*)-1-[2H]-**58** (113 mg, 0.61 mmol, 58 %) was obtained as colourless needles following the same method as described for (*R*)-**58** starting from (*R*)-1-[2H]-**34** (150 mg, 1.06 mmol).

1H NMR (600.25 MHz, D_2O , [61Oct2720/110], TD 105 Umk): $\delta_H = 4.35$ - 4.31 (m, CH-P impurity), 3.61 (ABP-System; A-part: dd, $J_{AB} = 14.3$ Hz, $J_{AP} = 4.6$ Hz; B-part: dd, $J_{AB} = 14.3$ Hz, $J_{BP} = 2.6$ Hz, 2H, CH_2), 3.24 (s, 9H, $3 \times CH_3$) ppm.

^{13}C NMR (150.93 MHz, D_2O , [61Oct2720/111], TD 105 Umk): $\delta_C = 67.99$ (td, $J = 12.7$ Hz, $J = 2.3$ Hz, CH_2), 64.17 (td, $J_{CP} = 151.3$ Hz, $J_{CD} = 21.4$ Hz, CD-P), 53.97 (s, CH_3), 53.95 (s, CH_3), 53.93 (s, CH_3) ppm.

^{31}P NMR (161.98 MHz, D_2O , [42Oct2720/231], TD 105 Umk): $\delta_P = 14.04$ (t, $J = 5.8$ Hz) ppm.

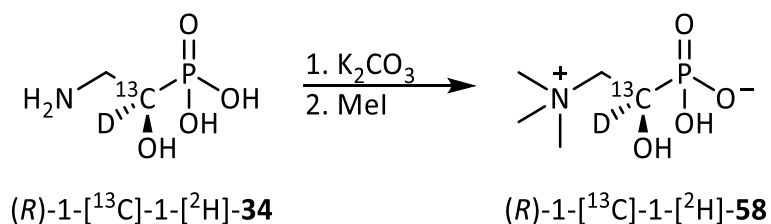
HRMS calculated for $C_5H_{13}DNO_4P$ (184.15 g/mol): $[M+Na]^+$ 207.0621; found: $[M+Na]^+$ 207.0613.

Elemental analysis for $C_5H_{13}DNO_4P \times 0.25 H_2O$ (% calculated/ % found): C (31.83/31.51), H (7.74/7.65), N (7.437.72), O (36.04/35.69). (hygroscopic)

Specific optical rotation: $\alpha_D^{20} = -29.3$ (c 0.50, D_2O).

Degree of deuteration: 1H -NMR: $\delta_H = 4.35$ - 4.31 ppm (m, CH-P, non-deuterated compound, f 0.0143), 3.61 (ABP-System deuterated compound, CH_2 , f 2.0000) \rightarrow degree of deuteration \geq 98%.

4.8.7 (*R*)-1-[¹³C]-1-[²H]-[1-hydroxy-2-(trimethylammonio)ethyl]phosphonic acid {(*R*)-1-[¹³C]-1-[²H]-**58**}



With the same method 1-[¹³C]-1-[²H]-**58** (108 mg, 0.58 mmol, 55%) was obtained as colourless needles starting from 1-[¹³C]-1-[²H]-**34** (150 mg, 1.05 mmol).

¹H NMR (600.25 MHz, D₂O, [61Oct2720/120], TD 106 Umk): δ_H = 4.50-4.20 (m, ¹³CH-P impurity), 4.36-4.31 (m, CH-P impurity), 3.61 (ABXP-System; A-part: dd, *J*_{AB} = 14.2 Hz, *J*_{AP} = 4.6 Hz; B-part: ddd, *J*_{AB} = 14.2 Hz, *J*_{BX} = 5.4 Hz, *J*_{BP} = 2.8 Hz, 2H, CH₂), 3.24 (s, 9H, 3 × CH₃) ppm.

¹³C NMR (150.93 MHz, D₂O, [61Oct2720/121], TD 106 Umk): δ_C = 67.99 (ddd, *J*_{CC} = 41.3 Hz, *J*_{CD} = 13.2 Hz, *J*_{CP} = 1.9 Hz, CH₂), 63.83 (td, *J* = 151.3 Hz, *J* = 21.3 Hz, CD), 53.97 (s, CH₃), 53.95 (s, CH₃), 53.93 (s, CH₃) ppm.

³¹P NMR (162.02 MHz, D₂O, [41Oct2720/201], TD 106 Umk): δ_P = 14.04 (td, *J*_{C-P} = 151.3 Hz, *J* = 5.7 Hz).

HRMS calculated for C₄¹³CH₁₃DNO₄P (185.14 g/mol): [M+Na]⁺ 208.0654; found: [M+Na]⁺ 208.0641.

Elemental analysis for C₄¹³CH₁₃DNO₄P × 0.33 H₂O (calculated/found): C (31.43/31.06), H (7.73/7.50), N (7.33/7.61), O (36.27/35.91). (hygroscopic)

Specific optical rotation: α_D²⁰ = -27.0 (c 0.54, D₂O).

Degree of labeling: ¹H-NMR: δ_H = 4.50-4.20 (m, ¹³CH-P, non-deuterated compound, f0.0483), 4.36-4.31 (m, CH-P, non-deuterated, non ¹³C-labeled compound, f0.0049), 3.61 (ABXP-System deuterated compound, CH₂, f2.0000) → degree of ¹³C-labeling ≥ 99%; degree of deuteration ≥ 94%.

5. Abstract

5.1 English abstract

During this work two main topics were worked on. This master thesis deals with the synthesis of a set of isotopically-labeled phosphonic acid compounds, which are of great interest for mechanistic studies as well as with the synthesis of chiral α -aminophosphonic acids for future medicinal applications.

Recently, a new oxidative cleavage route for the natural occurring trimethylated analog to 2-AEP was discovered. This pathway, which consists of the enzymes TmpA and TmpB, is currently under investigation. To further elucidate the mechanism of TmpB, its substrate, which is naturally produced by TmpA, (*R*)-[1-hydroxy-2-(trimethylammonio)ethyl]phosphonic acid [(*R*)-**58**] and its isotopically labeled analogs (*R*)-1-[²H]-**58** and (*R*)-1-[¹³C]-1-[²H]-**58** were successfully synthesized in six synthetic steps and can now be used for mechanistic studies by our collaborators. The first steps of this synthetic pathway were already known for the non-labeled and singly deuterated compound. Thus, they only needed slight adaptations. The last reaction step and purification of the final products was developed only during the work for this thesis.

The second part of this thesis deals with the synthesis of the phosphonic acid analogs to the 21 proteinogenic aminocarboxylic acids, which are of high scientific interest due to their favorable enzyme-inhibitory properties. These compounds have the ability to effectively mimic enzymatic transition states. Enantiopure phosphoalanine [(*R*)-**20**] and phosphoisoleucine [(1*R*,2*S*)-**59**] were synthesized using a newly designed synthetic method, which was only slightly adapted for each compound. This procedure involves an Arbuzov reaction, a catalytic asymmetric transfer hydrogenation, a Mitsunobu reaction, a reductive hydrogenation and final global deprotection as key steps. Using this method, the azide intermediate (*R*)-**82** which can be used for the synthesis of (*R*)-**88** and finally phosphoarginine [(*R*)-**61**] was also successfully synthesized. All following transformations to finally yield phosphoarginine are literature known. Furthermore, two sulfur-containing amino-carboxylic acid analogs, phosphomethionine [(*R*)-**60**] and phosphoisocysteine [(*R*)-**62**], were synthesized in their protected form [(*S*)-**92** and (*S*)-**93**].

(*R*)-**20** was synthesized with an overall yield of 42% and an *ee* of over 98% in 5 reaction steps. (*1R,2S*)-**59** could be obtained over 6 steps with an *ee* of over 97% and an overall yield of 68%. Starting from **103** the azide (*R*)-**88** was obtained with an overall yield of 29% and an *ee* of over 97% in 5 reaction steps. (*S*)-**92** was synthesized with an *ee* of over 99% and a yield of 38% over two steps, starting from (*S*)-**83**. Over 6 steps (*S*)-**93** could be obtained with an overall yield of 46% and an *ee* of over 98%.

5.2 Deutsche Zusammenfassung

Während dieser Arbeit wurden zwei Hauptthemen bearbeitet. Diese Masterarbeit befasst sich mit der Synthese einer Reihe von isotopenmarkierten Phosphonsäureverbindungen, die für mechanistische Studien von großem Interesse sind, sowie mit der Synthese chiraler α -Aminophosphonsäuren für zukünftige medizinische Anwendungen.

Kürzlich wurde ein neuer oxidativer Abbauweg für das natürlich vorkommende trimethylierte Analogon zu 2-AEP entdeckt. Dieser Weg, der aus den Enzymen TmpA und TmpB besteht, wird derzeit untersucht. Zur weiteren Aufklärung des Mechanismus von TmpB, wurden seine Substrat, das auf natürliche Weise von TmpA hergestellt wird, (*R*)-[1-Hydroxy-2-(trimethylammonio)ethyl]phosphonsäure [(*R*)-**58**] und seine isotopenmarkierten Analoga (*R*)-1-[²H]-**58** und (*R*)-1-[¹³C]-1-[²H]-**58** erfolgreich in sechs Syntheseschritten synthetisiert, welche jetzt von unseren Kooperationspartnern für mechanistische Studien verwendet werden können. Die ersten Schritte dieses Synthesewegs waren bereits für die nicht markierte und einfach deuterierte Verbindung bekannt. Sie bedurften daher nur geringfügiger Anpassungen. Der letzte Reaktionsschritt und die Reinigung der Endprodukte wurden gänzlich während der Arbeit für diese Masterarbeit entwickelt.

Der zweite Teil dieser Arbeit befasst sich mit der Synthese der Phosphonsäureanaloge zu den 21 proteinogenen Aminosäuren, die aufgrund ihrer vorteilhaften, enzymhemmenden Eigenschaften von hohem wissenschaftlichem Interesse sind. Diese Verbindungen haben die Fähigkeit, enzymatische Übergangszustände effektiv nachzuahmen. Enantiomerenreines Phosphaalanin [(*R*)-**20**] und Phosphaisoleucin [(*1R,2S*)-**59**] wurden unter Verwendung einer neu entwickelten Synthesemethode hergestellt, die für jede Verbindung nur geringfügig angepasst wurde. Dieses Verfahren beinhaltet eine Arbuzov-Reaktion, eine katalytische asymmetrische Transferhydrierung, eine Mitsunobu-Reaktion, eine reduktive Hydrierung und

eine globale Entschützung als Schlüsselschritte. Mit dieser Methode wurde auch das azidische Zwischenprodukt (*R*)-**82**, welches zur Synthese von (*R*)-**88** und später Phosphaarginin [(*R*)-**61**] verwendet werden kann, erfolgreich synthetisiert. Alle folgenden Transformationen, um schließlich Phosphaarginin zu erhalten, sind Literaturbekannt. Des Weiteren wurden zwei schwefelhaltige Aminocarbonsäureanaloge, Phosphamethionin [(*R*)-**60**] und Phosphaisocystein [(*R*)-**62**], in ihrer geschützten Form [(*S*)-**92** and (*S*)-**93**] hergestellt.

(*R*)-**20** wurde mit einer Gesamtausbeute von 42% und einem *ee* von über 98% in 5 Reaktionsschritten synthetisiert. (*1R,2S*)-**59** konnte über 6 Stufen mit einem *ee* von über 97% und einer Gesamtausbeute von 68% erhalten werden. Ausgehend von **103** wurde das Azid (*R*)-**88** mit einer Gesamtausbeute von 29% und einem *ee* von über 97% in 5 Reaktionsschritten erhalten. (*S*)-**92** wurde mit einem *ee* von über 99% und einer Ausbeute von 38% über zwei Schritte ausgehend von (*S*)-**83** synthetisiert. Über 6 Stufen konnten (*S*)-**93** mit einer Gesamtausbeute von 46% und einem *ee* von über 98% erhalten werden.

6. References

1. Ashley, K., Cordell, D. & Mavinic, D. A brief history of phosphorus: From the philosopher's stone to nutrient recovery and reuse. *Chemosphere* 84, 737–746 (2011).
2. Smil, V. PHOSPHORUS IN THE ENVIRONMENT: Natural Flows and Human Interferences. *Annu. Rev. Energy Environ.* 25, 53–88 (2000).
3. Vaccari, D. A. Phosphorus: A Looming Crisis. *Sci. Am.* 300, 54–59 (2009).
4. McGrath, J. W., Chin, J. P. & Quinn, J. P. Organophosphonates revealed: new insights into the microbial metabolism of ancient molecules. *Nat. Rev. Microbiol.* 11, 412–419 (2013).
5. Max, E. & Josef, P. Organic compound and process of preparing the same. 4 (1942).
6. Metcalf, W. W. & van der Donk, W. A. Biosynthesis of Phosphonic and Phosphinic Acid Natural Products. *Annu. Rev. Biochem.* 78, 65–94 (2009).
7. Quinn, J. P., Kulakova, A. N., Cooley, N. A. & McGrath, J. W. New ways to break an old bond: the bacterial carbon–phosphorus hydrolases and their role in biogeochemical phosphorus cycling. *Environ. Microbiol.* 9, 2392–2400 (2007).
8. Jia, Y., Lu, Z., Huang, K., Herzberg, O. & Dunaway-Mariano, D. Insight into the Mechanism of Phosphoenolpyruvate Mutase Catalysis Derived from Site-Directed Mutagenesis Studies of Active Site Residues. *Biochemistry* 38, 14165–14173 (1999).
9. Horiguchi, M. & Kandatstu, M. Isolation of 2-Aminoethane Phosphonic Acid from Rumen Protozoa. *Nature* 184, 901–902 (1959).
10. Missinou, M. A. *et al.* Fosmidomycin for malaria. *The Lancet* 360, 1941–1942 (2002).
11. Lanaspá, M. *et al.* Inadequate Efficacy of a New Formulation of Fosmidomycin-Cлиндamycin Combination in Mozambican Children Less than Three Years Old with Uncomplicated Plasmodium falciparum Malaria. *Antimicrob. Agents Chemother.* 56, 2923–2928 (2012).
12. Courtens, C. *et al.* Double prodrugs of a fosmidomycin surrogate as antimalarial and antitubercular agents. *Bioorg. Med. Chem. Lett.* 29, 1232–1235 (2019).
13. Silver, L. L. Fosfomycin: Mechanism and Resistance. *Cold Spring Harb. Perspect. Med.* 7, 1–11 (2017).
14. Falagas, M. E., Athanasaki, F., Voulgaris, G. L., Triarides, N. A. & Vardakas, K. Z. Resistance to fosfomycin: Mechanisms, Frequency and Clinical Consequences. *Int. J. Antimicrob. Agents* 53, 22–28 (2019).
15. Tajik, S. *et al.* Fosfomycin: A look at its various aspects. *Gene Rep.* 19, 100640 (2020).
16. Kahan, F. M., Kahan, J. S., Cassidy, P. J. & Kropp, H. The Mechanism of Action of Fosfomycin (phosphonomycin). *Ann. N. Y. Acad. Sci.* 235, 364–386 (1974).
17. Blodgett, J. A. V. *et al.* Unusual transformations in the biosynthesis of the antibiotic phosphinothricin tripeptide. *Nat. Chem. Biol.* 3, 480–485 (2007).
18. Zhou, H. *et al.* Biocatalytic asymmetric synthesis of l-phosphinothricin using a one-pot three enzyme system and a continuous substrate fed-batch strategy. *Appl. Catal. Gen.* 589, 117239 (2020).
19. Pallitsch, K., Happl, B. & Stieger, C. Determination of the Absolute Configuration of (–)-Hydroxynitrilaphos and Related Biosynthetic Questions. *Chem. – Eur. J.* 23, 15655–15665 (2017).
20. Ju, K.-S., Doroghazi, J. R. & Metcalf, W. W. Genomics-enabled discovery of phosphonate natural products and their biosynthetic pathways. *J. Ind. Microbiol. Biotechnol.* 41, 345–356 (2014).

21. Pallitsch, K., Kalina, T. & Stanković, T. Synthetic Phosphonic Acids as Potent Tools to Study Phosphonate Enzymology. *Synlett* 30, 770–776 (2019).
22. Walsh, C. Suicide substrates: mechanism-based enzyme inactivators. *Tetrahedron* 38, 871–909 (1982).
23. Anderson, D. K., Sikorski, J. A., Reitz, D. B. & Pilla, L. T. Triazole phosphonates. Electrophilic substitution of 1-substituted-1H-1,2,4-triazoles via lithiated triazole intermediates. *J. Heterocycl. Chem.* 23, 1257–1262 (1986).
24. Bunik, V. I., Tylicki, A. & Lukashov, N. V. Thiamin diphosphate-dependent enzymes: from enzymology to metabolic regulation, drug design and disease models. *FEBS J.* 280, 6412–6442 (2013).
25. Kukhar, V. & Romanenko, V. Phosphorus and Fluorine - The Union for Bioregulators. *Kem. U Ind.* 56, (2007).
26. Dill, G. M. *et al.* Glyphosate: Discovery, Development, Applications, and Properties. in *Glyphosate Resistance in Crops and Weeds* 1–33 (John Wiley & Sons, Ltd, 2010). doi:10.1002/9780470634394.ch1.
27. Alibhai, M. F. & Stallings, W. C. Closing down on glyphosate inhibition—with a new structure for drug discovery. *Proc. Natl. Acad. Sci.* 98, 2944–2946 (2001).
28. Oryan, A. & Sahvieh, S. Effects of bisphosphonates on osteoporosis: Focus on zoledronate. *Life Sci.* 118681 (2020) doi:10.1016/j.lfs.2020.118681.
29. Ralston, S. H. Bisphosphonates in the management of Paget's disease. *Bone* 138, 115465 (2020).
30. Fleisch, H., Reszka, A., Rodan, G. & Rogers, M. Chapter 78 - Bisphosphonates: Mechanisms of Action. in *Principles of Bone Biology (Second Edition)* (eds. Bilezikian, J. P., Raisz, L. G. & Rodan, G. A.) 1361–XLIII (Academic Press, 2002). doi:10.1016/B978-012098652-1.50180-3.
31. Galezowska, J. & Gumienna-Kontecka, E. Phosphonates, their complexes and bio-applications: A spectrum of surprising diversity. *Coord. Chem. Rev.* 256, 105–124 (2012).
32. Robbins, B. L., Srinivas, R. V., Kim, C., Bischofberger, N. & Fridland, A. Anti-Human Immunodeficiency Virus Activity and Cellular Metabolism of a Potential Prodrug of the Acyclic Nucleoside Phosphonate 9-R-(2-Phosphonomethoxypropyl)adenine (PMPA), Bis(isopropylloxymethylcarbonyl)PMPA. *Antimicrob. Agents Chemother.* 42, 612–617 (1998).
33. Clercq, E. D. Discovery and Development of Tenofovir Disoproxil Fumarate. in *Antiviral Drugs* 85–101 (John Wiley & Sons, Ltd, 2011). doi:10.1002/9780470929353.ch7.
34. de Clercq, E. Milestones in the discovery of antiviral agents: nucleosides and nucleotides. *Acta Pharm. Sin. B* 2, 535–548 (2012).
35. Lou, L. Advances in Nucleotide Antiviral Development from Scientific Discovery to Clinical Applications: Tenofovir Disoproxil Fumarate for Hepatitis B. *J. Clin. Transl. Hepatol.* 1, 33–38 (2013).
36. Huang, J. & Chen, R. An overview of recent advances on the synthesis and biological activity of α -aminophosphonic acid derivatives. *Heteroat. Chem.* 11, 480–492 (2000).
37. Kafarski, P. & Lejczak, B. Biological Activity of Aminophosphonic Acids. *Phosphorus Sulfur Silicon Relat. Elem.* 63, 193–215 (1991).
38. Mucha, A., Kafarski, P. & Berlicki, Ł. Remarkable Potential of the α -Aminophosphonate/Phosphinate Structural Motif in Medicinal Chemistry. *J. Med. Chem.* 54, 5955–5980 (2011).

39. Stamper, G., F., Morollo, A. A. & Ringe, D. Reaction of Alanine Racemase with 1-Aminoethylphosphonic Acid Forms a Stable External Aldimine. *Biochemistry* 38, 6714–6714 (1999).
40. Gu, L. & Jin, C. Synthesis and antitumor activity of α -aminophosphonates containing thiazole[5,4-b]pyridine moiety. *Org. Biomol. Chem.* 10, 7098–7102 (2012).
41. Wanat, W., Talma, M., Hurek, J., Pawełczak, M. & Kafarski, P. Substituted phosphonic analogues of phenylglycine as inhibitors of phenylalanine ammonia lyase from potatoes. *Biochimie* 151, 119–127 (2018).
42. Shaikh, S., Dhavan, P., Ramana, M. M. V. & Jadhav, B. L. Design, synthesis and evaluation of new chromone-derived aminophosphonates as potential acetylcholinesterase inhibitor. *Mol. Divers.* (2020) doi:10.1007/s11030-020-10060-y.
43. Pasek, M. A., Sampson, J. M. & Atlas, Z. Redox chemistry in the phosphorus biogeochemical cycle. *Proc. Natl. Acad. Sci.* 111, 15468–15473 (2014).
44. Morales, M. E., Allegrini, M., Basualdo, J., Villamil, M. B. & Zabaloy, M. C. Primer design to assess bacterial degradation of glyphosate and other phosphonates. *J. Microbiol. Methods* 169, 105814 (2020).
45. Clark, L. L., Ingall, E. D. & Benner, R. Marine phosphorus is selectively remineralized. *Nature* 393, 426–426 (1998).
46. Horsman, G. P. & Zechel, D. L. Phosphonate Biochemistry. *Chem. Rev.* 117, 5704–5783 (2017).
47. Björkman, K. M. & Karl, D. M. Bioavailability of dissolved organic phosphorus in the euphotic zone at Station ALOHA, North Pacific Subtropical Gyre. *Limnol. Oceanogr.* 48, 1049–1057 (2003).
48. Kamat, S. S., Williams, H. J., Dangott, L. J., Chakrabarti, M. & Raushel, F. M. The catalytic mechanism for aerobic formation of methane by bacteria. *Nature* 497, 132–136 (2013).
49. Metcalf, W. W. *et al.* Synthesis of methylphosphonic acid by marine microbes: a source for methane in the aerobic ocean. *Science* 337, 1104–1107 (2012).
50. Peck, S. C. & van der Donk, W. A. Phosphonate biosynthesis and catabolism: a treasure trove of unusual enzymology. *Curr. Opin. Chem. Biol.* 17, 580–588 (2013).
51. Khatun, S. *et al.* Aerobic methane production by planktonic microbes in lakes. *Sci. Total Environ.* 696, 133916 (2019).
52. Villarreal-Chiu, J. F., Quinn, J. P. & McGrath, J. W. The Genes and Enzymes of Phosphonate Metabolism by Bacteria, and Their Distribution in the Marine Environment. *Front. Microbiol.* 3, 1–13 (2012).
53. Chin, J. P., McGrath, J. W. & Quinn, J. P. Microbial transformations in phosphonate biosynthesis and catabolism, and their importance in nutrient cycling. *Curr. Opin. Chem. Biol.* 31, 50–57 (2016).
54. Nair, S. K. & van der Donk, W. A. Structure and mechanism of enzymes involved in biosynthesis and breakdown of the phosphonates fosfomycin, dehydrophos, and phosphinothricin. *Arch. Biochem. Biophys.* 505, 13–21 (2011).
55. Diddens, H. *et al.* On the transport of tripeptide antibiotics in bacteria. *Eur J Biochem* 11–23 (1976).
56. Michigami, T., Kawai, M., Yamazaki, M. & Ozono, K. Phosphate as a Signaling Molecule and Its Sensing Mechanism. *Physiol. Rev.* 98, 2317–2348 (2018).
57. Lamarche, M. G., Wanner, B. L., Crépin, S. & Harel, J. The phosphate regulon and bacterial virulence: a regulatory network connecting phosphate homeostasis and pathogenesis. *FEMS Microbiol. Rev.* 32, 461–473 (2008).

58. Crépin, S. *et al.* The Pho regulon and the pathogenesis of *Escherichia coli*. *Vet. Microbiol.* 153, 82–88 (2011).
59. Uluşeker, C. *et al.* Quantifying dynamic mechanisms of auto-regulation in *Escherichia coli* with synthetic promoter in response to varying external phosphate levels. *Sci. Rep.* 9, 2076 (2019).
60. Santos-Beneit, F. The Pho regulon: a huge regulatory network in bacteria. *Front. Microbiol.* 6, 1–13 (2015).
61. Zechel, D. L. PhnK: Another Piece of the Carbon-Phosphorus Lyase Puzzle. *Structure* 24, 3–4 (2016).
62. Wackett, L. P., Shames, S. L., Venditti, C. P. & Walsh, C. T. Bacterial carbon-phosphorus lyase: products, rates, and regulation of phosphonic and phosphinic acid metabolism. *J. Bacteriol.* 169, 710–717 (1987).
63. Cook, A. M., Daughton, C. G. & Alexander, M. Phosphonate utilization by bacteria. *J. Bacteriol.* 133, 85–90 (1978).
64. Seweryn, P. *et al.* Structural insights into the bacterial carbon-phosphorus lyase machinery. *Nature* 525, 68–72 (2015).
65. Morales, M. E., Allegrini, M., Basualdo, J., Villamil, M. B. & Zabaloy, M. C. Primer design to assess bacterial degradation of glyphosate and other phosphonates. *J. Microbiol. Methods* 169, 105814 (2020).
66. Horsman, G. P. & Zechel, D. L. Phosphonate Biochemistry. *Chem. Rev.* 117, 5704–5783 (2017).
67. Kamat, S. S., Singh, S., Rajendran, A., Gama, S. R. & Zechel, D. L. 4.16 - Enzymatic Strategies for the Catabolism of Organophosphonates. in *Comprehensive Natural Products III* (eds. Liu, H.-W. (Ben) & Begley, T. P.) 399–429 (Elsevier, 2020). doi:10.1016/B978-0-12-409547-2.14617-7.
68. Kamat, S. S., Williams, H. J. & Raushel, F. M. Intermediates in the Transformation of Phosphonates to Phosphate by Bacteria. *Nature* 480, 570 (2011).
69. Yang, K., Ren, Z., Raushel, F. M. & Zhang, J. Structures of the Carbon-Phosphorus Lyase Complex Reveal the Binding Mode of the NBD-like PhnK. *Structure* 24, 37–42 (2016).
70. Kamat, S. S. & Raushel, F. M. PhnJ – A novel radical SAM enzyme from the C–P lyase complex. *Perspect. Sci.* 4, 32–37 (2015).
71. Becker, A. *et al.* Structure and mechanism of the glycy radical enzyme pyruvate formate-lyase. *Nat. Struct. Biol.* 6, 969–975 (1999).
72. Hove-Jensen, B., Rosenkrantz, T. J., Haldimann, A. & Wanner, B. L. *Escherichia coli* phnN, Encoding Ribose 1,5-Bisphosphokinase Activity (Phosphoribosyl Diphosphate Forming): Dual Role in Phosphonate Degradation and NAD Biosynthesis Pathways. *J. Bacteriol.* 185, 2793–2801 (2003).
73. Ghodge, S. V., Cummings, J. A., Williams, H. J. & Raushel, F. M. Discovery of a cyclic phosphodiesterase that catalyzes the sequential hydrolysis of both ester bonds to phosphorus. *J. Am. Chem. Soc.* 135, 16360–16363 (2013).
74. Hove-Jensen, B. *et al.* Phosphoribosyl Diphosphate (PRPP): Biosynthesis, Enzymology, Utilization, and Metabolic Significance. *Microbiol. Mol. Biol. Rev.* 81, 1–83 (2017).
75. Hove-Jensen, B., Rosenkrantz, T. J., Haldimann, A. & Wanner, B. L. *Escherichia coli* phnN, encoding ribose 1,5-bisphosphokinase activity (phosphoribosyl diphosphate forming): Dual role in phosphonate degradation and NAD biosynthesis pathways. *J. Bacteriol.* 185, 2793–2801 (2003).

76. Fox, E. M. & Mendz, G. L. Phosphonate degradation in microorganisms. *Enzyme Microb. Technol.* 40, 145–150 (2006).
77. Villarreal-Chiu, J. F., Quinn, J. P. & McGrath, J. W. The genes and enzymes of phosphonate metabolism by bacteria, and their distribution in the marine environment. *Front. Microbiol.* 3, 1–13 (2012).
78. La Nauze, J. M., Rosenberg, H. & Shaw, D. C. The enzymic cleavage of the carbon-phosphorus bond: Purification and properties of phosphonatase. *Biochim. Biophys. Acta BBA - Enzymol.* 212, 332–350 (1970).
79. Jiang, W., Metcalf, W. W., Lee, K. S. & Wanner, B. L. Molecular cloning, mapping, and regulation of Pho regulon genes for phosphonate breakdown by the phosphonatase pathway of *Salmonella typhimurium* LT2. *J. Bacteriol.* 177, 6411–6421 (1995).
80. Dumora, C., Lacoste, A.-M. & Cassaigne, A. Purification and Properties of 2-Aminoethylphosphonate: Pyruvate Aminotransferase from *Pseudomonas aeruginosa*. *Eur. J. Biochem.* 133, 119–125 (1983).
81. Koonin, E. V. & Tatusov, R. L. Computer analysis of bacterial haloacid dehalogenases defines a large superfamily of hydrolases with diverse specificity. Application of an iterative approach to database search. *J. Mol. Biol.* 244, 125–132 (1994).
82. Lahiri, S. D., Zhang, G., Dunaway-Mariano, D. & Allen, K. N. Diversification of Function in the Haloacid Dehalogenase Enzyme Superfamily: The Role of the Cap Domain in Hydrolytic Phosphorus-Carbon Bond Cleavage. *Bioorganic Chem.* 34, 394–409 (2006).
83. Morais, M. C. *et al.* X-ray crystallographic and site-directed mutagenesis analysis of the mechanism of Schiff-base formation in phosphonoacetaldehyde hydrolase catalysis. *J. Biol. Chem.* 279, 9353–9361 (2004).
84. Ternan, N. G. & Quinn, J. P. In Vitro Cleavage of the Carbon-Phosphorus Bond of Phosphonopyruvate by Cell Extracts of an Environmental *Burkholderia cepacia* Isolate. *Biochem. Biophys. Res. Commun.* 248, 378–381 (1998).
85. Chen, C. C. H. *et al.* Structure and Kinetics of Phosphonopyruvate Hydrolase from *Voriovorax* sp. Pal2: New Insight into the Divergence of Catalysis within the PEP Mutase/Isocitrate Lyase Superfamily. *Biochemistry* 45, 11491–11504 (2006).
86. Kamat, S. S. & Raushel, F. M. The enzymatic conversion of phosphonates to phosphate by bacteria. *Curr. Opin. Chem. Biol.* 17, 589–596 (2013).
87. McGrath, J. W., Wisdom, G. B., McMullan, G., Larkin, M. J. & Quinn, J. P. The purification and properties of phosphonoacetate hydrolase, a novel carbon-phosphorus bond-cleavage enzyme from *Pseudomonas fluorescens* 23F. *Eur. J. Biochem.* 234, 225–230 (1995).
88. Agarwal, V., Borisova, S. A., Metcalf, W. W., van der Donk, W. A. & Nair, S. K. Structural and Mechanistic Insights into C-P Bond Hydrolysis by Phosphonoacetate Hydrolase. *Chem. Biol.* 18, 1230–1240 (2011).
89. McMullan, G., Harrington, F. & Quinn, J. P. Metabolism of Phosphonoacetate as the Sole Carbon and Phosphorus Source by an Environmental Bacterial Isolate. *Appl. Environ. Microbiol.* 58, 1364–1366 (1992).
90. Martinez, A., Tyson, G. W. & DeLong, E. F. Widespread known and novel phosphonate utilization pathways in marine bacteria revealed by functional screening and metagenomic analyses. *Environ. Microbiol.* 12, 222–238 (2010).
91. McSorley, F. R. *et al.* PhnY and PhnZ Comprise a New Oxidative Pathway for Enzymatic Cleavage of a Carbon-Phosphorus Bond. *J. Am. Chem. Soc.* 134, 8364–8367 (2012).

92. Staalduinen, L. M. van *et al.* Crystal structure of PhnZ in complex with substrate reveals a di-iron oxygenase mechanism for catabolism of organophosphonates. *Proc. Natl. Acad. Sci.* 111, 5171–5176 (2014).
93. Gama, S. R. *et al.* C-H Bond Cleavage Is Rate-Limiting for Oxidative C-P Bond Cleavage by the Mixed Valence Diiron-Dependent Oxygenase PhnZ. *Biochemistry* 58, 5271–5280 (2019).
94. Rajakovich, L. J. *et al.* 5.10 - Emerging Structural and Functional Diversity in Proteins With Dioxygen-Reactive Dinuclear Transition Metal Cofactors. in *Comprehensive Natural Products III* (eds. Liu, H.-W. (Ben) & Begley, T. P.) 215–250 (Elsevier, 2020). doi:10.1016/B978-0-12-409547-2.14864-4.
95. Gama, S. R. *et al.* An Oxidative Pathway for Microbial Utilization of Methylphosphonic Acid as a Phosphate Source. *ACS Chem. Biol.* 14, 735–741 (2019).
96. Zhao, C. & Chen, H. Mechanism of Organophosphonate Catabolism by Diiron Oxygenase PhnZ: A Third Iron-Mediated O–O Activation Scenario in Nature. *ACS Catal.* 7, 3521–3531 (2017).
97. Metcalf, W. W. & van der Donk, W. A. Biosynthesis of Phosphonic and Phosphinic Acid Natural Products. *Annu. Rev. Biochem.* 78, 65–94 (2009).
98. Rajakovich, L. J. *et al.* A New Microbial Pathway for Organophosphonate Degradation Catalyzed by Two Previously Misannotated Non-Heme-Iron Oxygenases. *Biochemistry* 58, 1627–1647 (2019).
99. Ordonez, M., Luis Viveros-Ceballos, J., Cativiela, C. & Arizpe, A. Stereoselective Synthesis of α -Aminophosphonic Acids Analogs of the 20 Proteinogenic α -Amino Acids. *Curr. Org. Synth.* 9, 310–341 (2012).
100. Qian, R. *et al.* Preparation of Phosphonic Acid Analogues of Proline and Proline Analogues and Their Biological Evaluation as δ 1-Pyrroline-5-carboxylate Reductase Inhibitors. *ACS Omega* 3, 4441–4452 (2018).
101. Corbett, M. T. & Johnson, J. S. Diametric Stereocontrol in Dynamic Catalytic Reduction of Racemic Acyl Phosphonates: Divergence from α -Keto Ester Congeners. *J. Am. Chem. Soc.* 135, 594–597 (2013).
102. Yokomatsu, T., Yamagishi, T. & Shibuya, S. Enantioselective synthesis of α -hydroxyphosphonates through asymmetric Pudovik reactions with chiral lanthanoid and titaniumalkoxides. *J. Chem. Soc. Perkin 1* 1527–1534 (1997) doi:10.1039/A608161D.
103. Cheng, X., Goddard, R., Buth, G. & List, B. Direct Catalytic Asymmetric Three-Component Kabachnik–Fields Reaction. *Angew. Chem. Int. Ed.* 47, 5079–5081 (2008).
104. Hammerschmidt, F. Addition von Dialkylphosphiten und Dialkyl(trimethylsilyl)phosphiten an 2-(Benzoyloxy)propanal Darstellung aller vier stereoisomeren (1,2-Dihydroxy-[1-2H1]propyl)phosphonsäuren aus chiralen Lactaten. *Liebigs Ann. Chem.* 1991, 469–475 (1991).
105. Stankovic, T. Synthesis of Potentially Bioactive Compounds: α -Aminophosphonates as Enzyme Inhibitors and an Improved TSPO Ligand for PET Diagnosis. (University of Vienna, 2019).
106. Ma, X. *et al.* Alcohol-based Michaelis–Arbuzov reaction: an efficient and environmentally-benign method for C–P(O) bond formation. *Green Chem.* 20, 3408–3413 (2018).
107. Cade, J. A. 449. Methylenebisphosphonates and related compounds. Part II. Synthesis from α -keto-phosphonates. *J. Chem. Soc. Resumed* 2272–2275 (1959) doi:10.1039/JR9590002272.

108. Platzer, S. *et al.* Task-specific thioglycolate ionic liquids for heavy metal extraction: Synthesis, extraction efficacies and recycling properties. *J. Hazard. Mater.* 324, 241–249 (2017).
109. Noyori, R. Asymmetric Catalysis: Science and Opportunities (Nobel Lecture). *Angew. Chem. Int. Ed.* 41, 2008–2022 (2002).
110. Hashiguchi, S., Fujii, A., Takehara, J., Ikariya, T. & Noyori, R. Asymmetric Transfer Hydrogenation of Aromatic Ketones Catalyzed by Chiral Ruthenium(II) Complexes. *J. Am. Chem. Soc.* 117, 7562–7563 (1995).
111. Fujii, A., Hashiguchi, S., Uematsu, N., Ikariya, T. & Noyori, R. Ruthenium(II)-Catalyzed Asymmetric Transfer Hydrogenation of Ketones Using a Formic Acid–Triethylamine Mixture. *J. Am. Chem. Soc.* 118, 2521–2522 (1996).
112. Noyori, R. & Hashiguchi, S. Asymmetric Transfer Hydrogenation Catalyzed by Chiral Ruthenium Complexes. *Acc. Chem. Res.* 30, 97–102 (1997).
113. Corbett, M. T. & Johnson, J. S. Diametric Stereocontrol in Dynamic Catalytic Reduction of Racemic Acyl Phosphonates: Divergence from α -Keto Ester Congeners. *J. Am. Chem. Soc.* 135, 594–597 (2013).
114. Oudar, J. Sulfur Adsorption and Poisoning of Metallic Catalysts. *Catal. Rev.* 22, 171–195 (1980).
115. Drescher, M. *et al.* ENZYMES IN ORGANIC CHEMISTRY 7.[1] EVALUATION OF HOMOCHIRAL t-BUTYL(PHENYL)PHOSPHINOTHIOIC ACID FOR THE DETERMINATION OF ENANTIOMERIC EXCESSES AND ABSOLUTE CONFIGURATIONS OF α -SUBSTITUTED PHOSPHONATES. *Phosphorus Sulfur Silicon Relat. Elem.* 140, 79–93 (1998).
116. Mitsunobu, O. & Yamada, M. Preparation of Esters of Carboxylic and Phosphoric Acid via Quaternary Phosphonium Salts. *Bull. Chem. Soc. Jpn.* 40, 2380–2382 (1967).
117. Fletcher, S. The Mitsunobu reaction in the 21st century. *Org. Chem. Front.* 2, 739–752 (2015).
118. Qian, R., Kuliszewska, E., Macoratti, E. & Hammerschmidt, F. Chemoenzymatic Synthesis of Racemic and Enantiomerically Pure Phosphaaspartic Acid and Phosphaarginine. *Eur. J. Org. Chem.* 2017, 4836–4845 (2017).
119. Hammerschmidt, F. & Hanbauer, M. Transformation of Arylmethylamines into α -Aminophosphonic Acids via Metalated Phosphoramidates: Rearrangement of Partly Configurationally Stable N-Phosphorylated α -Aminocarbanions. *J. Org. Chem.* 65, 6121–6131 (2000).
120. Pallitsch, K., Roller, A. & Hammerschmidt, F. The Stereochemical Course of the α -Hydroxyphosphonate-Phosphate Rearrangement. *Chem. - Eur. J.* 21, (2015).
121. Staalduinen, L. M. van *et al.* Crystal structure of PhnZ in complex with substrate reveals a di-iron oxygenase mechanism for catabolism of organophosphonates. *Proc. Natl. Acad. Sci.* 111, 5171–5176 (2014).
122. Wolff, H. The Schmidt Reaction. in *Organic Reactions* 307–336 (American Cancer Society, 2011). doi:10.1002/0471264180.or003.08.
123. Dolomanov, O. V., Bourhis, L. J., Gildea, R. J., Howard, J. a. K. & Puschmann, H. OLEX2: a complete structure solution, refinement and analysis program. *J. Appl. Crystallogr.* 42, 339–341 (2009).
124. Sheldrick, G. M. A short history of SHELX. *Acta Crystallogr. A* 64, 112–122 (2008).
125. Hammerschmidt, F., Kvaternik, H., Schweifer, A., Mereiter, K. & Aigner, R. M. Improved Synthesis of No-Carrier-Added [14 C]MIBG and Its Precursor. *Synthesis* 44, 3387–3391 (2012).

7. Appendix

Data from crystal structure analysis of (*R*)-**20** (mo_TD87_P212121), (*R*)-**34** (mo_TD70_P212121) and (*R*)-**58** (mo_TB55_2_C2c):

Identification code	(<i>R</i>)- 20	(<i>R</i>)- 34	(<i>R</i>)- 58
Empirical formula	C ₂ H ₈ NO ₃ P	C ₂ H ₈ NO ₄ P	C ₅ H ₁₉ NO _{6.5} P
Formula weight	125.06	141.06	228.18
Temperature/K	100.0	100.0	100.0
Crystal system	orthorhombic	orthorhombic	monoclinic
Space group	P2 ₁ 2 ₁ 2 ₁	P2 ₁ 2 ₁ 2 ₁	C2/c
a/Å	4.8215(3)	6.3103(6)	15.8461(13)
b/Å	10.3632(7)	7.1033(7)	6.0690(5)
c/Å	10.4822(10)	11.5814(17)	23.2674(17)
α/°	90	90	90
β/°	90	90	99.882(6)
γ/°	90	90	90
Volume/Å ³	523.76(7)	519.12(10)	2204.4(3)
Z	4	4	8
ρ _{calc} /g/cm ³	1.586	1.805	1.375
μ/mm ⁻¹	0.424	0.453	0.258
F(000)	264.0	296.0	984.0
Crystal size/mm ³	0.1 × 0.08 × 0.05	0.06 × 0.05 × 0.02	0.1 × 0.09 × 0.01
Radiation	MoKα (λ = 0.71073)	MoKα (λ = 0.71073)	MoKα (λ = 0.71073)
2θ range for data collection/°	7.866 to 60.098	6.73 to 60.196	3.554 to 60.338
Index ranges	-6 ≤ h ≤ 6, -13 ≤ k ≤ 13, -14 ≤ l ≤ 14	-8 ≤ h ≤ 8, -8 ≤ k ≤ 8, -13 ≤ l ≤ 16	-22 ≤ h ≤ 22, -8 ≤ k ≤ 8, -32 ≤ l ≤ 32
Reflections collected	3581	2791	38703
Independent reflections	1464 [R _{int} = 0.0414, R _{sigma} = 0.0506]	1389 [R _{int} = 0.0425, R _{sigma} = 0.0552]	3249 [R _{int} = 0.0495, R _{sigma} = 0.0242]
Data/restraints/parameters	1464/0/67	1389/0/76	3249/1/144
Goodness-of-fit on F ²	1.292	1.177	1.101
Final R indexes [I > 2σ (I)]	R ₁ = 0.0316, wR ₂ = 0.0754	R ₁ = 0.0296, wR ₂ = 0.0657	R ₁ = 0.0453, wR ₂ = 0.1116
Final R indexes [all data]	R ₁ = 0.0445, wR ₂ = 0.1139	R ₁ = 0.0429, wR ₂ = 0.0815	R ₁ = 0.0538, wR ₂ = 0.1152
Largest diff. peak/hole /e Å ⁻³	0.76/-1.33	0.42/-0.64	0.82/-0.40
Flack parameter	0.04(7)	-0.10(8)	

(R)-20:

Fractional Atomic Coordinates ($\times 10^4$) and Equivalent Isotropic Displacement Parameters ($\text{\AA}^2 \times 10^3$); U_{eq} is defined as 1/3 of the trace of the orthogonalised U_{ij} tensor.									
Atom	x	y	z	U(eq)					
P1	3768(2)	4149.0(8)	6115.0(8)	8.9(2)					
O1	1709(6)	5273(2)	6461(3)	12.9(5)					
N1	3466(7)	1550(3)	6593(3)	9.6(6)					
C1	2712(8)	2832(3)	7172(3)	11.0(7)					
O2	3491(6)	3693(2)	4759(2)	11.6(5)					
C2	3852(12)	2965(4)	8522(3)	19.7(8)					
O3	6598(6)	4610(3)	6503(3)	14.6(6)					
Anisotropic Displacement Parameters ($\text{\AA}^2 \times 10^3$); the Anisotropic displacement factor exponent takes the form: $-2\pi_2[h_2a^* \cdot U_{11} + 2hka^*b^*U_{12} + \dots]$.									
Atom	U_{11}	U_{22}	U_{33}	U_{23}	U_{13}	U_{12}			
P1	9.6(4)	8.6(4)	8.5(3)	-0.8(3)	0.7(3)	0.1(3)			
O1	11.5(13)	9.6(11)	17.7(12)	-1.6(10)	0.6(10)	-1.5(10)			
N1	6.8(14)	12.1(13)	9.8(12)	0.3(10)	0.0(12)	0.4(11)			
C1	13.2(17)	9.7(16)	10.2(15)	0.6(12)	2.2(13)	-0.5(13)			
O2	11.2(12)	13.2(11)	10.4(11)	-0.3(9)	0.1(10)	2.0(11)			
C2	34(2)	15.7(16)	9.6(14)	-1.8(12)	-0.8(18)	-2.4(19)			
O3	12.7(13)	15.2(12)	15.9(11)	-3.5(10)	1.6(10)	0.9(11)			
Bond Lengths									
Atom	Atom	Length/ \AA	Atom	Atom	Length/ \AA				
P1	O1	1.573(3)	P1	O3	1.502(3)				
P1	C1	1.830(4)	N1	C1	1.505(4)				
P1	O2	1.504(3)	C1	C2	1.524(5)				
Bond Angles									
Atom	Atom	Atom	Angle/ $^\circ$	Atom	Atom	Atom	Angle/ $^\circ$		
O1	P1	C1	103.71(16)	O3	P1	O2	115.89(16)		
O2	P1	O1	113.26(15)	N1	C1	P1	110.3(2)		
O2	P1	C1	108.26(16)	N1	C1	C2	111.6(3)		
O3	P1	O1	105.97(15)	C2	C1	P1	113.2(3)		
O3	P1	C1	109.02(17)						
Torsion Angles									
A	B	C	D	Angle/ $^\circ$	A	B	C	D	Angle/ $^\circ$
O1	P1	C1	N1	153.7(2)	O2	P1	C1	C2	158.9(3)
O1	P1	C1	C2	-80.5(3)	O3	P1	C1	N1	-93.7(3)
O2	P1	C1	N1	33.1(3)	O3	P1	C1	C2	32.0(3)

(R)-34:

Fractional Atomic Coordinates ($\times 10^4$) and Equivalent Isotropic Displacement Parameters ($\text{\AA}^2 \times 10^3$); U_{eq} is defined as 1/3 of the trace of the orthogonalised U_{ij} tensor.									
Atom	x	y	z	U(eq)					
P1	5686.2(12)	5888.3(11)	6508.5(6)	7.17(18)					
O3	4570(3)	5652(3)	7660.6(16)	10.2(4)					
O1	2191(3)	4406(3)	5479.4(18)	10.6(4)					
O4	8017(3)	5495(3)	6524.1(18)	11.3(4)					
C1	4453(4)	4344(4)	5439(2)	8.0(5)					
C2	5321(5)	4782(4)	4243(2)	9.7(6)					
N1	4548(4)	3424(4)	3355(2)	9.7(5)					
O2	5153(3)	7891(3)	6005.4(18)	10.2(5)					
Anisotropic Displacement Parameters ($\text{\AA}^2 \times 10^3$); the Anisotropic displacement factor exponent takes the form: $-2\pi_2[h_2a^*2U_{11}+2hka^*b^*U_{12}+\dots]$.									
Atom	U_{11}	U_{22}	U_{33}	U_{23}	U_{13}	U_{12}			
P1	8.7(3)	6.7(3)	6.2(3)	-0.1(3)	0.0(3)	0.3(3)			
O3	12.6(10)	10.0(10)	8.1(9)	1.3(8)	1.5(8)	1.1(9)			
O1	8.7(9)	10.0(11)	13.0(9)	2.3(9)	0.6(8)	-0.2(8)			
O4	10.5(10)	13.8(12)	9.6(9)	-2.1(9)	-0.7(9)	0.5(8)			
C1	6.7(12)	8.7(15)	8.4(11)	0.5(11)	-0.3(10)	1.1(12)			
C2	12.1(14)	9.4(14)	7.6(12)	-0.2(10)	0.7(11)	-2.7(11)			
N1	10.8(12)	10.1(12)	8.3(12)	-0.7(9)	0.7(10)	1.0(9)			
O2	16.6(11)	6.3(11)	7.6(10)	-1.1(8)	0.1(8)	1.2(8)			
Bond Lengths									
Atom	Atom	Length/ \AA	Atom	Atom	Length/ \AA				
P1	O3	1.518(2)	O1	C1	1.429(3)				
P1	O4	1.497(2)	C1	C2	1.521(4)				
P1	C1	1.829(3)	C2	N1	1.492(4)				
P1	O2	1.574(2)							
Bond Angles									
Atom	Atom	Atom	Angle/ $^\circ$	Atom	Atom	Atom	Angle/ $^\circ$		
O3	P1	C1	109.38(12)	O2	P1	C1	101.57(12)		
O3	P1	O2	109.02(12)	O1	C1	P1	112.59(19)		
O4	P1	O3	115.13(12)	O1	C1	C2	112.5(2)		
O4	P1	C1	108.30(13)	C2	C1	P1	109.93(19)		
O4	P1	O2	112.53(12)	N1	C2	C1	112.2(2)		
Torsion Angles									
A	B	C	D	Angle/ $^\circ$	A	B	C	D	Angle/ $^\circ$
P1	C1	C2	N1	173.73(19)	O4	P1	C1	O1	171.13(18)
O3	P1	C1	O1	44.9(2)	O4	P1	C1	C2	-62.5(2)
O3	P1	C1	C2	171.26(18)	O2	P1	C1	O1	-70.2(2)
O1	C1	C2	N1	-59.9(3)	O2	P1	C1	C2	56.1(2)

(R)-58:

Fractional Atomic Coordinates ($\times 10^4$) and Equivalent Isotropic Displacement Parameters ($\text{\AA}^2 \times 10^3$); U_{eq} is defined as 1/3 of the trace of the orthogonalised U_{ij} tensor.						
Atom	x	y	z	U(eq)		
P1	3057.2(2)	5534.5(7)	5724.2(2)	16.73(11)		
O1	3946.0(7)	3204(2)	5032.6(5)	21.3(3)		
N1	5372.7(9)	2512(3)	6193.1(6)	21.4(3)		
C1	3886.1(10)	3522(3)	5632.9(7)	20.2(3)		
O2	3439.4(8)	7828(2)	5593.2(6)	25.7(3)		
C2	4741.9(10)	4320(3)	5955.9(7)	21.0(3)		
O3	2277.2(7)	4989(2)	5278.3(5)	20.6(2)		
C3	5078.2(14)	1304(4)	6679.3(8)	33.5(4)		
O4	2953.5(8)	5426(2)	6351.8(5)	24.5(3)		
C4	6205.2(12)	3666(4)	6426.7(10)	35.6(5)		
C5	5509.8(12)	916(4)	5726.8(8)	29.4(4)		
O1S (water)	5000	4112(3)	2500	33.7(4)		
O4S (water)	7487(5)	7117(11)	6942(3)	43.4(9)		
O2S (water)	6534.1(9)	1844(3)	2752.4(6)	35.5(3)		
O3S (water)	2139(4)	2979(7)	2885(2)	43.4(9)		
Anisotropic Displacement Parameters ($\text{\AA}^2 \times 10^3$); the Anisotropic displacement factor exponent takes the form: $-2\pi_2[h_2a^*U_{11}+2hka^*b^*U_{12}+\dots]$.						
Atom	U_{11}	U_{22}	U_{33}	U_{23}	U_{13}	U_{12}
P1	15.89(18)	20.3(2)	13.96(18)	0.80(14)	2.43(13)	3.18(15)
O1	18.9(5)	31.2(7)	14.2(5)	-4.9(5)	4.4(4)	-1.8(5)
N1	17.3(6)	29.7(7)	16.7(6)	-2.5(5)	1.2(5)	6.9(6)
C1	20.3(7)	24.9(8)	15.3(7)	-1.4(6)	3.2(5)	3.6(6)
O2	25.5(6)	24.1(6)	24.1(6)	5.0(5)	-5.1(5)	-3.8(5)
C2	19.3(7)	23.1(8)	20.0(7)	-0.2(6)	1.5(6)	3.0(6)
O3	17.8(5)	20.5(6)	22.1(6)	2.9(4)	-0.4(4)	0.2(4)
C3	43.2(11)	34.5(10)	22.8(8)	5.7(8)	5.5(8)	8.7(9)
O4	30.4(6)	27.8(7)	17.2(5)	0.4(5)	9.1(5)	6.2(5)
C4	22.6(8)	41.6(12)	40.4(11)	-8.5(9)	-0.7(8)	1.8(8)
C5	25.7(8)	37.6(10)	24.8(8)	-8.5(8)	4.0(7)	12.6(8)
O1S	28.9(9)	27.5(10)	42.5(12)	0	0.1(8)	0
O4S	67(3)	26.4(9)	45(2)	12.1(14)	32.4(18)	11.7(19)
O2S	28.7(7)	48.9(9)	27.9(7)	-13.3(6)	2.4(5)	2.2(6)
O3S	67(3)	26.4(9)	45(2)	12.1(14)	32.4(18)	11.7(19)
Bond Lengths						
Atom	Atom	Length/ \AA	Atom	Atom	Length/ \AA	
P1	C1	1.8325(17)	N1	C2	1.522(2)	
P1	O2	1.5689(14)	N1	C3	1.489(3)	
P1	O3	1.5079(12)	N1	C4	1.510(2)	
P1	O4	1.4986(12)	N1	C5	1.498(2)	
O1	C1	1.4292(19)	C1	C2	1.513(2)	

Bond Angles									
Atom	Atom	Atom	Angle/°	Atom	Atom	Atom	Angle/°		
O2	P1	C1	105.11(8)	C3	N1	C5	109.57(16)		
O3	P1	C1	107.04(7)	C4	N1	C2	105.97(15)		
O3	P1	O2	111.06(7)	C5	N1	C2	111.80(13)		
O4	P1	C1	106.52(7)	C5	N1	C4	109.53(14)		
O4	P1	O2	109.80(8)	O1	C1	P1	111.86(11)		
O4	P1	O3	116.54(7)	O1	C1	C2	108.92(13)		
C3	N1	C2	111.01(14)	C2	C1	P1	109.16(12)		
C3	N1	C4	108.87(15)	C1	C2	N1	115.22(14)		
Torsion Angles									
A	B	C	D	Angle/°	A	B	C	D	Angle/°
P1	C1	C2	N1	149.66(12)	C3	N1	C2	C1	-68.88(19)
O1	C1	C2	N1	-87.95(17)	O4	P1	C1	O1	170.37(11)
O2	P1	C1	O1	-73.13(13)	O4	P1	C1	C2	-69.01(13)
O2	P1	C1	C2	47.48(13)	C4	N1	C2	C1	173.08(15)
O3	P1	C1	O1	45.04(14)	C5	N1	C2	C1	53.8(2)
O3	P1	C1	C2	165.65(11)					
Atomic Occupancy (water molecules)									
Atom	Occupancy	Atom	Occupancy	Atom	Occupancy	Atom	Occupancy		
H1SA	0.5	H1SB	0.5	O1S	0.5				
H4SA	0.399(7)	H4SB	0.399(7)	O4S	0.399(7)				
H3SA	0.601(7)	H3SB	0.601(7)	O3S	0.601(7)				